UNIVERSIDADE FEDERAL DE MINAS GERAIS
Programa de Pós-Graduação em Engenharia Metalúrgica, Materiais e de Minas

TESE DE DOUTORADO

Minérios Fosfáticos Ígneos com Ganga Carbonática: Estudos Fundamentais

Autor: Leandro Henrique Santos
Orientador: Prof. PhD. Antônio Eduardo Clark Peres
Coorientador: Prof. PhD. Gilberto Rodrigues da Silva

Março/2022

UNIVERSIDADE FEDERAL DE MINAS GERAIS
Programa de Pós-Graduação em Engenharia Metalúrgica, Materiais e de Minas

Leandro Henrique Santos

TESE DE DOUTORADO

Minérios Fosfáticos Ígneos com Ganga Carbonática: Estudos Fundamentais

Tese apresentada ao Programa de Pós-Graduação em Engenharia Metalúrgica, Materiais e de Minas da Universidade Federal de Minas Gerais como requisito parcial para obtenção do título de Doutor em Engenharia Metalúrgica, Materiais e de Minas.

Área de Concentração: Tecnologia Mineral

Orientador: Prof. PhD. Antônio Eduardo Clark Peres

Coorientador: Prof. PhD. Gilberto Rodrigues da Silva

Março/2022

Santos, Leandro Henrique.
S237m Minérios fosfáticos ígneos com ganga carbonática [recurso eletrônico]: estudos fundamentais / Leandro Henrique Santos. – 2022.
1 recurso online (133 f.: il., color.): pdf.

Orientador: Antônio Eduardo Clark Peres
Coorientador: Gilberto Rodrigues da Silva.

Tese (doutorado) - Universidade Federal de Minas Gerais, Escola de Engenharia.

Inclui bibliografia.
Exigências do sistema: Adobe Acrobat Reader.

1. Engenharia de minas - Teses. 2. Tecnologia mineral - Teses. 3. Apatita - Teses. 4. Carbonatos - Teses. I. Peres, Antonio Eduardo Clark. II. Silva, Gilberto Rodrigues da. III. Universidade Federal de Minas Gerais. Escola de Engenharia. IV. Título.

CDU: 622(043)

Ficha catalográfica elaborada pelo bibliotecário Reginaldo Cesar Vital dos Santos CRB-6/2165
Biblioteca Prof. Mário Werneck - Escola de Engenharia da UFMG

FOLHA DE APROVAÇÃO

UNIVERSIDADE FEDERAL DE MINAS GERAIS
ESCOLA DE ENGENHARIA
Programa de Pós-Graduação em Engenharia Metalúrgica, Materiais e de Minas

Tese intitulada **"Minérios Fosfáticos Ígneos com Ganga Carbonática: Estudos Fundamentais"**, área de concentração: Tecnologia Mineral, apresentada pelo candidato **Leandro Henrique Santos**, para obtenção do grau de Doutor em Engenharia Metalúrgica, Materiais e de Minas, aprovada pela comissão examinadora constituída pelos seguintes membros:

Antônio Eduardo Clark Peres
Orientador - PhD (UFMG)

Gilberto Rodrigues da Silva
Coorientador - PhD (UFMG)

Michelly dos Santos Oliveira
Drª (CEFET/MG/Araxá)

Andréia Bicalho Henriques
Drª (UFMG)

Carlos Alberto Pereira
Dr. (UFOP)

Fábio de São José
Dr. (CEFET/MG)

Coordenador do Programa de Pós-Graduação em Engenharia Metalúrgica, Materiais e de Minas/UFMG

Belo Horizonte, 24 de março de 2022

Dedicatória

A Deus, sempre presente na minha vida, à minha mãe, meu alicerce, à minha irmã e irmão (*in memoriam*) e à minha grande companheira Larissa. Dedico este trabalho.

AGRADECIMENTOS

À Universidade Federal de Minas Gerais, ao Departamento de Engenharia Metalúrgica e de Materiais, ao Departamento de Química e ao Programa de Pós-Graduação em Engenharia Metalúrgica, Materiais e de Minas (PPGEM-UFMG), pela infraestrutura disponibilizada para a realização deste trabalho.

À Coordenação de Aperfeiçoamento de Pessoal de Nível Superior (CAPES), ao Conselho Nacional de Desenvolvimento Cientifico e Tecnológico (CNPq), à Fundação de Amparo a Pesquisa do Estado de Minas Gerais (FAPEMIG) pelo auxílio financeiro.

Aos membros da banca de qualificação, professora Michelly dos Santos Oliveira e engenheiro Eliomar Ferreira, e da banca de defesa, professora Andréia Bicalho Henriques, professora Michelly dos Santos Oliveira, professor Carlos Alberto Pereira e professor Fábio de São José, pelas valiosas contribuições para o desenvolvimento e para o aprimoramento deste trabalho.

Aos professores Antônio Eduardo Clark Peres e Gilberto Rodrigues da Silva por todo apoio, ensinamentos e orientações, além de companheirismo e amizade, durante a execução do trabalho. Ainda, por serem parte fundamental da minha história e do meu crescimento, e pelo cuidado ao longo desses anos. Vocês são exemplos de profissionalismo, dedicação e excelência para mim.

Aos alunos Adriele Mércia Alves dos Santos, Augusto Henrique Lacerda Paiva, Guilherme Otávio dos Santos e Joyce Aparecida Silva pela parceria durante toda a atividade experimental do trabalho nos laboratórios de Química e Tratamento de Minérios do CEFET-MG (Unidade Araxá). Vocês foram fundamentais para a realização do trabalho. Ainda, à professora Tamiris Fonseca de Souza pelo apoio e amizade, pelos conselhos e toda a força que me deu durante todo esse período. Ao engenheiro e amigo João Victor da Silva Alves pela contribuição fundamental e pela disponibilidade em momentos essenciais. Ao Luciano Fernandes de Magalhães, por todo apoio durante o fechamento do trabalho.

A todos os professores do PPGEM-UFMG, pelos ensinamentos e pela dedicação. Em especial, ao professor Paulo Roberto Gomes Brandão, pelo privilégio da convivência e pelos preciosos ensinamentos. Também, à professora Andréia Bicalho Henriques, pelo

apoio durante a realização dos ensaios no Centro de Microscopia, além das orientações e conselhos.

Ao professor Carlos Alberto Pereira e todos os membros do laboratório de Flotação, por todo apoio e disponibilidade durante os ensaios realizados no DEMIN-UFOP.

À toda a equipe do CEFET-MG (Unidade Araxá), em especial aos parceiros do DMCAX, por me apoiarem durante o afastamento para me dedicar ao doutorado. Em especial, à professora e amiga Bruna Letícia dos Santos, por todo o apoio e parceria durante esse difícil período de concomitância entre Doutorado e Coordenação do Curso de Engenharia de Minas.

À Clariant e à Amazon Oil, por cederem as amostras de reagentes, fundamentais para a realização do trabalho.

À minha mãe, Marlene, por todo amor, criação, exemplo, preocupação, incentivo e por representar todo o sentido da minha vida.

À minha irmã, Patrícia (Nanda), pela compreensão e apoio, além dos momentos de descontração, mesmo com toda a sua seriedade.

Ao meu irmão, Luís, que esteve e estará sempre presente em minha vida, mesmo que seja “do andar de cima”.

À Larissa, pelo amor incondicional, companheirismo, paciência e dedicação, que foram essenciais para a conquista de mais um objetivo. Saber que sempre poderei contar com você faz de mim um homem mais forte para enfrentar todos os obstáculos do caminho. Este foi somente um dos muitos que vieram e virão.

Aos amigos Cláudio, Diogo e Felipe pelos tantos anos de amizade sincera e verdadeira, me fortalecendo para avançar cada dia mais em busca do sucesso.

Enfim, a todos que de alguma forma contribuíram, e que por ventura eu tenha esquecido, o meu eterno agradecimento.

RESUMO

A indústria mineral se reinventa a cada dia, em consonância com as crescentes demandas ambientais para redução de resíduos e substituição de insumos por alternativas ambientalmente sustentáveis. O fósforo é um recurso estratégico na segurança alimentar global e produção de biodiesel, obtido a partir de minérios fosfáticos, não renováveis. A sua complexidade, como associação a gangas silicatadas e carbonatadas, exige etapas de beneficiamento sofisticadas para atender à indústria de fertilizantes. Os óleos vegetais se apresentam como fonte de ácidos graxos, em proporções variadas, para a produção de coletores para a flotação. A ação sinérgica desses compostos presentes no coletor apresenta vantagens como redução no consumo de reagentes, melhor recuperação e teor, além de maior cobertura da superfície mineral e estabilidade da espuma. As fontes graxas de origem amazônica apresentam características como alta diponibilidade, baixo custo de extração, seletividade para alguns sistemas de flotação, além de proporcionar desenvolvimento para as comunidades locais. O presente estudo avaliou o desempenho dos óleos de Andiroba (*Carapas guianensi*) e Patauá (*Oenocarpus bataua*), e da gordura de Bacuri (*Platonia insiginis*), na flotação de apatita e carbonatos, presentes no minério fosfático. Inicialmente, foi realizada a caracterização dos minerais, amostras graxas e coletores. A proporção de saturação nos coletores, obtidos a partir da saponificação alcóolica a quente das amostras graxas, afetou a CMC e a adsorção destes, em relação aos coletores de ácidos graxos puros majoritários em sua composição. A CMC apresentou relação direta com a saturação das cadeias carbônicas do coletor. Em relação à adsorção, coletores majoritariamente saturados apresentaram melhor desempenho na hidrofobização da dolomita, já coletores com alta insaturação se mostraram eficientes na hidrofobização de apatita e calcita, ainda que de maneira distinta. O impacto positivo do tempo de condicionamento sobre hidrofobização das partículas corrobora com a hipótese de que esse fenômeno se dá através de quimissorção. Máxima seletividade foi alcançada a partir do coletor de Andiroba (20mg.L^{-1}) em pH 7,5 recuperando 90,2% de apatita, frente a 10,5% de calcita e 8,2% de dolomita. Por fim, os coletores a base de amostras graxas amazônicas se mostraram promissores na aplicação industrial para sistemas de flotação de fosfato.

Palavras-chave: *apatita, carbonatos, óleos amazônicos, novos coletores, sinergia.*

ABSTRACT

The mineral industry is reinventing itself every day, in line with growing environmental demands to reduce waste and replace inputs by environmentally sustainable alternatives. Phosphorus is a strategic resource for the global food security and biodiesel production, obtained from non-renewable phosphate ores. Its complexity, *i. e.*, association with silicate and carbonate ores, requires sophisticated beneficiation steps to supply the fertilizer industry. Vegetable oils are presented as a source of fatty acids, in varied proportions, for the production of collectors for phosphate flotation. The synergistic action of these compounds present in the collector can lead to advantages such as reduction in the consumption of reagents, better recovery and content, besides greater coverage of the mineral surface and stability of the foam. The grease sources of Amazonian origin present characteristics such as high availability, low extraction cost, selectivity for different flotation systems, besides providing development for the local communities. The present study evaluated the performance of Andiroba (*Carapas guianensi*) and Patauá (*Oenocarpus bataua*) oils, and Bacuri (*Platonia insiginis*) fat, in the flotation of apatite and carbonates, present in phosphate ore. Initially, the characterization of the minerals, grease samples and collectors was performed. The proportion of saturation in the collectors, obtained from the hot alcoholic saponification of the grease samples, affected the CMC and the adsorption process, in comparison to the collectors composed of pure fatty acids found in the oil samples. The CMC showed a direct relation with carbon chain saturation of collector. Regarding the adsorption process, mostly saturated collectors showed better performance in recovering dolomite, whereas collectors with high unsaturation were efficient in the collection of apatite and calcite. The positive impact of the conditioning time on particle recovery corroborates the hypothesis that this phenomenon occurs through chemisorption. Maximum selectivity was achieved with the Andiroba (20 mg.L-1) collector at pH 7.5 recovering 90.2% apatite, compared to 10.5% calcite and 8.2% dolomite. Finally, the Amazonian oil-based collectors based showed promising results for industrial application in phosphate flotation systems.

Keywords: *apatite, carbonates, Amazonian oils, novel collectors, synergy*

LISTA DE FIGURAS

LISTA DE TABELAS

LISTA DE Abreviaturas

AI	Acidity Index
AOC	Andiroba Oil Collector
AOCS	American Oil Chemist's Society
CACB	Complexo Alcalino-carbonatítico do Barreiro
CAD	Collector Adsorption Density
CG	Cromatografia Gasosa
CMC	Critical Micelle Concentration
DRX	Difratometria de Raios-X
FTIR	Fourier Transform Infrared Spectroscopy
ICDD	International Diffraction Data Center
II	Iodine Index
PCMC	Pré-critical Micelle Concentration
PDI	Potential Determining Ions
SI	Saponification Index
TOC	Total Organic Carbon
WDXRF	Wavelength Dispersive X-ray Fluorescence
XPS	X-ray Photoelectron Spectroscopy

SUMÁRIO

1. Introdução

1.1 Relevância da pesquisa

Fosfatos, juntamente com minerais portadores de nitrogênio e potássio, fazem parte do grupo classificado como agrominerais, os quais, como o nome sugere, são estratégicos para a agricultura. Eles são fundamentais na cadeia produtiva dos fertilizantes químicos NPK, cada vez mais relevantes no desenvolvimento da produção agrícola necessária para alimentar a crescente população mundial.

Os minerais da série das apatitas constituem os minerais-minério de fósforo, ocorrendo em depósitos sedimentares, ígneos e/ou biogenéticos, sendo o último de menor importância econômica. Mais de 90% do consumo mundial de minério fosfático se destina à indústria de fertilizantes, sendo o restante destinado a outros diversos usos. Não há, até o presente momento, substitutos para o minério fosfático como produto primário fornecedor de fósforo em larga escala para a agricultura, com viabilidade comprovada.

Desta forma, o Brasil, país de forte economia agropecuária, é extremamente dependente desse bem mineral para manutenção de sua posição destaque na economia agropecuária mundial. As reservas nacionais são majoritariamente de origem ígnea, as quais apresentam composição mais complexa. Além disso, a produção nacional de concentrado fosfático se apresenta pouco expressiva e o consumo de fertilizantes no Brasil demonstra crescimento superior à produção agrícola nas últimas décadas, motivada tanto pela intensificação do processo produtivo no campo, quanto pelo aumento recente da produção de biocombustíveis.

Os minérios fosfáticos apresentam como minerais de ganga silicatos e carbonatos, dentre outros, sendo submetidos ao beneficiamento via flotação para obtenção de concentrados dentro da especificação da indústria de fertilizantes. A separação da ganga carbonatada, principalmente calcita e dolomita, se mostra complexa devido às características similares entre estes e os minerais fosfatados, por se tratarem de minerais semi-solúveis. As suas características de superfície são semelhantes, prejudicando a seletividade na adsorção dos reagentes coletores durante a operação.

Atualmente, o mercado busca maior seletividade e menor custo dos coletores na flotação de apatita. Estudos avaliam técnicas de adsorção em superfície mineral em busca de

conhecimentos sobre o comportamento de potenciais coletores alternativos, confrontando o desempenho destes com o de ácidos graxos isolados, presentes em sua composição. O Brasil abriga uma das mais ricas variedades de espécies vegetais do mundo, sendo o sexto colocado em relação à biodiversidade. Os óleos e gorduras vegetais de fontes distintas, como andiroba, patauá e bacuri, de origem amazônica, se apresentam como sistemas constituídos por vários ácidos graxos em proporções variadas. Esses recursos apresentam alto potencial de aplicação na flotação, devido a sua ampla disponibilidade técnica e econômica. Os coletores obtidos a partir da saponificação desses óleos e gorduras podem apresentar ação sinérgica de seus diferentes ácidos, quando em proporção ideal, apresentando a vantagem da combinação das características individuais desses reagentes.

Diante disso, o presente trabalho aborda a caracterização de amostras graxas de origem amazônica, sendo estes os óleos de patauá e andiroba, e a gordura de bacuri, em relação ao perfil de ácidos graxos e propriedades físico-químicas. Ainda, o trabalho avalia a aplicação de seus respectivos sais sódicos como coletores na flotação de apatita, calcita e dolomita, por meio de ensaios de microflotação em tubo de Hallimond, buscando seletividade em relação à ganga carbonatada. Como parâmetro de comparação, é avaliado o desempenho desses coletores em relação aos ácidos graxos isolados (oleico e palmítico), majoritários na sua composição.

1.2 Objetivos

O objetivo geral deste trabalho consiste no estudo do desempenho de coletores alternativos na flotação aniônica direta da apatita, presente no minério fosfático de ganga carbonática, a partir de estudos fundamentais. Para tal, foram propostos os seguintes objetivos específicos:

i. caracterizar as amostras graxas (óleos de andiroba e patauá, e gordura de bacuri) empregados na produção dos coletores avaliados, através de técnicas de FTIR, CG, IA, IS e II;
ii. caracterizar as amostras de ácidos graxos puros (oleico e palmítico) através de técnicas de FTIR e CG;
iii. sintetizar coletores aniônicos a partir das amostras graxas e ácidos graxos puros avaliados, a partir da reação de saponificação alcoólica a quente com refluxo;
iv. caracterizar os coletores sintetizados através de técnica de FTIR e CMC;
v. caracterizar os minerais avaliados (apatita, calcita e dolomita) através de técnicas de DRX, WDXRF, FTIR e XPS;
vi. determinar o potencial zeta dos minerais avaliados (apatita, calcita e dolomita) através de ensaios de mobilidade eletroforética;
vii. caracterizar a adsorção dos coletores sintetizados sobre os minerais avaliados através de ensaios de FTIR e mobilidade eletroforética (potencial zeta).
viii. avaliar o efeito do tempo de condicionamento, pH do sistema e concentração dos coletores sintetizados sobre a flotabilidade dos minerais avaliados, através de ensaios de microflotação em tubo de Hallimond modificado;
ix. avaliar faixas e condições operacionais de seletividade no sistema apatita/carbonatos;
x. confrontar o desempenho dos coletores sintetizados a partir de amostras graxas com o dos ácidos graxos puros em relação à flotabilidade dos minerais avaliados;
xi. avaliar a relação entre o perfil de ácidos graxos, além da sinergia entre estes, nas amostras graxas amazônicas e seu desempenho sobre a flotabilidade dos minerais avaliados.

1.3 Estrutura da tese

A presente tese é dividida em cinco capítulos, que foram estruturados da seguinte forma: No capítulo 1, são apresentadas as justificativas para o desenvolvimento do projeto e seus objetivos. No capítulo 2, é realizada uma breve revisão da literatura referente aos fertilizantes fosfatados, minérios fosfáticos ígneos (peculiaridades e rotas de beneficiamento), seletividade nos sistemas de flotação apatita/carbonatos considerando as peculiaridades dos minerais semi-solúveis, além da sinergia de coletores em sistemas de flotação e as diferentes fontes de óleos vegetais, em especial, os de origem amazônica. Os capítulos 3 e 4 são constituídos pelos trabalhos submetidos para publicação durante a realização desta tese, na forma em que foram submetidos. Finalmente, no capítulo 5, são apresentadas as considerações finais, incluindo as principais conclusões, que integram os resultados dos trabalhos publicados, e as sugestões para trabalhos futuros.

2. Revisão Bibliográfica

Neste capítulo serão abordados tópicos importantes para o presente trabalho com foco no conhecimento de assuntos relevantes para o desenvolvimento do mesmo. Dentre esses, são abordados temas como fertilizantes fosfatados, minério fosfático e seu beneficiamento, solubilidade e flotabilidade de minerais semi-solúveis, seletividade no sistema apatita-carbonatos, coletores de apatita e sinergia de reagentes em sistemas de flotação, além de óleos vegetais amazônicos, entre outros pontos relevantes.

2.1 Fertilizantes Fosfatados

A indústria mineral se reinventa a cada dia na busca por processos menos poluidores e mais sustentáveis, em consonância com as crescentes demandas ambientais. Dentre as ações envolvidas na reestruturação do setor estão a menor geração de resíduos e a substituição de insumos por alternativas ambientalmente sustentáveis [1]. A indústria do fosfato se enquadra nesse cenário, já que o fósforo, recurso essencial na produção de fertilizantes para a agricultura é obtido a partir de minérios fosfáticos, sendo estes recursos não renováveis [2, 3].

Agrominerais correspondem ao grupo de minerais estratégicos e importantes para a agricultura, englobando representantes como os portadores de fosfato, enxofre e potássio. O elemento fósforo (P) [4, 5], juntamente com o Nitrogênio (N) [6-8] e o Potássio (K) [9, 10], compõem o grupo dos principais macronutrientes vegetais (NPK), essenciais para toda a vida na Terra [2, 11, 12].

A apatita, de fórmula química $Ca_{10}(PO_4)_6(OH,Cl,F)_2$, apresentada na Figura 2.1, é o principal mineral portador de fósforo, apresentando estrutura complexa, com possíveis substituições iônicas na sua composição, com variações como a fluorapatita, cloroapatita e hidroxiapatita.

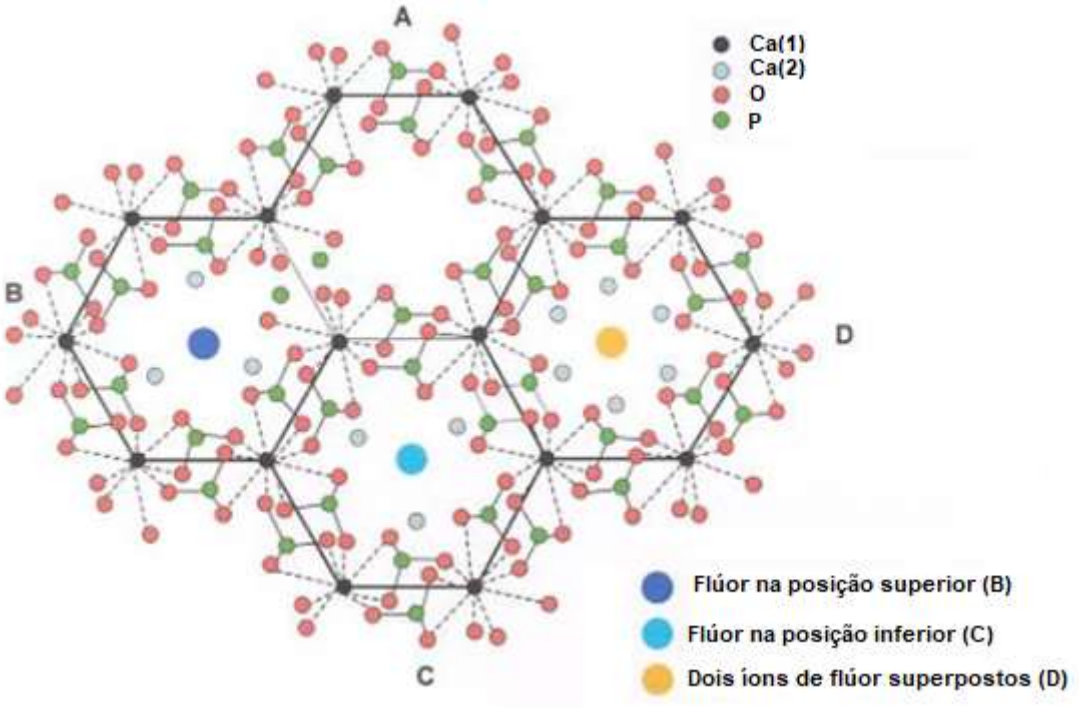

Figura 2.1 - Estrutura cristalina das apatitas [13]

O minério fosfático, contendo o mineral-minério apatita, é a fonte majoritária de P para indústria de fertilizantes e outros produtos, como ácido fosfórico e gesso [3, 14-17]. Esse recurso vem ganhando destaque diante da crescente demanda do setor agrícola, fundamental para a segurança alimentar global, diante do crescimento da população mundial, com uma demanda alimentar exponencial [18-21]. Adicionalmente, considera-se o aumento da produção de biodiesel como potencializador dessa demanda [22-26]. Cerca de 90% do consumo mundial de minério fosfático se destina à indústria de fertilizantes, e o restante direcionado, principalmente, para a indústria química e nutrição animal [27].

O Brasil se destaca pelas condições favoráveis ao setor agrícola e importância no desenvolvimento do agronegócio. O país apresenta clima diversificado, chuvas regulares, energia solar abundante e extenso território disponível para plantio, além de 13% de toda a água doce mundial. Apesar disso, por estar localizado na faixa intertropical, apresenta clima úmido, solos ácidos e mineralmente pobres em relação aos nutrientes principais, demandando emprego maciço de fertilizantes para reposição e manutenção das quantidades dos elementos vitais retirados do solo pelos processos de

intemperismo no decorrer dos anos [28].

No contexto brasileiro, os minérios portadores de fósforo são insuficientes, apresentando disponibilidade primária de recursos minerais que atende a um horizonte de menos de 25 anos e consumo interno extremamente dependente das importações, apresentando elevada dependência internacional. Logo, o país se mostra extremamente vulnerável em relação à este bem mineral para a manutenção de sua posição de destaque no setor de agronegócio mundial.

2.2 Minério Fosfático

Os depósitos de minério fosfático se diferem quanto à gênese, sendo os sedimentares os mais expressivos no cenário mundial [29-31], avaliados também em trabalhos científicos na área de concentração de minérios [32, 33]. Depósitos de origem ígnea são maioria no Brasil, apresentando mineralogia mais complexa [34], baixo teor de P_2O_5, associados a gangas silicatada e carbonatada [35]. Fosfatos de origem biogenética não apresentam relevância econômica devido à pequena quantidade encontrada na crosta terrestre [14].

O Marrocos se destaca como o principal produtor e exportador mundial de insumos fosfatados, com cerca de 30% das reservas mundiais, o que justifica sua baixa dependência externa [36]. A China apresentou produção de 120 milhões de toneladas de concentrado fosfático no ano de 2017, um aumento de 0,6% em relação ao ano anterior [37].

Apesar dos recentes avanços da tecnologia mineral, os depósitos de minério fosfático vêem sofrendo com a escassez de depósitos mais acessíveis e de alta qualidade, impondo restrições técnicas e econômicas de aproveitamento a longo prazo [38, 39]. Inclusive, durante sua aplicação, a eficiência de fertilizantes vem se mostrando baixa, contribuindo para o aumento da demanda [40, 41]. Logo, torna-se essencial a pesquisa e desenvolvimento, aplicando estratégias como *scientific research* [42], fontes alternativas de P [43-46], economia circular [47-53] e *text-mining* [36, 54, 55].

Dentre os depósitos fosfáticos brasileiros, o Complexo Alcalino-carbonatítico do Barreiro (CACB), situado a aproximadamente 6km ao sul da cidade de Araxá-MG, contempla um dos vinte complexos desse tipo no país, com 15km^2 [56]. O Complexo se

apresenta metassomatizado, sendo o metamorfismo restrito às mediações de um corpo intrusivo, causado pela ação de fluidos e gases, sendo formado por flogopititos cortados por veios carbonatíticos e veios de apatitito. O CACB se mostra coberto por um espesso manto de intemperismo, com espessura de até 230 metros. É composto por carbonatitos, foscoritos e um grande volume de flogopititos derivados do metassomatismo de rochas ultramáficas como bebedouritos e dunitos [57]. As formações são concêntricas e a ocorrência dos foscoritos é observada na parte central do domo, apresentando granulação fina e grossa (Figura 2.2). Entre a zona central, rica em carbonatitos e o anel de quartzitos, foi descrito uma auréola com predomínio de rochas silicáticas cortadas por diques de carbonatito. Estas rochas são constituídas por flogopita com quantidades menores de dolomita, magnetita e apatita [58].

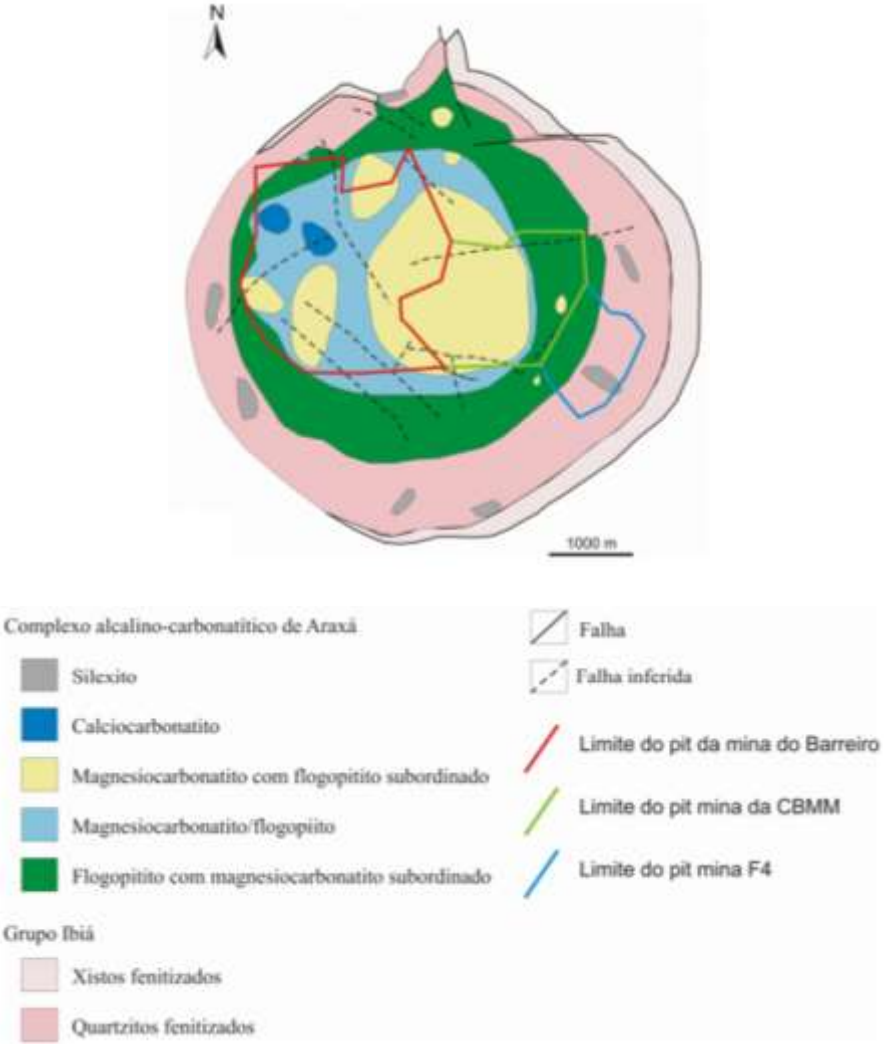

Figura 2.2 - Mapa geológico do Complexo de Araxá [57].

No Complexo, são observadas ocorrências de fosfato e pirocloro, integrando a Província Alcalina do Alto Paranaíba [59], registrando a produção de 20.000 toneladas de concentrado fosfático, em 2018 [60]. Alguns estudos foram realizados avaliando o minério proveniente do Complexo e sua rota de beneficiamento mineral [61-63].

2.3 Beneficiamento de Minério Fosfático

A aplicação direta de rochas contendo macronutrientes (*i.e.* NPK) como fertilizantes é desfavorecida pela baixa taxa de intemperismo, inviabilizando a biodisponibilidade desses nutrientes para as plantas [64]. Carbonatitos são exemplos de rochas ígneas compostas principalmente de minerais carbonatados com taxa de intemperismo relativamente alta e geralmente contendo minerais acessórios com macronutrientes (*i.e.* apatita e biotita) [65]. Entretanto, para a grande maioria dos tipos de rocha fosfática, o beneficiamento mineral é fundamental para fornecer o concentrado fosfático, matéria-prima base para produção de ácido fosfórico e fertilizantes fosfatados [66-75].

A complexidade dos minérios fosfáticos, como associação a gangas silicatadas e carbonatadas, exige etapas de beneficiamento sofisticadas para atender às especificações da indústria de fertilizantes [34, 76, 77]. Os critérios de qualidade definidos levam em consideração os principais minerais de ganga que afetam negativamente o processo produtivo. Dentre esses, podem ser destacados calcita, dolomita, óxidos de ferro, alumínio e magnésio, além de silicatos e cloretos, sendo os carbonatos os mais prejudiciais, devido ao impacto expressivo na operação e custo de produção do ácido fosfórico [78]. A presença de minerais carbonatados no concentrado fosfático proporciona elevação no consumo de ácido sulfúrico (H_2SO_4) empregado na solubilização. Entre os carbonatos, a dolomita se apresenta como a impureza de maior impacto negativo no processo, devido à presença do magnésio em sua composição. Esse metal alcalino-terroso afeta a taxa de filtração e capacidade do equipamento, além de aumentar a viscosidade do ácido superfosfórico e reduzir a quantidade de P_2O_5 solúvel durante a acidulação [79].

O processamento de minérios fosfáticos ígneos envolve etapas de fragmentação, separação por tamanho, concentração e, eventualmente, métodos químicos e térmicos,

principalmente em áreas com disponibilidade de energia a baixo custo e limitação de recursos hídricos [77, 80]. Alguns métodos alternativos podem ser empregados na concentração de minério fosfático, inclusive a separação magnética [81] e biolixiviação [82, 83]. Entretanto, desde 1920, a operação de concentração majoritariamente aplicada corresponde à flotação em espuma [84]. A técnica é utilizada para separar partículas minerais contidas no minério, sob a forma de polpa, com base nas suas diferentes propriedades de superficie. Para tal, explora o fenômeno de partículas hidrofóbicas se aderirem às bolhas de ar em fluxo ascendente, devido ao empuxo, sendo carreadas até a interface polpa-espuma (flotado). Enquanto isso, partículas hidrofílicas permanecem na fase líquida (afundado) [74, 85-89].

A flotação em espuma é amplamente aplicada em rotas de concentração de minério fosfático. No caso dos minérios fosfáticos brasileiros, as apatitas ígneas, com baixa área superficial, apresentam maior solubilidade e flotabilidade em condições ácidas, evidenciando a precipitação superficial como mecanismo de adsorção do coletor [90-93]. A rota clássica de beneficiamento de minério fosfático ígneo engloba operações de britagem e moagem, podendo ser incluídas etapas de lavagem, deslamagem e separação magnética, em função da ganga presente, via flotação aniônica direta. Ela envolve a aplicação de sais de ácidos graxos (*i.e.* oleato) como coletores de apatita e amido gelatinizado para a depressão de ganga carbonatada e óxidos de ferro, em pH alcalino. Geralmente é empregado estágio *rougher*, sendo o rejeito desta etapa direcionado para estágios *scavenger*. O concentrado fosfático da etapa inicial segue para estágios duplos ou triplos de etapa de limpeza (*cleaner*) [34, 62, 66, 94-99]. Alternativamente, podem ser empregados outros depressores de ganga como o silicato de sódio, atuando sobre os carbonatos [100, 101]. O processamento de minérios fosfáticos pode ser realizado, ainda, por rotas envolvendo flotação cariônica reversa, empregando aminas como coletor de silicatos em pH levemente básico [102, 103], e flotação aniônica reversa, com a depressão da apatita realizada por íons fosfato, sulfato e oxalato provenientes de seus respectivos ácidos e sais solúveis, em pH levemente ácido [104-106].

O Processo Crago, outra rota desenvolvida para concentração de minério fosfático, se baseia em uma mescla entre flotação aniônica direta e catiônica reversa [77, 107-109]. O desenvolvimento da rota conhecida como Processo Crago Inverso, contempla uma sequência de flotação contrária à convencional, iniciando com a flotação catiônica

reversa, seguida da aniônica direta. Assim, inicialmente são flotadas areias finas de quartzo e silicatos, empregando dosagem mínima de aminas. A rota foi desenvolvida pelo Instituto de Pesquisa de Fosfato da Flórida (*Florida Institute of Phosphate Research* – FIPR), motivado pelo comportamento do quartzo durante a rota Crago convencional [93]. O Projeto Serrana é um marco na história da tecnologia mineral brasileira para o beneficiamento de minérios fosfatados de origem ígnea, sendo desenvolvido entre 1960 e 1962 a partir do minério rico em ganga carbonatada, principalmente calcítica, da mina de Cajati/SP [99].

Apatitas amorfas podem demandar concentrações de oleato até dez vezes maiores em relação à apatita cristalina, devido às caraterísticas distintas na estrutura cristalina das partículas, principalmente nas bordas, onde ocorre a adsorção do reagente, demandando maior tempo de condicionamento com os reagentes, além de alta solubilidade, acarretando menor estabilidade na interação com o coletor [34, 100, 102].

A granulometria das partículas está diretamente ligada à sua área superficial. Esta característica pode influenciar o desempenho na flotação de fosfato sob duas vertentes. Uma delas afirma que partículas de granulometria mais fina demandam maior quantidade de reagentes para serem recobertas, aumentando o custo da operação. A segunda vertente afirma que o carboxilato pode interagir com íons cálcio no *bulk* da polpa e precipitar sob a forma de carboxilato de cálcio. Assim, altas concentrações deste íon bivalente na solução, potencializados pela elevada taxa de dissolução das partículas mais finas, pode acarretar a insuficiência ou até o esgotamento do coletor para a adsorção nas partículas minerais e, consequentemente, sua coleta, prejudicando o desempenho da flotação [32, 93, 110].

A adsorção de surfactantes na superfície de partículas minerais em polpa é determinante no controle de vários processos industriais como flotação [111-115], floculação/dispersão [116-121], dentre outros (*i.e.* farmacêuticos [122], ambientais [123]). No campo do processamento mineral, as interações energeticamente efetivas entre as fases adsorvente (mineral) e adsorvida (surfactante) são afetadas pelas propriedades superficiais das partículas, do coletor e da fase líquida do sistema [124]. A adsorção pode ser estabelecida através de atração eletrostática, ligações covalente ou de hidrogênio, além de interações não polares, em função das características químicas da solução e da superfície mineral [124]. Quando a adsorção ocorre entre a porção polar do

coletor e superfície mineral (*head on*), a hidrofobização das partículas é favorecida, resultando em sua maior recuperação na espuma. Entretanto, quando ocorre a interação inversa (*head out*), a porção polar do surfatante se volta para a fase líquida, causando a reversão da hidrofobicidade da partícula, prejudicando sua adesão à bolha e, consequentemente, sua recuperação na espuma. Esse cenário é típico quando são empregadas sobredosagens de surfactantes no sistema [125].

Compreender o mecanismo de adsorção do coletor na superfície dos diversos minerais presentes em um sistema de flotação é essencial para controlar a seletividade da separação [126]. Vários estudos avaliaram o mecanismo de adsorção do oleato na superfíce das partículas de minerais do tipo óxido, principalmente os portadores de cálcio (Ca) [127-129], incluindo os minerais envolvidos no presente estudo (apatita [130-135], calcita [136-138] e dolomita [139-141]).

Os ácidos graxos e seus respectivos sais, provenientes da sua neutralização com bases inorgânicas, são amplamente utilizados como coletores na flotação [90, 91, 142-146]. Estes são compostos por cadeia hidrocarbônica extensa e grupo carboxila (COOH), sendo caracterizados pelo tamanho da cadeia, além de número e posição das insaturações, características que determinam diferenças nas suas propriedades químicas e físicas [96, 147]. O ácido oleico é o coletor mais comum e tradicionalmente usado para flotação de apatita [148], dentre outros minerais, apresentando sensibilidade a granulometria [149], temperatura [150] e presença de íons na polpa [130]. A especiação do ácido oleico/oleato (sal respectivo) e suas variações ocorre em função da concentração e do pH, influenciando a natureza e estrutura da camada superficial adsorvida em superfícies minerais [151] e na formação da espuma [152].

A interação entre coletores e o mineral apatita envolve a adsorção química do reagente e sítios metálicos presentes na superfície do mineral, através da precipitação de um sal proveniente da reação química entre estes. Em sistemas contendo apatita e carbonatos, a seletividade fica comprometida, uma vez que o mecanismo de adsorção do coletor sobre os minerais se apresenta similar, a partir de sítios ativos semelhantes, prejudicando o desempenho da operação.

2.4 Seletividade no sistema apatita-carbonatos

Dentre os minerais de ganga presentes no minério fosfático, destacam-se os silicatos e carbonatos. Este último, quando em grande proporção no minério, proporciona enormes desafios, principalmente pelas propriedades minerais superficiais semelhantes entre eles e o mineral-minério [76, 153]. Como o mineral-minério (apatita) e a ganga carbonatada (calcita e dolomita) são minerais portadores de Ca, a seletividade do processo fica comprometida. Isso porque os sais de ácidos graxos, principalmente o oleato, se adsorvem através dos sítios desse cátion metálico na superfície dos minerais [100]. A literatura científica demonstra que a adsorção deste surfactante ocorre de maneira distinta na superfície dos minerais calcita (monocamada) e apatita (bicamada) [100, 154]. Essa peculiaridade afeta, inclusive, a dosagem necessária de coletor para atingir a máxima flotabilidade. Para a apatita, essa dosagem se apresenta menor, sendo sensível ao emprego de altas dosagens [101, 131, 155]. Além disso, a cinética de adsorção do oleato sobre a apatita é mais rápida em relação calcita, mesmo ambas seguindo o modelo de primeira ordem para a cinética de formação da primeira camada [156]. Ainda, a interação interfacial ocorre via quimissorção, através da adsorção imediata do dioleato de cálcio na superfície do mineral, formado entre os íons Ca^{2+} liberados pela solubilização parcial dos minerais e os íons oleato presentes na solução. Assim, a solubilidade parcial do mineral apresenta correlação com a sua hidrofobização pelo coletor e, logo, sua flotabilidade [130]. Outros trabalhos corroboram com essa proposição, uma vez que tanto o oleato [157] quanto a superfície dos minerais apatita e calcita [100] se apresentam negativas no pH investigado (alcalino).

Os carbonatos compõem o grupo dos minerais classificados como semi-solúveis, juntamente com os fosfatos. Estes minerais de ganga podem ocorrer tanto como pequenas inclusões ou veios, quanto na forma de grãos livres [17]. A solubilidade dos minerais semi-solúveis corresponde a um parâmetro de grande relevância quando se trata do processamento mineral via flotação. Esse grupo de minerais é caracterizado pela considerável solubilidade, superior a da maioria dos minerais constituídos por óxidos e silicatos e inferior a dos minerais altamente solúveis, como halita e silvita. Vários estudos avaliaram o efeito da solubilidade dos minerais sobre outros sistemas de flotação contendo limonita [158], malaquita [159], espodumênio [160], bastenasita [161], smithsonita [162], schellita [162, 163], powellita [164] e apatitas primárias e

secundárias [165].

Em contato com a água, esses minerais entram em processo de dissolução, dependendo das condições do sistema, como força iônica, temperatura, pH e a presença de outras espécies químicas na solução [166]. O comportamento da fluorapatita em meio aquoso, em função do pH do sistema, segue apresentada na Figura 2.3. A solubilidade deste mineral apresenta relação inversa com o pH do sistema, em meio ácido. Na faixa de pH entre 7 e 11, a solubilidade do mineral independe do pH do meio. Em meio fortemente alcalino, a solubilidade se mostra diretamente proporcional ao pH do sistema. A solubilização parcial desses minerais e as características químicas do sistema mineral-solução determinam a composição química da fase aquosa e a carga da superfície das partículas minerais presentes na polpa. No caso da apatita, o tipo de cálcio solúvel ou espécie de fósforo predominante dependem das condições da solução e do seu domínio de estabilidade.

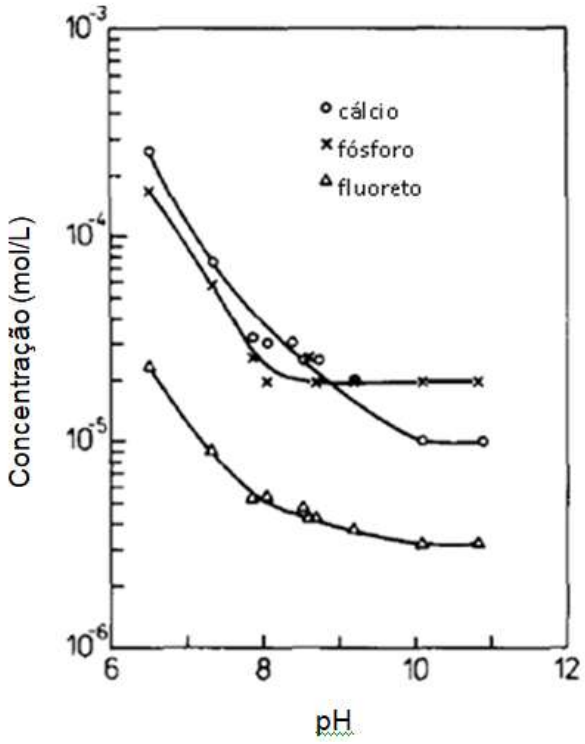

Figura 2.3 - Solubilidade da apatita em função do pH.

Fonte: HANUMANTHA RAO *et al.* (1990), adaptado [167]

Os mecanismos relacionados à ação dos reagentes de flotação na superfície dos minerais estão diretamente ligados ao potencial de superfície destes. No caso da apatita, calcita e dolomita, a carga superficial é controlada pela dissolução não estequiométrica das espécies químicas que fazem parte da sua estrutura cristalina. Desta maneira, os íons liberados são submetidos a reações adicionais, acarretando a readsorção das espécies formadas na superfície do mineral, afetando diretamente na etapa de desenvolvimento de cargas superficiais. Essas reações podem ser do tipo hidrólise, complexação, adsorção e precipitação *bulk* ou superficial. Logo, a eficiência da flotação de minérios fosfáticos contendo esses minerais sofre influência do balanço eletrostático ocasionado pelas reações adicionais que os íons provenientes da solubilidade parcial destes minerais estabelecem com as espécies presentes na polpa [131, 167, 168].

O equilíbrio químico do sistema mineral-solução sofre influência das modificações na estrutura cristalina do sólido, presença de impurezas, bem como adição de eletrólitos. O emprego de eletrólitos contendo íons comuns à composição química dos minerais presentes no sistema reduz a solubilidade destes quando comparado ao cenário onde eram empregados eletrólitos denominados indiferentes. Considerando a solubilidade em água pura, à mesma temperatura, a calcita se apresenta mais solúvel que a apatita em toda a faixa de pH avaliada, sendo que ambas apresentam relação inversa entre solubilidade e pH do sistema (Figura 2.4). Considerando a possibilidade de coexistência destes minerais no minério fosfático com ganga carbonática e, consequentemente, na polpa de flotação, torna-se necessário avaliar o comportamento destes quando condicionados em polpa contendo íons constituintes da rede cristalina do outro (sobrenadante). A concentração total de íons cálcio presente na polpa contendo apatita e calcita depende da solubilidade do carbonato nas condições do sistema, devido à sua maior solubilidade, se comportando como principal fonte deste cátion ao sistema [166].

Considerando o sistema composto por calcita condicionada em sobrenadante de apatita, pode ser observada uma redução na sua solubilidade em toda a faixa de pH avaliada, sendo essa queda mais expressiva em condições mais alcalinas (Figura 2.4).

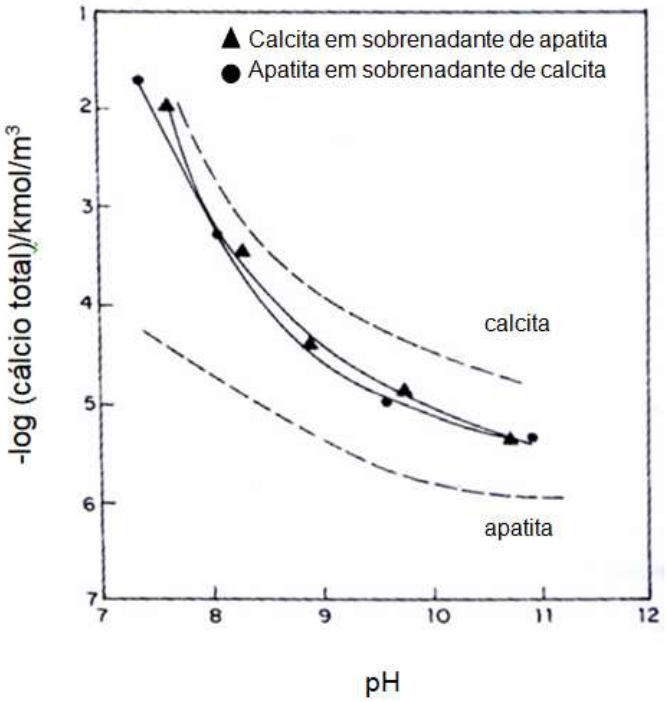

Figura 2.4 - Solubilidade de apatita e calcita em água (linha tracejada) e em soluções sobrenadantes (linha cheia), considerando [KNO_3] = $2x10^{-3}$ kmol/m^3.

Fonte: OFORI AMANKONAH *et al.* (1985) [166] adaptado

Como o sobrenadante apresenta o íon fosfato (PO_4^{3-}) como principal ânion, proveniente da dissolução da apatita, a redução pode ser atribuída ao efeito da presença desta espécie química, que torna a calcita mais estável nestas condições, quando proporciona a precipitação de apatita sobre a superfície desta. Logo, caso apatita seja condicionada em sobrenadante de calcita, a precipitação deste mineral na superfície da apatita será favorecida, aumentando sua solubilidade e alterando suas características de superfície, como apresentado na Figura 2.5 [168].

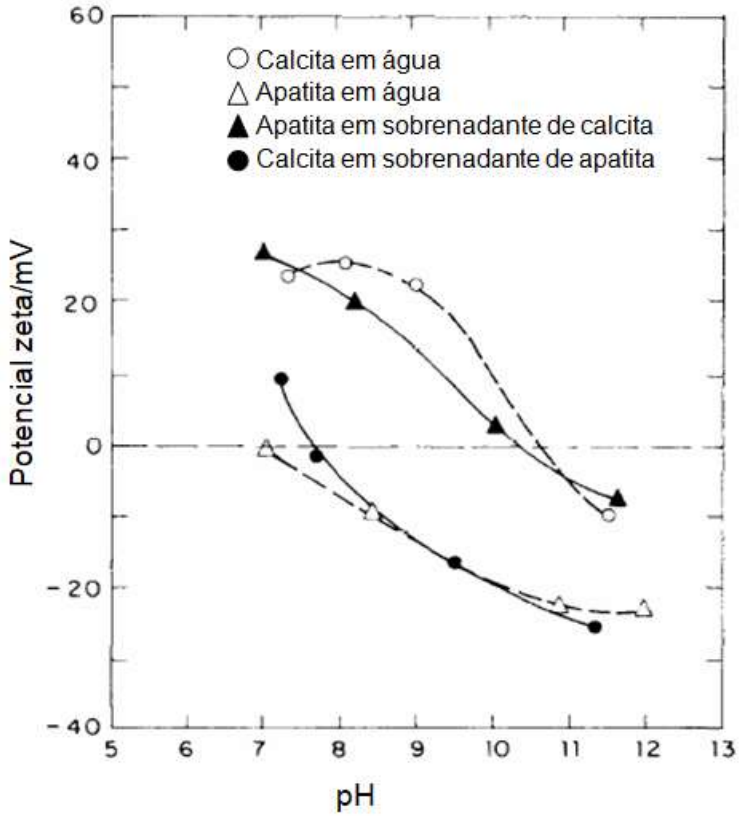

Figura 2.5 - Efeito do sobrenadante no PIE da calcita e apatita, considerando [KNO_3]= $2x10^{-3}$ kmol/m^3.

Fonte: SOMASUNDARAN e OFORI AMANKONAH (1985) [168] adaptado

Esse equilíbrio químico é representado na equação (2.1) e evidenciado pela sobreposição das respectivas curvas de solubilidade e potencial zeta, demonstrando a semelhança das características superficiais destes minerais quando coexistem na polpa, sendo este o grande desafio do processamento de minério fosfático com ganga carbonatada [79, 166, 169].

$$Ca_{10}(PO)_6(OH)_{2(s)} + 10CO_3^{2-} \leftrightarrow 10CaCO_{3(s)} + 6PO_4^{3-} + 2OH^- \quad (2.1)$$

Para os sistemas calcita/dolomita e apatita/dolomita o pH de transição entre as espécies correspondem a 8,2 e 8,8, respectivamente, sendo a dolomita a espécie mais estável em valores elevados de pH. Considerando o sistema calcita/apatita/dolomita, para pH abaixo de 8,8 a apatita se apresenta como a espécie mais estável, apresentando menor

solubilidade (Figura 2.6). A partir daí, a dolomita adquire maior estabilidade, determinando as características químicas do sistema. Em toda a faixa de pH a calcita não se apresenta como a espécie menos solúvel dentre as representadas [168].

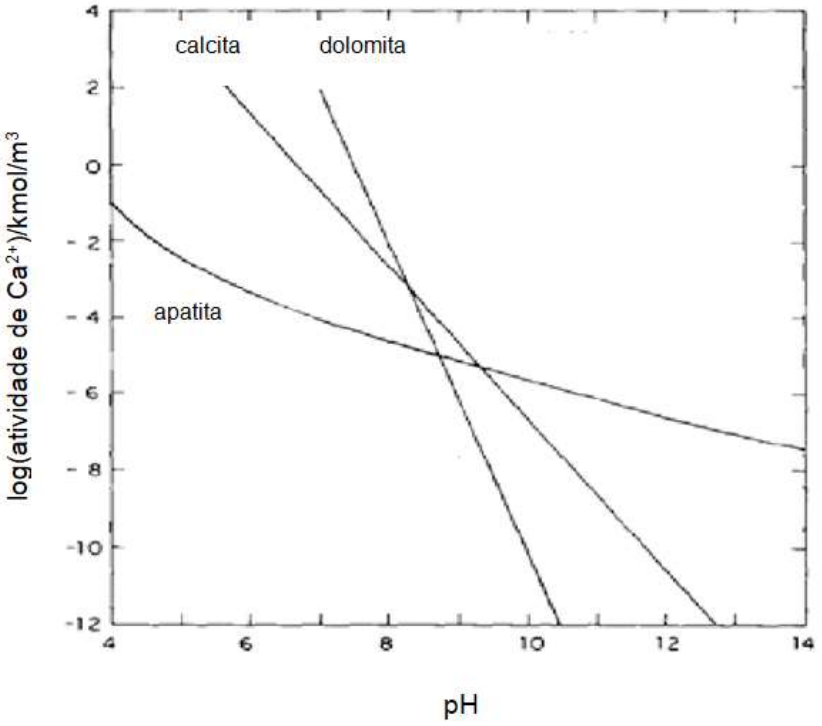

Figura 2.6 - Relações de estabilidade no sistema calcita/apatita/dolomita a 25ºC, $[Mg^{2+}]=5x10^{-4}$ kmol/m^3 considerando o sistema aberto para a atmosfera.

Fonte: SOMASUNDARAN *et al.* (1985) [168]adaptado

Na busca por seletividade na separação entre o mineral-minério e os carbonatos, várias estratégias foram empregadas como uso de depressores de calcita [100, 170-173], dolomita [174, 175] ou apatita [176], inclusive empregando microorganismos [177], além de rotas estagiadas de flotação [178], desenvolvimento/aplicação de novos reagentes [98, 179-189] e métodos, como calcinação [190] e flotação reativa [191]. A presença de íons Fe nas apatitas primárias proporciona a estas potencial zeta semelhante ao da hematita, enquanto os íons Ca e Mg no sistema adicionam cargas superficiais positivas nas apatitas e nos minerais de ganga, em pH 10,5 em função da adsorção específica dos hidroxicomplexos formados [98]. O comportamento químico da calcita

quando condicionada em solução de ácido fosfórico, típico depressor de apatita, evidencia a formação de fosfato de cálcio na superfície do mineral em determinadas condições de concentração do ácido, pH e tempo de condicionamento, indicando um cenário de perda de seletividade no sistema de flotação direta de apatita contendo calcita como ganga carbonatada [192]. Flotação de minério fosfático de ganga carbonatada foi objeto de vários estudos científicos [68, 76, 101, 106, 110, 174, 178, 193-198].

A acidez do sistema promove a interação entre os íons H^+ e os carbonatos contidos na estrutura cristalina dos minerais de ganga, proporcionando a dissolução contínua da superfície mineral destes, removendo contaminantes e criando novos sítios de adsorção do coletor aniônico. Essa reação entre o ácido e o carbonato produz micro bolhas de gás carbônico (CO_2) na superfície dos minerais de ganga, reduzindo a interação desta com as moléculas de água, através de ligações de hidrogênio. Logo, a cinética de adsorção do coletor é favorecida, potencializando a flotabilidade dos carbonatos [106, 199].

A presença de cátions na fase líquida do sistema provenientes da água de processo [200] ou da solubilização parcial dos minerais [201], afeta a dinâmica da flotação, sendo inevitáveis no processo [202]. Caso a taxa de liberação e difusão do cátion através das camadas limite for maior que a difusão do coletor até a superfície mineral, a interação dos cátions e coletores ocorrerá no seio da solução, resultando em precipitação do composto formado entre eles e o aumento do consumo do coletor. Caso contrário, a precipitação do oleato de cátion ocorrendo na superfície da partícula mineral, ocasiona o aumento da sua hidrofobicidade, sem a perda do coletor por precipitação na polpa [203]. Logo, é importante minimizar a dissolução do próprio mineral ou imobilizar os íons gerados na fase líquida, amenizando seu impacto deletério. O efeito dos íons na fase líquida também foi investigado sobre a dispersão de partículas finas em polpa, demonstrando que altas valências prejudicam o fenômeno uma vez que, via medidas de potencial zeta e aplicação da teoria da DLVO extendida, observa-se que a estabilidade da dispersão depende da repulsão eletrostática e da repulsão de hidratação [203].

Apatitas ígneas, com baixa área superficial são mais solúveis para valores de pH mais baixos, apresentando maior flotabilidade [93]. Isso evidencia a teoria de precipitação superficial durante a adsorção do oleato, uma vez que as condições que favorecem a solubilidade do mineral, proporcional a liberação mais pronunciada de íons Ca^{2+} próximo à partícula [92].

2.5 Coletores no sistema de flotação de minério fosfático

Diante dos altos custos dos ácidos graxos puros, a indústria de fosfato emprega óleos vegetais (misturas complexas de ácidos graxos) como coletores, devido ao seu baixo custo e alta eficiência em temperatura ambiente [66]. Os ácidos graxos mais comuns em óleos e gorduras comestíveis apresentam cadeia carbônica contendo 16 a 18 átomos, sendo os ácidos palmítico (C16:0), oleico (C18:1) e linoleico (C18:2) responsáveis por aproximadamente 80% da composição de óleos e gorduras [148, 204]. O ácido oleico e seu sal (oleato) apresentam bom desempenho na função de coletor, sendo que ambos apresentam cadeia carbônica insaturada constituída por uma ligação dupla entre os carbonos. Diante disso, geralmente torna-se necessária a realização da hidrogenação parcial prévia dos ácidos graxos poli-insaturados, diminuindo o número de insaturações nas suas respectivas cadeias carbônicas. Assim, é possível elevar o teor de ácido oleico na mistura de ácidos graxos empregados [96].

Existem estudos empregando óleos de origem animal [205] e reuso [206-209] na flotação. No passado, o *tall oil*, subproduto da industria de papel, foi amplamente utilizado na rota, mas devido ao aumento da demanda do insumo, afetando seu custo e disponibilidade, este foi substituído recentemente por fontes vegetais alternativas [79, 210, 211]. O seu emprego e o do óleo vegetal, como coletores de apatita, foram avaliados, demonstrando melhor desempenho para o primeiro [212].

O Brasil abriga uma das variedades mais ricas de espécies vegetais do mundo, sendo o sexto colocado em relação à biodiversidade [213], sendo que apenas uma fração desse potencial é conhecida e utilizada adequadamente, tanto do ponto de vista alimentício [214], quanto tecnológico [215] e ambiental [216]. Os óleos vegetais são ricos em ácidos graxos, sendo objeto de vários estudos sobre seu potencial como agentes coletores, devido a sua alta disponibilidade técnica e econômica.

No cenário brasileiro, óleos de milho (*Zea mays*), soja (*Glycine max*) e farelo de arroz (*Oryza sativa*), apresentam resultados satisfatórios como coletores na flotação de apatita [217]. Óleos de arroz, soja e linhaça (*Linum usitatissimum*) foram avaliados, demonstrando o bom desempenho do óleo com grande proporção de ácido linoleico (soja) em pH básico [95]. Óleo de jojoba (*Simmondsia chinensis*) demonstrou ser capaz de hidrofobizar a calcita em pH 6,5 em concentração de 200mgL^{-1}, enquanto a apatita permaneceu hidrofílica, mesmo na ausência de depressores [218], enquanto o óleo de

coco (*Cocos nucifera*) foi avaliado para minério com ganga silico-carbonatada do mesmo depósito, fornecendo um concentrado com 30,5% P_2O_5 e 80,8% de recuperação para o circuito *rougher-cleaner* [196]. Óleo de pequi amarelo (*Caryocar brasiliense*) apresentou resultados similares ao coletor empregado industrialmente (FLOTIGAM 5806) na microflotação de apatita, atingindo recuperação superior a 95% [219]. Óleo de farelo de arroz foi avaliado na flotação em coluna com rejeitos de minério fosfático, fornecendo teor de 29,4% P_2O_5 no concentrado final com 46,2% de recuperação, quando associado ao coletor aniônico sintético do tipo sulfosuccinato [63]. Todos estes óleos avaliados se apresentam como mistura de ácidos graxos, caracterizada pelo seu perfil graxo, podendo experimentar o efeito sinérgico destes ácidos graxos variados no mesmo sistema de flotação.

2.6 Sinergia entre reagentes no sistema de flotação

A ação sinérgica de coletores em um sistema de flotação, quando empregados em proporção ideal, apresenta a vantagem da combinação das características individuais desses reagentes, atendendo a vários requisitos do sistema [220]. Essa sinergia pode promover a redução no consumo de reagentes com recuperações e teores semelhantes e/ou proporcionar melhores resultados para o mesmo consumo. Os principais mecanismos propostos para a interação entre os coletores são maior cobertura da superfície mineral, interação entre os coletores na polpa ou na superfície mineral e alteração das características da espuma, aumentando sua estabilidade [221]. Os sistemas de coletores mistos podem ser classificados, de acordo com a natureza dos reagentes, como aniônico-catiônico, aniônico-não iônico e catiônico-não iônico [222]. O desempenho desses sistemas depende do tipo de interação coletor-partícula (eletrostática, ligação de hidrogênio ou adsorção química), estruturas dos coletores e proporção entre os reagentes [223].

O emprego simultâneo de mais de um tipo de coletor no mesmo sistema de flotação foi amplamente avaliado em diversos trabalhos, sempre buscando potencializar a seletividade e eficiência na separação de partículas minerais [189, 221, 222, 224-226], inclusive para as naturalmente hidrofóbicas [227, 228]. Para o oleato não foi diferente, sendo combinado com vários co-coletores catiônicos [220, 223, 229, 230], aniônicos [231, 232] e não-iônicos [233].

Os reagentes não iônicos, quando empregados juntamente com carboxilatos, sendo classificados como extensores de cadeia, buscam aumento da seletividade, economia de reagentes e melhoria das condições de viscosidade da polpa. A ação destes pode ser explicada pela atuação das cadeias carbônicas na desidratação de superfícies através da co-adsorção dos compostos apolares sobre elas [167]. Além disso, proporcionaram a redução da concentração micelar crítica e a tensão superficial da solução, demonstrando que os surfactantes se concentram na interface líquido/gás [139, 233]. Tal fato favorece o umedecimento, solubilização e formação de espuma mais estável, devido à redução da taxa de ruptura das bolhas, o que causa maior probabilidade de colisão das partículas minerais com essas bolhas, potencializando sua flotabilidade [139]. A sinergia entre o oleato e os coletores não-iônicos proporciona o aumento do ângulo de contato [150], redução do consumo de coletor e suavização do efeito deletério de íons Ca^{2+}, que causam a precipitação do coletor [232, 234]. A interação entre oleato/ácido hidroxâmico proporcionou alta seletividade e recuperação no sistema de flotação calcita/scheelita [112] e dolomita/smithsonita [235], além de proporcionar adsorção mais intensa e maior recuperação na flotação de bastenasita [236] e óxidos de elementos de terras raras [237]. Já o par oleato/querosene foi empregado na flotação em célula/coluna de minério fosfático sedimentar com ganga carbonatada em pH levemente ácido, apresentando resultados satisfatórios [197]. Para o sistema apatita/calcita, foi observado que quando o oleato e o iso-tridecanol (álcool graxo) foram empregados em conjunto, a adsorção deste sobre as partículas minerais se mostrou superior ao cenário de aplicação isolada, mesmo mantendo a densidade de adsorção do oleato, demonstrando maior afinidade entre o complexo álcool-oleato e a superfície mineral em relação ao dímero dioleato e a mesma, o que proporcionou hidrofobização mais efetiva das partículas [238].

Como discutido anteriormente, considerando os óleos vegetais como um sistema composto por vários ácidos graxos, a interação entre a ação desses como coletores pode ser discutida sob a óptica de uma sinergia do tipo aniônico-aniônico. O desempenho do sistema composto por ácido oleico (54%), linoleico (36%) e linolenico (10%) foi avaliado na flotação de apatita, apresentando baixa concentração micelar e menor consumo de reagente em relação ao desempenho do ácido oleico isolado [217]. A flotação de tungstênio, aplicando o sistema ácido oleico/linoleico, com de diferentes proporções de ácido ricínico, apresentou ganho de seletividade em um único estágio em relação ao emprego de ácido oleico puro [239]. Entretanto, os registros em relação à

sinergia de ácidos graxos presentes nos óleos vegetais na flotação de minérios são escassos, principalmente a discussão sobre a repulsão eletrostática entre eles [231].

Para os coletores provenientes de óleos e gorduras, tanto de origem vegetal quanto animal, a sinergia entre os ácidos graxos em sua composição também desempenha papel fundamental no desempenho e seletividade da operação de flotação. Diante da sensibilidade do ácido oleico como coletor à presença de lamas e íons Ca^{2+} na fase líquida, o efeito sinérgico deste (54%), juntamente com linoleico (36%) e linolenico (10%) foi avaliado na flotação de apatita, apresentando baixa concentração micelar e menor consumo de reagente [217]. A abordagem utilizando efeitos sinérgicos da mistura de coletores carboxílicos também foi empregada para o sistema de flotação de tungstênio, aplicando coletor de composição predominante de ácidos oleico e linoleico, além de diferentes proporções de ácido ricínico, elevando substancialmente a seletividade do processo em um único estágio [239].

As primeiras discussões sobre efeito sinérgico de coletores do tipo ácido graxo se basearam na formação complexos iono-molecurares, embora tenha sido elaborada analisando sistemas contendo um único ácido, sendo pouco desenvolvida até então [240]. A formação de compostos iono-moleculares, provenientes da interação das formas neutras e dissociadas dos coletores aniônicos, demonstrou favorecer a flotabilidade devido à atividade superficial mais alta do complexo em relação aos componentes isoladamente. O aumento efetivo da cadeia carbônica nos complexos formados reforça essa discussão [241-243]. Até então, a formação de cargas superficiais em função do pH do meio era considerada como fator predominante para a intensidade da interação entre o coletor e a partícula. A partir da discussão sobre a formação de compostos ionomoleculares, esse fenômeno passou a ser considerado como relevante na hidrofobização de partículas minerais [240]. A flotação de hematita em sistema contendo oleato foi discutida sob a luz da formação de compostos iono-moleculares, sendo observado a mesma condição de pH para a máxima flotabilidade do mineral e maior formação dos compostos [244]. Essa abordagem também foi empregada na discussão da flotação de quartzo em sistema contendo amina/cloreto de amônio a partir de estudos termogravimétricos, demonstrando a maior atividade dos compostos iono-moleculares na superfície das partículas [245].

Registros em relação à sinergia de ácidos graxos presentes nos óleos vegetais na flotação de minérios são escassos, principalmente a discussão sobre a estabilidade,

configuração e grau de hidrofobicidade do filme formado [217, 231, 239]. Atualmente, o mercado busca maior efetividade, menor custo e melhor seletividade na ação dos coletores de flotação de fosfato. Visando atender a essa demanda, estudos avaliam técnicas de adsorção em superfície mineral em busca de conhecimentos sobre o comportamento de potenciais coletores alternativos, confrontando o desempenho destes com o de ácidos graxos isolados, presentes em sua composição [212].

2.7 Óleos Amazônicos

O Brasil abriga uma das variedades mais ricas de espécies vegetais do mundo, sendo o sexto colocado em relação à biodiversidade [213]. Entretanto, apenas uma fração desse potencial é conhecida e utilizada adequadamente, tanto do ponto de vista alimentício, quanto tecnológico e ambiental [214-216]. A região amazônica é rica em recursos vegetais, como frutas e oleaginosas, cuja exploração comercial é fator importante no desenvolvimento econômico e social das comunidades [246-249]. A caracterização destes óleos derivados dessas oleaginosas foi amplamente investigada visando o levantamento de dados para embasar sua aplicação [250-252]. A composição, em ácidos graxos, das principais oleaginosas amazônicas apresentam alto nível de insaturação, típico de espécies do tipo palmeiras, sendo os ácidos oleico e linoleico os mais expressivos [253], habilitando-os para potencial emprego industrial [254].

As palmeiras demonstraram boa adaptação a áreas tropicais, com mais de 150 espécies na região, fornecendo vários tipos de óleos com alto rendimento de polpa e semente, mesmo em condições adversas, representando alto potencial para aplicação industrial [255, 256].

O patauá (*Oenocarpus bataua*) é fruto de uma palmeira encontrada no norte da América do Sul, incluindo Panamá e Trinidad, sendo abundante na região amazônica e útil para comunidades indígenas da região. O fruto é usado principalmente como fonte de óleo para fins medicinais, cosméticos ou culinários, além da preparação de uma bebida semelhante ao leite. O óleo de patauá é tradicionalmente extraído da polpa e sementes do fruto, apresentando aspecto característico amarelo-esverdeado, semelhante ao óleo de oliva. Apesar de escassos, estudos confirmam o perfil de ácidos graxos do óleo de patauá como sendo majoritariamente composto por ácidos oleico (80%) e palmítico (15%), com pequenas proporções de esteárico, láurico e mirístico [257, 258].

A andiroba (*Carapas guianensi*), é uma árvore endêmica em florestas úmidas da América do Sul, presente em toda a Amazônia, e que produz frutos redondos com sementes de coloração marrom, de onde é extraído seu óleo espesso (60% em peso), que solidifica a temperaturas abaixo de 25°C e atinge rapidamente o ranço após a extração [251, 259-261]. Esse óleo é tradicionalmente utilizado na indústria cosmética e farmacêutica devido a suas propriedades febrífuga, analgésica, antibacteriana, antiparasitária, inseticida e repelente, em função dos liminóides presentes em sua fração não saponificável (2 a 5%) [249, 262-266]. Já a fração saponificável é composta majoritariamente por ácidos oleico (57%), palmítico (25%) e esteárico (10%) [267].

O bacuri (*Platonia insiginis*) é uma espécie nativa da Amazônia brasileira, explorada para produção de madeira e frutas. Seu fruto pode ser consumido cru ou sob a forma de suco, sorvete ou geléia. Já a gordura extraída de sua semente é amplamente utilizada no campo medicinal para tratamentos anti-inflamatório e anti-eplético [268, 269]. No campo industrial, a gordura de bacuri pode ser aplicada na produção do biodiesel devido ao seu potencial antioxidante [254]. Seu perfil graxo é composto por ácidos de cadeia saturada (palmítico (65%)), além do oleico (25%), resultando em seu aspecto sólido a temperatura ambiente [250, 252].

Alguns óleos amazônicos foram objeto de estudo no campo da flotação em espuma [270, 271], inclusive o patauá [204]. Entretanto, não foram encontrados trabalhos empregando óleo de andiroba e gordura de bacuri saponificados como coletores na literatura.

2.8 Referências

1. Dubiński J. Sustainable Development of Mining Mineral Resources. Journal of Sustainable Mining. 2013;12(1):1-6. https://doi.org/10.7424/jsm130102.

2. Geissler B, Mew MC, Matschullat J, Steiner G. Innovation potential along the phosphorus supply chain: A micro and macro perspective on the mining phase. Science of The Total Environment. 2020;714:136701. https://doi.org/10.1016/j.scitotenv.2020.136701.

3. Zhang P. Comprehensive Recovery and Sustainable Development of Phosphate Resources. Procedia Engineering. 2014;83:37-51. https://doi.org/10.1016/j.proeng.2014.09.010.

4. Billah M, Khan M, Bano A, Hassan TU, Munir A, Gurmani AR. Phosphorus and phosphate solubilizing bacteria: Keys for sustainable agriculture. Geomicrobiology Journal. 2019;36(10):904-16. https://doi.org/10.1080/01490451.2019.1654043.

5. Dari B, Rogers CW, Liang X. Plant, grain, and soil response of irrigated malt barley as affected by cultivar, phosphorus, and sulfur applications on an alkaline soil. Journal of Plant Nutrition. 2019;42(9):1061-71. https://doi.org/10.1080/01904167.2019.1589504.

6. Ayadi S, Jallouli S, Landi S, Capasso G, Chamekh Z, Cardi M, Paradisone V, Lentini M, Karmous C, Trifa Y, Esposito S. Nitrogen assimilation under different nitrate nutrition in Tunisian durum wheat landraces and improved genotypes. Plant Biosystems - An International Journal Dealing with all Aspects of Plant Biology. 2020;1-11. https://doi.org/10.1080/11263504.2020.1722274.

7. Yu F, Li Y, Li F, Zhou Z, Chen C, Liang X, Li C, Liu K. Nitrogen fertilizers promote plant growth and assist in manganese (Mn) accumulation by Polygonum pubescens Blume cultured in Mn tailings soil. International Journal of Phytoremediation. 2019;21(12):1225-33. https://doi.org/10.1080/15226514.2019.1619161.

8. Tian D, Wang Y, Xing J, Sun Q, Song J, Li X. Nitrogen loss process in hypoxic seawater based on the culture experiment. Marine Pollution Bulletin. 2020;152:110912. DOI: 10.1016/j.marpolbul.2020.110912.

9. Shirale AO, Meena BP, Gurav PP, Srivastava S, Biswas AK, Thakur JK, Somasundaram J, Patra AK, Rao AS. Prospects and challenges in utilization of indigenous rocks and minerals as source of potassium in farming. Journal of Plant Nutrition. 2019;42(19):2682-701. https://doi.org/10.1080/01904167.2019.1659353.

10. Liu C, Wang W, Yang F, Ma J, Yang W, Wang T, Wang C. The intensified leaching mechanism of phosphorus-potassium associated ore in HCl-CaF2 system with sodium dodecyl sulfate. Chemical Engineering and Processing - Process Intensification. 2020;149:107847. https://doi.org/10.1016/j.cep.2020.107847.

11. Paramasivam CR, Anbazhagan S. Soil fertility analysis in and around magnesite mines, Salem, India. Geology, Ecology, and Landscapes. 2020;4(2):140-150. https://doi.org/10.1080/24749508.2019.1608407.

12. Gao C, Zhang M, Song K, Wei Y, Zhang S. Spatiotemporal analysis of anthropogenic phosphorus fluxes in China. Science of The Total Environment. 2020;721(2):137588. https://doi.org/10.1016/j.scitotenv.2020.137588.

13. Barros LAF, Caracterização Tecnológica de Minério Fosfático de Salitre - Patrocínio-MG. UFMG, 2005.

14. Owens CL, Nash GR, Hadler K, Fitzpatrick RS, Anderson CG, Wall F. Apatite enrichment by rare earth elements: A review of the effects of surface properties. Advances in Colloid and Interface Science. 2019;265:14-28. https://doi.org/10.1016/j.cis.2019.01.004.

15. Louw I. Potential radiological impact of the phosphate industry in South Africa on the public and the environment (Paper 1). Journal of Environmental Radioactivity. 2020;217:106214. https://doi.org/10.1016/j.jenvrad.2020.106214.

16. Lieberman RN, Izquierdo M, Córdoba P, Moreno NP, Querol X, de la Campa AMS, Font O, Cohen H, Knop Y, Torres-Sánchez R, Sánchez-Rodas D, Muñoz-Quiros C, de la Rosa JD. The geochemical evolution of brines from phosphogypsum deposits in Huelva (SW Spain) and its environmental implications. Science of The Total Environment. 2020;700:134444. https://doi.org/10.1016/j.scitotenv.2019.134444.

17. Santana RC, Farnese ACC, Fortes MCB, Ataíde CH, Barrozo MAS. Influence of particle size and reagent dosage on the performance of apatite flotation. Separation and Purification Technology. 2008;64(1):8-15. https://doi.org/10.1016/j.seppur.2008.09.004.

18. Huang W, Cai W, Huang H, Lei Z, Zhang Z, Tay JH, Lee D-J. Identification of inorganic and organic species of phosphorus and its bio-availability in nitrifying aerobic granular sludge. Water Research. 2015;68:423-31. https://doi.org/10.1016/j.watres.2014.09.054.

19. Lei Y, Song B, Saakes M, van der Weijden RD, Buisman CJN. Interaction of calcium, phosphorus and natural organic matter in electrochemical recovery of phosphate. Water Research. 2018;142:10-17. https://doi.org/10.1016/j.watres.2018.05.035.

20. Xing B, Ouyang M, Graham N, Yu W. Enhancement of phosphate adsorption during mineral transformation of natural siderite induced by humic acid: Mechanism and application. Chemical Engineering Journal. 2020;393:124730. https://doi.org/10.1016/j.cej.2020.124730.

21. Oita A, Wirasenjaya F, Liu J, Webeck E, Matsubae K. Trends in the food nitrogen and phosphorus footprints for Asia's giants: China, India, and Japan. Resources, Conservation and Recycling. 2020;157:104752. https://doi.org/10.1016/j.resconrec.2020.104752.

22. Mahlia TMI, Syazmi ZAHS, Mofijur M, Abas AEP, Bilad MR, Ong HC, Silitonga AS. Patent landscape review on biodiesel production: Technology updates. Renewable and Sustainable Energy Reviews. 2020;118:109526. https://doi.org/10.1016/j.rser.2019.109526.

23. Singh D, Sharma D, Soni SL, Sharma S, Kumar Sharma P, Jhalani A. A review on feedstocks, production processes, and yield for different generations of biodiesel. Fuel. 2020;262:116553. https://doi.org/10.1016/j.fuel.2019.116553.

24. Galadima A, Muraza O. Waste materials for production of biodiesel catalysts: Technological status and prospects. Journal of Cleaner Production. 2020;263:121358. https://doi.org/10.1016/j.jclepro.2020.121358.

25. Wan Isahak WNR, Che Ramli ZA, Ismail M, Mohd Jahim J, Yarmo MA. Recovery and Purification of Crude Glycerol from Vegetable Oil Transesterification.

Separation & Purification Reviews. 2015;44(3):250-67. https://doi.org/10.1080/15422119.2013.851696.

26. Onoji SE, Iyuke SE, Igbafe AI, Daramola MO. Hevea brasiliensis (rubber seed) oil: modeling and optimization of extraction process parameters using response surface methodology and artificial neural network techniques. Biofuels. 2019;10(6):677-91. https://doi.org/10.1080/17597269.2017.1338122.

27. Awadallah RM, Mohamed AE, El Hazek NT, Hassan MY. Beneficiation of west sibaiya phosphate ores by flotation in alkaline media. Metallurgical and Materials Transactions B. 1998;29(6):1149-56. https://doi.org/10.1007/s11663-998-0036-8.

28. Gontijo VLS, Santos LH, Rodrigues GD, Carvalho PLG. Método alternativo para purificação de P2O5 do minério fosfático silico-carbonatado da região de Araxá, na retirada de íons cálcio e magnésio via sistema aquoso bifásico (SAB). Holos. 2017;8:1-11. https://doi.org/10.15628/holos.2017.6596.

29. El Bamiki R, Séranne M, Chellaï EH, Merzeraud G, Marzoqi M, Melinte-Dobrinescu MC. The Moroccan High Atlas phosphate-rich sediments: Unraveling the accumulation and differentiation processes. Sedimentary Geology. 2020;403:105655. https://doi.org/10.1016/j.sedgeo.2020.105655.

30. Kechiched R, Laouar R, Bruguier O, Kocsis L, Salmi-Laouar S, Bosch D, Ameur-Zaimeche O, Foufou A, Larit H. Comprehensive REE + Y and sensitive redox trace elements of Algerian phosphorites (Tébessa, eastern Algeria): A geochemical study and depositional environments tracking. Journal of Geochemical Exploration. 2020;208:106396. https://doi.org/10.1016/j.gexplo.2019.106396.

31. Jiang X-D, Sun X-M, Chou Y-M, Hein JR, He G-W, Fu Y, Li D-f, Liao J-L, Ren J-B. Geochemistry and origins of carbonate fluorapatite in seamount FeMn crusts from the Pacific Ocean. Marine Geology. 2020;423:106135. https://doi.org/10.1016/j.margeo.2020.106135.

32. Singh R, Pradip, Sankar TAP. Selective flotation of Maton (India) phosphate ore slimes with particular reference to the effects of particle size. International Journal of Mineral Processing. 1992;36(3-4):283-93. https://doi.org/10.1016/0301-7516(92)90050-7.

33. Hoang DH, Kupka N, Peuker UA, Rudolph M. Flotation study of fine grained carbonaceous sedimentary apatite ore – Challenges in process mineralogy and impact of hydrodynamics. Minerals Engineering. 2018;121:196-204. https://doi.org/10.1016/j.mineng.2018.03.021.

34. Rodrigues AJ, Brandao PRG. The influence of crystal chemistry properties on the floatability of apatites with sodium oleate. Minerals Engineering. 1993;6(6):643-53. https://doi.org/10.1016/0892-6875(93)90118-7.

35. Barbosa ESR, Brod JA, Cordeiro PFO, Junqueira-Brod TC, Santos RV, Dantas EL. Phoscorites of the Salitre I complex: Origin and petrogenetic implications. Chemical Geology. 2020;535:119463. https://doi.org/10.1016/j.chemgeo.2020.119463.

36. Pérez C, Claveria O. Natural resources and human development: Evidence from mineral-dependent African countries using exploratory graphical analysis. Resources Policy. 2020;65:101535. https://doi.org/10.1016/j.resourpol.2019.101535.

37. Resources MN. China mineral resources. Disponível em https://www.gov.cn/xinwen/2018-10/22/5333589/files/01d0517b9d6c430bbb927ea5e48641b4.pdf. 2018. Acessado em 10/04/2020.

38. Smil V. Phosphorus in the environment: natural flows and human interferences. Annual Review of Energy and the Environment. 2000;25(1):53-88. https://doi.org/10.1146/annurev.energy.25.1.53.

39. Withers PJA, Elser JJ, Hilton J, Ohtake H, Schipper WJ, van Dijk KC. Greening the global phosphorus cycle: how green chemistry can help achieve planetary P sustainability. Green Chemistry. 2015;17(4):2087–99. https://doi.org/10.1039/c4gc02445a.

40. Mayer BK, Baker LA, Boyer TH, Drechsel P, Gifford M, Hanjra MA, Parameswaran P, Stoltzfus J, Westerhoff P, Rittmann BE. Total Value of Phosphorus Recovery. Environmental Science and Technology. 2016;50(13):6606-20. https://doi.org/20. 10.1021/acs.est.6b01239.

41. Chen Y, Zhang X, Yang X, Lv Y, Wu J, Lin L, Zhang Y, Wang G, Xiao Y, Zhu X, Yu X, Peng H. Emergy evaluation and economic analysis of compound fertilizer production: A case study from China. Journal of Cleaner Production. 2020;260:121095. https://doi.org/10.1016/j.jclepro.2020.121095.

42. Oumenskou H, El Baghdadi M, Barakat A, Aquit M, Ennaji W, Karroum LA, Aadraoui M. Multivariate statistical analysis for spatial evaluation of physicochemical properties of agricultural soils from Beni-Amir irrigated perimeter, Tadla plain, Morocco. Geology, Ecology, and Landscapes. 2019;3(2):83-94. https://doi.org/10.1080/24749508.2018.1504272.

43. Ramphisa PD, Collins PH, Bair EK, Davenport RJ. Corn biomass, uptake and fractionation of soil phosphorus in five soils amended with organic wastes as P fertilizers. Journal of Plant Nutrition. 2020;43(3):335-53. https://doi.org/10.1080/01904167.2019.1683194.

44. Codling EE. Effects of phosphorus amended low phosphorus soil on soybean (Glycine max L.) and wheat (Titicum aestivum L.) yield and phosphorus uptake. Journal of Plant Nutrition. 2019;42(8):891-99. https://doi.org/10.1080/01904167.2019.1589506.

45. Castro JS, Calijuri ML, Ferreira J, Assemany PP, Ribeiro VJ. Microalgae based biofertilizer: A life cycle approach. Science of The Total Environment. 2020;724:138138. https://doi.org/10.1016/j.scitotenv.2020.138138.

46. Gypser S, Freese D. Phosphorus release from vivianite and hydroxyapatite by organic and inorganic compounds. Pedosphere. 2020;30(2):190-200. https://doi.org/10.1016/S1002-0160(20)60004-2.

47. Chojnacka K, Moustakas K, Witek-Krowiak A. Bio-based fertilizers: A practical approach towards circular economy. Bioresource Technology. 2020;295:122223. https://doi.org/10.1016/j.biortech.2019.122223.

48. Scholtz M. Creating a circular economy for phosphorus fertilizers. Disponível em http://ostara.com/wp-content/uploads/2017/09/Scholz_FF_Sept_Oct_2017.pdf 2017 Acessado em 08/04/2020.

49. Hansen J. EU must get serious about promoting the circular economy. Disponível em https://www.theparliamentmagazine.eu/news/article/eu-must-get-serious-about-promoting-the-circular-economy. 2018. Acessado em 09/04/2020.

50. Li L, Pang H, He J, Zhang J. Characterization of phosphorus species distribution in waste activated sludge after anaerobic digestion and chemical precipitation with Fe3+ and Mg2+. Chemical Engineering Journal. 2019;373:1279-85. https://doi.org/10.1016/j.cej.2019.05.146.

51. Barquet K, Järnberg L, Rosemarin A, Macura B. Identifying barriers and opportunities for a circular phosphorus economy in the Baltic Sea region. Water Research. 2020;171:115433. https://doi.org/10.1016/j.watres.2019.115433.

52. Mackey KRM, Mooy BV, Cade-Menum CJ, Paytan A. Phosphorus Dynamics in the Environment. Encyclopedia of Microbiology (Fourth Edition). 2019;4:506-19. https://doi.org/10.1016/B978-0-12-809633-8.20911-4

53. Golroudbary SR, El Wali M, Kraslawski A. Rationality of using phosphorus primary and secondary sources in circular economy: Game-theory-based analysis. Environmental Science and Policy. 2020;106:166-76. https://doi.org/10.1016/j.envsci.2020.02.004.

54. Gokhberg L, Kuzminov I, Khabirova E, Thurner T. Advanced text-mining for trend analysis of Russia's Extractive Industries. Futures. 2020;115:102476. https://doi.org/10.1016/j.futures.2019.102476

55. Angelopoulos J, Sahoo S, Visvikis ID. Commodity and transportation economic market interactions revisited: New evidence from a dynamic factor model. Transportation Research Part E: Logistics and Transportation Review. 2020;133:101836. https://doi.org/10.1016/j.tre.2019.101836.

56. Seer HJ, Pimentel MM, Fonseca MA, Moraes LC. Grupo Ibiá na sinforma de Araxá: um terreno tectonoestratigráfico ligado à evolução de arcos magmáticos. Revista Brasileira de Geociências. 2000;30(4):737-44. https://doi.org/10.25249/0375-7536.2000304737744.

57. Gomide CS, Brod JA, Junqueira-Brod TC, Buhn BM, Santos RV, Barbosa ESR, Cordeiro PFO, Palmieri M, Grasso CB, Torres MG. Sulfur isotopes from Brazilian alkaline carbonatite complexes. Chemical Geology. 2013;341:38-49. https://doi.org/10.1016/j.chemgeo.2013.01.006.

58. Traversa GG, Gomes CB, Brotzu, P, Buraglini N, Morbidelli L, Principato MS, Ronca S, Ruberti E. Petrography and mineral chemistry of carbonatites and mica-rich rocks from the Araxá complex (Alto Paranaíba Province, Brazil). Anais da Associação brasileira de Ciências. 2001;73(1):71-98. https://doi.org/10.1590/S0001-37652001000100008.

59. Raposo DB, Pereira SY. Caracterização litológica e hidrodinâmica do aquífero associado ao Complexo Alcalino Carbonatítico do Barreiro, oeste de Minas Gerais. Geociências. 2013;32(1):33-50.

60. Bonotto DM. Hydrogeochemical study of surface waters from Araxá city, Minas Gerais State, Brazil. Journal of Geochemical Exploration. 2020;213:106521. http://dx.doi.org/10.1016/j.gexplo.2020.106521.

61. Santana RC, Duarte CR, Ataíde CH, Barrozo MAS. Flotation Selectivity of Phosphate Ore: Effects of Particle Size and Reagent Concentration. Separation Science and Technology. 2011;46(9):1511-18. https://doi.org/10.1080/01496395.2011.561268.

62. Barrozo MAS, Lobato FS. Multi-objective optimization of column flotation of an igneous phosphate ore. International Journal of Mineral Processing. 2016;146:82-9. https://doi.org/10.1016/j.minpro.2015.12.001.

63. Oliveira MS, Santana RC, Ataíde CH, Barrozo MAS. Recovery of apatite from flotation tailings. Separation and Purification Technology. 2011;79(1):79-84. https://doi.org/10.1016/j.seppur.2011.03.015.

64. Jones JMC, Guinel FC, Antunes PM. Carbonatites as rock fertilizers: A review. Rhizosphere. 2020;13:100188. https://doi.org/10.1016/j.rhisph.2020.100188.

65. Feng M, Song W, Kynicky J, Smith M, Cox C, Kotlanova M, Brtnicky M, Fu W, Wei C. Primary rare earth element enrichment in carbonatites: Evidence from melt inclusions in Ulgii Khiid carbonatite, Mongolia. Ore Geology Reviews. 2020;117:103294. https://doi.org/10.1016/j.oregeorev.2019.103294.

66. Sis H, Chander S. Reagents used in the flotation of phosphate ores: a critical review. Minerals Engineering. 2003;16(7):577-85. https://doi.org/10.1016/S0892-6875(03)00131-6.

67. Wen Qi G. Use of the QEM-SEM analysis in flotation testwork on a phosphate ore containing monazite. International Journal of Mineral Processing. 1993;37(1-2):89-108. https://doi.org/10.1016/0301-7516(93)90007-W.

68. Su F, Hanumantha Rao K, Forssberg KSE, Samskog PO. The influence of temperature on the kinetics of apatite flotation from magnetite fines. International Journal of Mineral Processing. 1998;54(3-4):131-45. https://doi.org/10.1016/S0301-7516(98)00021-0.

69. Al-Wakeel MI, Lin CL, Miller JD. Significance of liberation characteristics in the fatty acid flotation of Florida phosphate rock. Minerals Engineering. 2009;22(3):244-53. https://doi.org/10.1016/j.mineng.2008.07.011.

70. Nanthakumar B, Grimm D, Pawlik M. Anionic flotation of high-iron phosphate ores - Control of process water chemistry and depression of iron minerals by starch and guar gum. International Journal of Mineral Processing. 2009;92(1-2):49-57. https://doi.org/10.1016/j.minpro.2009.02.003.

71. Li G, Cao Y, Liu J, Wang D. Cyclonic flotation column of siliceous phosphate ore. International Journal of Mineral Processing. 2012;110-111:6-11. https://doi.org/10.1016/j.minpro.2012.03.008.

72. Santana RC, Ribeiro JA, Santos MA, Reis AS, Ataíde CH, Barrozo MAS. Flotation of fine apatitic ore using microbubbles. Separation and Purification Technology. 2012;98:402-09. https://doi.org/10.1016/j.seppur.2012.06.014.

73. Zhang Y, Chen H, Yang B, Fu S, Yu J, Wang Z. Prediction of phosphate concentrate grade based on artificial neural network modeling. Results in Physics. 2018;11:625-28. https://doi.org/10.1016/j.rinp.2018.10.011.

74. Reis AS, Reis Filho AM, Demuner LR, Barrozo MAS. Effect of bubble size on the performance flotation of fine particles of a low-grade Brazilian apatite ore. Powder Technology. 2019;356:884-91. https://doi.org/10.1016/j.powtec.2019.09.029.

75. Elbendary A, Aleksandrova T, Nikolaeva N. Influence of operating parameters on the flotation of the Khibiny Apatite-Nepheline Deposits. Journal of Materials Research and Technology. 2019;8(6):5080-90. https://doi.org/10.1016/j.jmrt.2019.08.027.

76. Abouzeid AZM, Negm AT, Elgillani DA. Upgrading of calcareous phosphate ores by flotation: Effect of ore characteristics. International Journal of Mineral Processing. 2009;90(1-4):81-89. https://doi.org/10.1016/j.minpro.2008.10.005.

77. Abouzeid A-ZM. Physical and thermal treatment of phosphate ores - An overview. International Journal of Mineral Processing. 2008;85(4):59-84. https://doi.org/10.1016/j.minpro.2007.09.001.

78. Peng FF, Gu Z. Processing Florida dolomitic phosphate pebble in a double reverse fine flotation process. Mining, Metallurgy & Exploration. 2005;22:23-30. https://doi.org/10.1007/BF03403192.

79. El-Shall H, Zhang P, Abdel Khalek N, El-Mofty S. Beneficiation technology of phosphates: challenges and solutions. Minerals and Metallurgical Processing. 2004;21:17-26. https://doi.org/10.1007/BF03403297.

80. Ibrahim SS, Yassin KE, Boulos TR. Processing of an East Mediterranean phosphate ore sample by an integrated attrition scrubbing/classification scheme (part one). Separation Science and Technology. 2020;55(5):967-79. https://doi.org/10.1080/01496395.2019.1575413.

81. Shaikh AMH, Dixit SG. Beneficiation of phosphate ores using high gradient magnetic separation. International Journal of Mineral Processing. 1993;37(1-2):149-62. https://doi.org/10.1016/0301-7516(93)90010-8.

82. Behera SK, Mulaba-Bafubiandi AF. Microbes Assisted Mineral Flotation a Future Prospective for Mineral Processing Industries: A Review. Mineral Processing and Extractive Metallurgy Review. 2017;38(2):96-105. https://doi.org/10.1080/08827508.2016.1262861.

83. Chandraprabha MN, Natarajan KA. Microbially Induced Mineral Beneficiation. Mineral Processing and Extractive Metallurgy Review. 2009;31(1):1-29. https://doi.org/10.1080/08827500903404682.

84. Bulatovic SM. Flotation of Phosphate Ore. In: Bulatovic SM, organizador. Handbook of Flotation Reagents: Chemistry, Theory and Practice. Amsterdam: Elsevier; 2015, p. 1-19. https://doi.org/10.1016/B978-0-444-53083-7.00026-9.

85. Hoang DH, Heitkam S, Kupka N, Hassanzadeh A, Peuker UA, Rudolph M. Froth properties and entrainment in lab-scale flotation: A case of carbonaceous sedimentary phosphate ore. Chemical Engineering Research and Design. 2019;142:100-10. https://doi.org/10.1016/j.cherd.2018.11.036.

86. Foucaud Y, Badawi M, Filippov L, Filippova I, Lebègue S. A review of atomistic simulation methods for surface physical-chemistry phenomena applied to froth flotation. Minerals Engineering. 2019;143:106020. https://doi.org/10.1016/j.mineng.2019.106020.

87. Krasowska M, Zawala J, Bradshaw-Hajek BH, Ferri JK, Beattie DA. Interfacial characterisation for flotation: 1. Solid-liquid interface. Current Opinion in Colloid and Interface Science. 2018;37:61-73. https://doi.org/10.1016/j.cocis.2018.06.004.

88. Pawliszak P, Krasowska M, Zawala J, Bradshaw-Hajek BH, Ferri JK, Beattie DA. Interfacial characterisation for flotation: 2. Air-water interface. Current Opinion in Colloid and Interface Science. 2018;37:115-27. https://doi.org/10.1016/j.cocis.2018.07.002.

89. Achaye I, Wiese J, McFadzean B. Effect of mineral particle size on froth stability. Mineral Processing and Extractive Metallurgy. 2021;130(3):253-61. https://doi.org/10.1080/25726641.2019.1606147.

90. Guo W, Han Y, Zhu Y, Li Y, Tang Z. Effect of amide group on the flotation performance of lauric acid. Applied Surface Science. 2020;505:144627. https://doi.org/10.1016/j.apsusc.2019.144627.

91. Nan N, Zhu Y, Han Y. Flotation performance and mechanism of α-Bromolauric acid on separation of hematite and fluorapatite. Minerals Engineering. 2019;132:162-68. https://doi.org/10.1016/j.mineng.2018.11.048.

92. Horta D, Monte MBM, Leal Filho LS. The effect of dissolution kinetics on flotation response of apatite with sodium oleate. International Journal of Mineral Processing. 2016;146:97-104. https://doi.org/10.1016/j.minpro.2015.12.003.

93. Zhong K, Vasudevan TV, Somasundaran P. Floatability of apatites of different type and origin: role of surface area and porosity. International Journal of Mineral Processing. 1993;38(3-4):177-88. https://doi.org/10.1016/0301-7516(93)90074-K.

94. Dehghani A, Azizi A, Mojtahedzadeh SH, Gharibi K. Optimizing Rougher Flotation Parameters of the Esfordi Phosphate Ore. Mineral Processing and Extractive Metallurgy Review. 2012;33(4):260-68. https://doi.org/10.1080/08827508.2011.584092.

95. Brandao PRG, Caires LG, Queiroz DSB. Vegetable lipid oil-based collectors in the flotation of apatite ores. Minerals Engineering. 1994;7(7):917-25. https://doi.org/10.1016/0892-6875(94)90133-3.

96. Oliveira MS, Peres AEC. Flotabilidade da apatita e minerais de ganga provenientes de minério sílico-carbonatado com oleato de sódio. Revista da Escola de Minas. 2010;63(3):551-7. https://doi.org/10.1590/S0370-44672010000300019.

97. Gaspar JC, Monte MBM, Paiva PRP. Concentração por flotação da apatita proveniente de rochas de filiação carbonatítica. Revista Escola de Minas. 2011;64(1):111-16. https://doi.org/10.1590/S0370-44672011000100015.

98. Barros LAF, Ferreira EE, Peres AEC. Floatability of apatites and gangue minerals of an igneous phosphate ore. Minerals Engineering. 2008;21(12-14):994-99. https://doi.org/10.1016/j.mineng.2008.04.012.

99. Leal Filho LS, Assis SM, Araujo AC, Chaves AP. Process mineralogy studies for optimizing the flotation performance of two refractory phosphate ores. Minerals Engineering. 1993;6(8-10):907-16. https://doi.org/10.1016/0892-6875(93)90063-S.

100. Mishra SK. Electrokinetic properties and flotation behaviour of apatite and calcite in the presence of sodium oleate and sodium metasilicate. International Journal of Mineral Processing. 1982;9(1):59-73. https://doi.org/10.1016/0301-7516(82)90006-0.

101. Hanumantha Rao K, Antti B-M, Forssberg E. Flotation of phosphatic material containing carbonatic gangue using sodium oleate as collector and sodium silicate as modifier. International Journal of Mineral Processing. 1989;26(1-2):123-40. https://doi.org/10.1016/0301-7516(89)90047-1.

102. Mishra SK. The electrokinetic properties and flotation behaviour of apatite and calcite in the presence of dodecylamine chloride. International Journal of Mineral Processing. 1979;6(2):119-32. https://doi.org/10.1016/0301-7516(79)90017-6.

103. Hu Y, Xu Z. Interactions of amphoteric amino phosphoric acids with calcium-containing minerals and selective flotation. International Journal of Mineral Processing. 2003;72(1-4):87-94. https://doi.org/10.1016/S0301-7516(03)00089-9.

104. Rao DV, Narayanan MK, Nayak UB, Ananthapadmanabhan K, Somasundaran P. Flotation of calcareous Mussorie phosphate ore. International Journal of Mineral Processing. 1985;14(1):57-66. https://doi.org/10.1016/0301-7516(85)90014-6.

105. Ananthapadmanabhan KP, Somasundaran PJM. Role of Dissolved Mineral Species in Calcite-Apatite Flotation. Minerals and Metallurgical Processing. 1984;1:36-42. https://doi.org/10.1007/BF03402550.

106. Elgillani DA, Abouzeid AZM. Flotation of carbonates from phosphate ores in acidic media. International Journal of Mineral Processing. 1993;38(3-4):235-56. https://doi.org/10.1016/0301-7516(93)90077-N.

107. Zhang P, Yu Y, Bogan M. Challenging the “Crago” double float process II. Amine-fatty acid flotation of siliceous phosphates. Minerals Engineering. 1997;10(9):983-94. https://doi.org/10.1016/S0892-6875(97)00078-2.

108. Moudgil BM, Barnett DH. Agglomeration-Skin Flotation of Coarse Phosphate Rock. The American Institute of Mining, Metallurgical, and Petroleum Engineers. 1979, 7p.

109. Moudgil, BMS. Advances in phosphate flotation. In: SME, editor. Advances in Mineral Processing. Colorado; 1986, p. 426-441.

110. Houot R. Beneficiation of phosphatic ores through flotation: Review of industrial applications and potential developments. International Journal of Mineral Processing. 1982;9(4):353-84. https://doi.org/10.1016/0301-7516(82)90041-2.

111. Chanturiya VA, Kondratiev SA. Contemporary Understanding and Developments in the Flotation Theory of Non-Ferrous Ores. Mineral Processing and Extractive Metallurgy Review. 2019;40(6):390-401. https://doi.org/10.1080/08827508.2019.1657863.

112. Gao Y, Gao Z, Sun W, Yin Z, Wang J, Hu Y. Adsorption of a novel reagent scheme on scheelite and calcite causing an effective flotation separation. Journal of Colloid and Interface Science. 2018;512:39-46. https://doi.org/10.1016/j.jcis.2017.10.045.

113. Bjorklund RB, Arwin H. Distribution of an adsorbed anionic surfactant on the external and internal surfaces of a porous apatite mineral. Minerals Engineering. 1993;6(8-10):895-906. https://doi.org/10.1016/0892-6875(93)90062-R.

114. Nunes APL, Peres AEC, Chaves AP, Ferreira WR. Effect of alkyl chain length of amines on fluorapatite and aluminium phosphates floatabilities. Journal of Materials Research and Technology. 2019;8(4):3623-34. https://doi.org/10.1016/j.jmrt.2019.05.025.

115. Ding K, Laskowski JS. Application of a modified water glass in a cationic flotation of calcite and dolomite. Canadian Metallurgical Quarterly. 2006;45(2):199-206. https://doi.org/10.1179/cmq.2006.45.2.199.

116. Vu HP, Nguyen LN, Lesage G, Nghiem LD. Synergistic effect of dual flocculation between inorganic salts and chitosan on harvesting microalgae Chlorella vulgaris. Environmental Technology & Innovation. 2020;17:100622. https://doi.org/10.1016/j.eti.2020.100622.

117. Sun Y, Zhou S, Sun W, Zhu S, Zheng H. Flocculation activity and evaluation of chitosan-based flocculant CMCTS-g-P(AM-CA) for heavy metal removal. Separation and Purification Technology. 2020;241:116737. https://doi.org/10.1016/j.seppur.2020.116737.

118. Sun Y, Zhou S, Pan S-Y, Zhu S, Yu Y, Zheng H. Performance evaluation and optimization of flocculation process for removing heavy metal. Chemical Engineering Journal. 2020;385:123911. https://doi.org/10.1016/j.cej.2019.123911.

119. Feng X, Wan J, Deng J, Qin W, Zhao N, Luo X, He M, Chen X. Preparation of acrylamide and carboxymethyl cellulose graft copolymers and the effect of molecular weight on the flocculation properties in simulated dyeing wastewater under different pH conditions. International Journal of Biological Macromolecules. 2019;155:1142-56. https://doi.org/10.1016/j.ijbiomac.2019.11.081.

120. Pérez-Calderón J, Santos MV, Zaritzky N. Optimal clarification of emulsified oily wastewater using a surfactant/chitosan biopolymer. Journal of Environmental Chemical Engineering. 2018;6(4):3808-18. https://doi.org/10.1016/j.jece.2018.06.004.

121. Besra L, Sengupta DK, Roy SK, Ay P. Influence of surfactants on flocculation and dewatering of kaolin suspensions by cationic polyacrylamide (PAM-C) flocculant. Separation and Purification Technology. 2003;30(3):251-64. https://doi.org/10.1016/S1383-5866(02)00164-8.

122. Tunç MS, Hanay Ö, Yıldız B. Adsorption of chlortetracycline from aqueous solution by chitin. Chemical Engineering Communications. 2019;207(8):1138-47. https://doi.org/10.1080/00986445.2019.1677628.

123. Chakraborty R, Asthana A, Singh AK, Jain B, Susan ABH. Adsorption of heavy metal ions by various low-cost adsorbents: a review. International Journal of Environmental Analytical Chemistry. 2020;10:1-38. https://doi.org/10.1080/03067319.2020.1722811.

124. Salmani Nuri O, Irannajad M, Mehdilo A. Reagent adsorption on modified mineral surfaces: isotherm, kinetic and thermodynamic aspects. Journal of Molecular Liquids. 2019;291:111311. https://doi.org/10.1016/j.molliq.2019.111311.

125. Chang Z, Chen X, Peng Y. The adsorption behavior of surfactants on mineral surfaces in the presence of electrolytes – A critical review. Minerals Engineering. 2018;121:66-76. https://doi.org/10.1016/j.mineng.2018.03.002.

126. Mielczarski E, Mielczarski JA, Cases JM, Rai B, Pradip. Influence of solution conditions and mineral surface structure on the formation of oleate adsorption layers on fluorite. Colloids and Surfaces A: Physicochemical and Engineering Aspects. 2002;205(1-2):73-84. https://doi.org/10.1016/S0927-7757(01)01150-5.

127. Free ML, Miller JD. The significance of collector colloid adsorption phenomena in the fluorite/oleate flotation system as revealed by FTIR/IRS and solution chemistry analysis. International Journal of Mineral Processing. 1996;48(3-4):197-216. https://doi.org/10.1016/S0301-7516(96)00027-0.

128. Mielczarski E, Donato P, Mielczarski JA, Cases JM, Barres O, Bouquet E. Solution Chemistry in Adsorption Layer Formation of Oleate on Fluorite. Journal of

Colloid and Interface Science. 2000;226(2):269-76. https://doi.org/10.1006/jcis.2000.6793.

129. Chennakesavulu K, Raju GB, Prabhakar S, Nair CM, Murthy KVGK. Adsorption of oleate on fluorite surface as revealed by atomic force microscopy. International Journal of Mineral Processing. 2009;90(1-4):101-4. https://doi.org/10.1016/j.minpro.2008.10.011.

130. Filippova IV, Filippov LO, Lafhaj Z, Barres O, Fornasiero D. Effect of calcium minerals reactivity on fatty acids adsorption and flotation. Colloids and Surfaces A: Physicochemical and Engineering Aspects. 2018;545:157-66. https://doi.org/10.1016/j.colsurfa.2018.02.059.

131. Pugh R, Stenius P. Solution chemistry studies and flotation behaviour of apatite, calcite and fluorite minerals with sodium oleate collector. International Journal of Mineral Processing. 1985;15(3):193-218. https://doi.org/10.1016/0301-7516(85)90035-3.

132. Zhen W. The adsorption of oleate on powellite and fluorapatite: A joint experimental and theoretical simulation study. Applied Surface Science. 2017;409:65-70. https://doi.org/10.1016/j.apsusc.2017.02.227.

133. Yehia A, Miller JD, Ateya BG. Analysis of the adsorption behaviour of oleate on some synthetic apatites. Minerals Engineering. 1993;6(1):79-86. https://doi.org/10.1016/0892-6875(93)90165-J.

134. Ye J, Zhang Q, Li X, Wang X, Ke B, Li X, Shen Z. Effect of the morphology of adsorbed oleate on the wettability of a collophane surface. Applied Surface Science. 2018;444:87-96, https://doi.org/10.1016/j.apsusc.2018.03.020.

135. Gamage McEvoy J, Thibault Y. Impact of crystal chemistry properties on the collector-mineral interactions observed for REE orthophosphates and oxides. Applied Surface Science. 2019;466:970-81. https://doi.org/10.1016/j.apsusc.2018.10.103.

136. Young CA , Miller JD. Effect of temperature on oleate adsorption at a calcite surface: an FT-NIR/IRS study and review. International Journal of Mineral Processing. 2000;58(1-4):331-50. https://doi.org/10.1016/S0301-7516(99)00057-5.

137. Chamerois M, François M, Villiéras F, Yvon J. Modification of calcium carbonate surface properties: macroscopic and microscopic investigations. Journal of Adhesion Science and Technology. 1999;13(12):1481-93. https://doi.org/10.1163/156856199X00604.

138. Antti BM, Forssberg E. Pulp chemistry in calcite flotation. Modelling of oleate adsorption using theoretical equilibrium calculations. Minerals Engineering. 1989;2(1):93-109. https://doi.org/10.1016/0892-6875(89)90068-X.

139. Zhang H, Han C, Liu W, Hou D, Wei D. The chain length and isomeric effects of monohydric alcohols on the flotation of magnesite and dolomite by sodium oleate. Journal of Molecular Liquids. 2019;276:471-79. https://doi.org/10.1016/j.molliq.2018.11.143.

140. Espiritu ERL, Waters KE. Flotation studies of monazite and dolomite. Minerals Engineering. 2018;116:101-06. https://doi.org/10.1016/j.mineng.2017.02.010.

141. Araújo ACA, Lima RMF. Influence of cations Ca2+, Mg2+ and Zn2+ on the flotation and surface charge of smithsonite and dolomite with sodium oleate and sodium silicate. International Journal of Mineral Processing. 2017;167:35-41. https://doi.org/10.1016/j.minpro.2017.08.001.

142. Wang Y, Ahmed Khoso S, Luo X, Tian M. Understanding the depression mechanism of citric acid in sodium oleate flotation of Ca2+ activated quartz: Experimental and DFT study. Minerals Engineering. 2019;140:105878. https://doi.org/10.1016/j.mineng.2019.105878.

143. Wang Z, Wu H, Xu Y, Shu K, Fang S, Xu L. The effect of dissolved calcite species on the flotation of bastnaesite using sodium oleate. Minerals Engineering. 2020;145:106095. https://doi.org/10.1016/j.mineng.2019.106095.

144. Rath SS, Sinha N, Sahoo H, Das B, Mishra BK. Molecular modeling studies of oleate adsorption on iron oxides. Applied Surface Science. 2014;295:115-22. https://doi.org/10.1016/j.apsusc.2014.01.014.

145. Castro FHB, Borrego AG. The influence of temperature during flotation of celestite and calcite with sodium oleate and quebracho. International Journal of Mineral Processing. 1996;46(1-2):35-52. https://doi.org/10.1016/0301-7516(95)00059-3.

146. Pascoe RD, Doherty E. Shear flocculation and flotation of hematite using sodium oleate. International Journal of Mineral Processing. 1997;51(1-4):269-82 https://doi.org/10.1016/S0301-7516(97)00033-1.

147. Pereira E, Meirelles AJA, Maximo GJ. Predictive models for physical properties of fats, oils, and biodiesel fuels. Fluid Phase Equilibria. 2020;508:112440. https://doi.org/10.1016/j.fluid.2019.112440.

148. Liu W, Wang X, Miller JD. Collector Chemistry for Bastnaesite Flotation - Recent Developments. Mineral Processing and Extractive Metallurgy Review. 2019;40(6):370-9. https://doi.org/10.1080/08827508.2019.1647840.

149. Hernáinz F, Calero M, Blázquez G. Flotation of low-grade phosphate ore. Advanced Powder Technology. 2004;15(4):421-33. https://doi.org/10.1163/1568552041270491.

150. Sis H, Chander S. Adsorption and contact angle of single and binary mixtures of surfactants on apatite. Minerals Engineering. 2003;16(9):839-48. https://doi.org/10.1016/S0892-6875(03)00202-4.

151. Yang B, Huang P, Song S, Luo H, Zhang Y. Hydrophobic agglomeration of apatite fines induced by sodium oleate in aqueous solutions. Results in Physics. 2018;9:970-7. https://doi.org/10.1016/j.rinp.2018.03.049.

152. Atrafi A, Gomez CO, Finch JA, Pawlik M. Frothing behavior of aqueous solutions of oleic acid. Minerals Engineering. 2012;36-38:138-44. https://doi.org/10.1016/j.mineng.2012.03.020.

153. Hassanzadeh A, Hoang DH, Brockmann M. Assessment of flotation kinetics modeling using information criteria; case studies of elevated-pyritic copper sulfide and high-grade carbonaceous sedimentary apatite ores. Journal of Dispersion Science and Technology. 2020;40:1083-94. https://doi.org/10.1080/01932691.2019.1656640.

154. Hanumantha Rao K, Forssberg KSE. Mechanism of fatty acid adsorption in salt-type mineral flotation. Minerals Engineering. 1991;4(7-11):879-90. https://doi.org/10.1016/0892-6875(91)90071-3.

155. Antti BM, Forssberg E. Pulp chemistry in industrial mineral flotation. Studies of surface complex on calcite and apatite surfaces using FTIR spectroscopy. Minerals Engineering. 1989;2(2):217-27. https://doi.org/10.1016/0892-6875(89)90042-3.

156. O'Connor CT, Dunne RC, Martalas A. The adsorption of oleate and the guar-based gum, acrol LG-21, onto apatite and calcite. Colloids and Surfaces. 1987;27(4):357-65. https://doi.org/10.1016/0166-6622(87)80157-9.

157. Shu X, Meng Y, Wan L, Li G, Yang M, Jin W. pH-Responsive Aqueous Foams of Oleic Acid/Oleate Solution. Journal of Dispersion Science and Technology. 2014;35(2):293-300. https://doi.org/10.1080/01932691.2013.785363.

158. Wang Y, Lu D, Wang L. Flotation separation of limonite from calcite with sodium oleate: effects of calcite dissolution and addition of sodium pyrophosphate. Mineral Processing and Extractive Metallurgy. 2019;128(4):207-12. https://doi.org/10.1080/03719553.2018.1424684.

159. Li Z, Rao F, Guo B, Zuo W, Song S, López-Valdivieso A. Effects of calcium ions on malachite flotation with octyl hydroxamate. Minerals Engineering. 2019;141:105854. https://doi.org/10.1016/j.mineng.2019.105854.

160. Tanhua A, Sinche-Gonzalez M, Kalapudas R, Tanskanen P, Lamberg P. Effect of waste rock dilution on spodumene flotation. Minerals Engineering. 2020;150:106282. https://doi.org/10.1016/j.mineng.2020.106282.

161. Wang Z, Wu H, Xu Y, Shu K, Yang J, Luo L, Xu L. Effect of dissolved fluorite and barite species on the flotation and adsorption behavior of bastnaesite. Separation and Purification Technology. 2020;237:116387. https://doi.org/10.1016/j.seppur.2019.116387.

162. Zhang Z, Cao Y, Ma Z, Liao Y. Impact of calcium and gypsum on separation of scheelite from fluorite using sodium silicate as depressant. Separation and

Purification Technology. 2019;215:249-58. https://doi.org/10.1016/j.seppur.2019.01.021.

163. Foucaud Y, Filippova IV, Filippov LO. Investigation of the depressants involved in the selective flotation of scheelite from apatite, fluorite, and calcium silicates: Focus on the sodium silicate/sodium carbonate system. Powder Technology. 2019;352:501-12. https://doi.org/10.1016/j.powtec.2019.04.071.

164. Wang Z, Wang L, Zheng Y, Xiao J. Role of calcium dioleate in the flotation of powellite particles using oleate. Minerals Engineering. 2019;138:95-100. https://doi.org/10.1016/j.mineng.2019.04.040.

165. Nunes APL, Peres AEC, Valadão GES. The Influence of Lattice Ions on the Electrokinetic Potential of Primary and Secondary Phosphates. Separation Science and Technology. 2015;50(13):2023-31. https://doi.org/10.1080/01496395.2015.1004347.

166. Amankonah JO, Somasundaran P, Ananthapadmabhan KP. Effects of dissolved mineral species on the dissolution/ precipitation characteristics of calcite and apatite. Colloids and Surfaces. 1985;15:295-307. https://doi.org/10.1016/0166-6622(85)80080-9.

167. Rao KH, Antti B-M, Forssberg E. Mechanism of oleate interaction on salt-type minerals, Part II. Adsorption and electrokinetic studies of apatite in the presence of sodium oleate and sodium metasilicate. International Journal of Mineral Processing. 1990;28(1-2):59-79. https://doi.org/10.1016/0301-7516(90)90027-V.

168. Somasundaran P, Amankonah JO, Ananthapadmabhan KP. Mineral-solution equilibria in sparingly soluble mineral systems. Colloids and Surfaces. 1985;15:309-33. https://doi.org/10.1016/0166-6622(85)80081-0.

169. Amankonah JO, Somasundaran P. Effects of dissolved mineral species on the electrokinetic behavior of calcite and apatite. Colloids and Surfaces. 1985;15:335-53. https://doi.org/10.1016/0166-6622(85)80082-2.

170. Chen C, Hu Y, Zhu H, Sun W, Qin W, Liu R, Gao Z. Inhibition performance and adsorption of polycarboxylic acids in calcite flotation. Minerals Engineering. 2019;133:60-8. https://doi.org/10.1016/j.mineng.2018.12.027.

171. Dong L, Wei Q, Qin W, Jiao F. Selective adsorption of sodium polyacrylate on calcite surface: Implications for flotation separation of apatite from calcite. Separation and Purification Technology. 2020;241:116415. https://doi.org/10.1016/j.seppur.2019.116415.

172. Chen Y, Tang X. Selective flotation separation of smithsonite from calcite by application of amino trimethylene phosphonic acid as depressant. Applied Surface Science. 2020;512:145663. https://doi.org/10.1016/j.apsusc.2020.145663.

173. Gao J, Hu Y, Sun W, Liu R, Gao Z, Han H, Lyu F, Jiang W. Enhanced separation of fluorite from calcite in acidic condition. Minerals Engineering. 2019;133:103-5. https://doi.org/10.1016/j.mineng.2019.01.013.

174. Yu J, Ge Y, Guo X, Guo W. The depression effect and mechanism of NSFC on dolomite in the flotation of phosphate ore. Separation and Purification Technology. 2016;161:88-95. https://doi.org/10.1016/j.seppur.2016.01.044.

175. Ghosh C, Sinhamahapatra S, Tripathi HS, Sarkar U. Reverse Flotation of Natural Magnesite and Process Optimization Using Response Surface Methodology. Transactions of the Indian Ceramic Society. 2020;79(1):23-9. https://doi.org/10.1080/0371750X.2019.1699864.

176. Pan Z, Wang Y, Wei Q, Chen X, Jiao F, Qin W. Effect of sodium pyrophosphate on the flotation separation of calcite from apatite. Separation and Purification Technology. 2020;242:116408. https://doi.org/10.1016/j.seppur.2019.116408.

177. Zheng X, Arps PJ, Smith RW. Adsorption of Bacillus subtilis to minerals: effect on the flotation of dolomite and apatite. Process Metallurgy. 1999; 9: 127-36. https://doi.org/10.1016/S1572-4409(99)80012-1.

178. Zhong K, Vasudevan TV, Somasundaran P. Beneficiation of a high dolomitic phosphate ore: A bench scale optimization study. Minerals Engineering. 1991;4(5-6):563-71. https://doi.org/10.1016/0892-6875(91)90003-E.

179. Silva AC, Cara DVC, Silva EMS, Leal GS, Machado AM, da Silva LM. Apatite flotation using saponified baker's yeast cells (Saccharomyces cerevisiae) as a bioreagent. Journal of Materials Research and Technology. 2019;8(1):752-58. https://doi.org/10.1016/j.jmrt.2018.05.018.

180. Urbina RH. Recent developments and advances in formulations and applications of chemical reagents used in froth flotation. Mineral Processing and Extractive Metallurgy Review. 2003;24(2):139-82. https://doi.org/10.1080/08827500306898.

181. Khalek MAA. Separation of dolomite from phosphate minerals by flotation with a new amphoteric surfactant as collector. Mineral Processing and Extractive Metallurgy. 2001;110(2):89-93. https://doi.org/10.1179/mpm.2001.110.2.89.

182. Tripathy DB, Mishra A, Clark J, Farmer T. Synthesis, chemistry, physicochemical properties and industrial applications of amino acid surfactants: A review. Comptes Rendus Chimie. 2018;21(2):112-30. https://doi.org/10.1016/j.crci.2017.11.005.

183. Wang L, Tian M, Khoso SA, Hu Y, Sun W, Gao Z. Improved Flotation Separation of Apatite from Calcite with Benzohydroxamic Acid Collector. Mineral Processing and Extractive Metallurgy Review. 2019;40(6):427-36. https://doi.org/10.1080/08827508.2019.1666126.

184. Tang Y, Yin W, Kelebek S. Magnesite-dolomite separation using potassium cetyl phosphate as a novel flotation collector and related surface chemistry. Applied Surface Science. 2020;508:145191. https://doi.org/10.1016/j.apsusc.2019.145191.

185. Patra A, Taner HA, Bordes R, Holmberg K, Larsson AC. Selective flotation of calcium minerals using double-headed collectors. Journal of Dispersion Science and Technology. 2019;40(8):1205-16. https://doi.org/10.1080/01932691.2018.1503547.

186. Tang Y, Yin W, Kelebek S. Selective flotation of magnesite from calcite using potassium cetyl phosphate as a collector in the presence of sodium silicate. Minerals Engineering. 2020;146:106154. https://doi.org/10.1016/j.mineng.2019.106154.

187. Jong K, Han Y, Ryom S. Flotation mechanism of oleic acid amide on apatite. Colloids and Surfaces A: Physicochemical and Engineering Aspects. 2017;523:127-31. https://doi.org/10.1016/j.colsurfa.2016.11.038.

188. Pedain K-U, Bezuidenhout J, Lipowsky G. Synergistic Effects of Environmentally Friendly Collectors in the Preconcentration Step of a Double Float Process on Sedimentary Phosphate Ore. Procedia Engineering. 2014;83:139-47. https://doi.org/10.1016/j.proeng.2014.09.031.

189. Jong K, Paek I, Kim Y, Li I, Jang D. Flotation mechanism of a novel synthesized collector from Evodiaefructus onto fluorite surfaces. Minerals Engineering. 2020;146:106017. https://doi.org/10.1016/j.mineng.2019.106017.

190. García AC, Latifi M, Chaouki J. Kinetics of calcination of natural carbonate minerals. Minerals Engineering. 2020;150:106279. https://doi.org/10.1016/j.mineng.2020.106279.

191. Deng R, Huang Y, Hu Y, Ku J, Zuo W, Yin W. Study of reverse flotation of calcite from scheelite in acidic media. Applied Surface Science. 2018;439:139-47. https://doi.org/10.1016/j.apsusc.2017.12.231.

192. Filippov LO, Kaba OB, Filippova IV. Surface analyses of calcite particles reactivity in the presence of phosphoric acid. Advanced Powder Technology. 2019;30(10):2117-25. https://doi.org/10.1016/j.apt.2019.06.026.

193. Hoang DH, Hassanzadeh A, Peuker UA, Rudolph M. Impact of flotation hydrodynamics on the optimization of fine-grained carbonaceous sedimentary apatite ore beneficiation. Powder Technology. 2019;345:223-33. https://doi.org/10.1016/j.powtec.2019.01.014.

194. Li G, Liu J, Cao Y, Wang D. Effect of a cyclonic flotation column on the separation of magnesium from phosphate ore. Mining Science and Technology (China). 2011;21(5):647-50. https://doi.org/10.1016/j.mstc.2011.10.009.

195. Mohammadkhani M, Noaparast M, Shafaei SZ, Amini A, Amini E, Abdollahi H. Double reverse flotation of a very low grade sedimentary phosphate rock, rich in carbonate and silicate. International Journal of Mineral Processing. 2011;100(3-4):157-65. https://doi.org/10.1016/j.minpro.2011.06.001.

196. Albuquerque RO, Peres AEC, Aquino JA, Praes PE, Pereira CA. Pilot Scale Direct Flotation of a Phosphate Ore with Silicate-Carbonate Gangue. Procedia Engineering. 2012;46:105-10. https://doi.org/10.1016/j.proeng.2012.09.452.

197. Al-Fariss TF, El-Nagdy KA, Abd El-Aleem FA, El-Midany AA. Column versus Mechanical Flotation for Calcareous Phosphate Fines Upgrading. Particulate Science and Technology. 2013;31(5):488-93. https://doi.org/10.1080/02726351.2013.776999.

198. Boulos TR, Yehia A, Ibrahim SS, Yassin KE. A modification in the flotation process of a calcareous–siliceous phosphorite that might improve the process economics. Minerals Engineering. 2014;69:97-101. https://doi.org/10.1016/j.mineng.2014.07.017.

199. Abdel-Khalek NA. Evaluation of flotation strategies for sedimentary phosphates with siliceous and carbonates gangues. Minerals Engineering. 2000;13(7):789-93. https://doi.org/10.1016/S0892-6875(00)00064-9.

200. Guimarães RC, Peres AEC. Interfering ions in the flotation of a phosphate ore in a batch column. Minerals Engineering. 1999;12(7):757-68. https://doi.org/10.1016/S0892-6875(99)00062-X.

201. Rootare HM, Deitz VR, Carpenter FG. Solubility product phenomena in hydroxyapatite-water systems. Journal of Colloid Science. 1962;17(3):179-206. https://doi.org/10.1016/0095-8522(62)90035-1.

202. Yehia A, Youseff MA, Boulos TR. Different alternatives for minimizing the collector consumption in phosphate fatty acid flotation. Minerals Engineering. 1990;3(3-4):273-78. https://doi.org/10.1016/0892-6875(90)90122-R.

203. Ananthapadmanabhan KP, Somasundaran P. Surface precipitation of inorganics and surfactants and its role in adsorption and flotation. Colloids and Surfaces. 1985;13:151-67. https://doi.org/10.1016/0166-6622(85)80014-7.

204. Oliveira P, Mansur H, Mansur A, Silva Gd, Peres AEC. Apatite flotation using pataua palm tree oil as collector. Journal of Materials Research and Technology. 2019;8(5):4612-19. https://doi.org/10.1016/j.jmrt.2019.08.005.

205. Yu H, Wang H, Sun C. Comparative studies on phosphate ore flotation collectors prepared by hogwash oil from different regions. International Journal of Mining Science and Technology. 2018;28(3):453-59. https://doi.org/10.1016/j.ijmst.2018.04.010.

206. Liu X, Li C, Luo H, Cheng R, Liu F. Selective reverse flotation of apatite from dolomite in collophanite ore using saponified gutter oil fatty acid as a collector. International Journal of Mineral Processing. 2017;165:20-27. https://doi.org/10.1016/j.minpro.2017.06.004.

207. Zhu X-n, Lyu X-j, Wang Q, Qiu J, Wang S-s, Liu X-y, Li L. Clean utilization of waste oil: Soap collectors prepared by alkaline hydrolysis for fluorite flotation. Journal of Cleaner Production. 2019;240:118179. https://doi.org/10.1016/j.jclepro.2019.118179.

208. Zhu X-n, Wang D-z, Ni Y, Wang J-x, Nie C-c, Yang C, Lyu X-j, Qiu J, Li L. Cleaner approach to fine coal flotation by renewable collectors prepared by waste

oil transesterification. Journal of Cleaner Production. 2020;252:119822. https://doi.org/10.1016/j.jclepro.2019.119822.

209. Han DY, Yu WQ, Luo KY, Cao ZB. Study on the process of oil recovery from oil sludge and tailing oil sands by blending extraction. Petroleum Science and Technology. 2019;37(22):2269-74. https://doi.org/10.1080/10916466.2019.1633347.

210. Srinivas K, Sekhar DMR. Comparative Study of Jhamarkotra Soap Emulsion and Tall Oil Soap Emulsion as Flotation Collectors. Indian Chemical Engineer. 2010;52(3):248-53. https://doi.org/10.1080/00194506.2010.547973.

211. Guimarães RC, Araujo AC, Peres AEC. Reagents in igneous phosphate ores flotation. Minerals Engineering. 2005;18(2):199-204. https://doi.org/10.1016/j.mineng.2004.08.022.

212. Kou J, Tao D, Xu G. Fatty acid collectors for phosphate flotation and their adsorption behavior using QCM-D. International Journal of Mineral Processing. 2010;95(1-4):1-9. https://doi.org/10.1016/j.minpro.2010.03.001.

213. Silva KLC, Silva MMC, Moraes MM, Camara CAG, Santos ML, Fagg CW. Chemical composition and acaricidal activity of essential oils from two species of the genus Bauhinia that occur in the Cerrado biome in Brazil. Journal of Essential Oil Research. 2020;32(1):23-31. https://doi.org/10.1080/10412905.2019.1662338.

214. Teixeira N, Melo JCS, Batista LF, Paula-Souza J, Fronza P, Brandão MGL. Edible fruits from Brazilian biodiversity: A review on their sensorial characteristics versus bioactivity as tool to select research. Food Research International. 2019;119:325-48. https://doi.org/10.1016/j.foodres.2019.01.058.

215. Razak DM, Syahrullail S, Sapawe N, Azli Y, Nuraliza N. A New Approach Using Palm Olein, Palm Kernel Oil, and Palm Fatty Acid Distillate as Alternative Biolubricants: Improving Tribology in Metal-on-Metal Contact. Tribology Transactions. 2015;58(3):511-17. https://doi.org/10.1080/10402004.2014.989348.

216. Pentyala V-B, Eapen S. High efficiency phytoextraction of uranium using Vetiveria zizanioides L. Nash. International Journal of Phytoremediation. 2020;22(11):1137-46. doi: 10.1080/15226514.2020.1741506.

217. Cao Q, Cheng J, Wen S, Li C, Bai S, Liu D. A mixed collector system for phosphate flotation. Minerals Engineering. 2015;78:114-21. https://doi.org/10.1016/j.mineng.2015.04.020.

218. Santos EP, Dutra AJB, Oliveira JF. The effect of jojoba oil on the surface properties of calcite and apatite aiming at their selective flotation. International Journal of Mineral Processing. 2015;143:34-38. https://doi.org/10.1016/j.minpro.2015.08.002.

219. Silva AC, Silva EMS, Silva TC, Alves BE. Apatite microflotation using pequi oil. Mineral Processing and Extractive Metallurgy. 2015;124(4):233-39. https://doi.org/10.1179/1743285515Y.0000000015.

220. Xu L, Jiao F, Jia W, Pan Z, Hu C, Qin W. Selective flotation separation of spodumene from feldspar using mixed anionic/nonionic collector. Colloids and Surfaces A: Physicochemical and Engineering Aspects. 2020;594:124605. https://doi.org/10.1016/j.colsurfa.2020.124605.

221. Buckley AN, Hope GA, Parker GK, Steyn J, Woods R. Mechanism of mixed dithiophosphate and mercaptobenzothiazole collectors for Cu sulfide ore minerals. Minerals Engineering. 2017;109:80-97. https://doi.org/10.1016/j.mineng.2017.03.002.

222. Wu H, Tian J, Xu L, Fang S, Zhang Z, Chi R. Flotation and adsorption of a new mixed anionic/cationic collector in the spodumene-feldspar system. Minerals Engineering. 2018;127:42-7. https://doi.org/10.1016/j.mineng.2018.07.024.

223. Wang Z, Wang L, Wang J, Xiao J, Liu J, Xu L, Fu K. Strengthened floatation of molybdite using oleate with suitable co-collector. Minerals Engineering. 2018;122:99-105. https://doi.org/10.1016/j.mineng.2018.03.042.

224. Shen L, Zhu J, Liu L, Wang H. Flotation of fine kaolinite using dodecylamine chloride/fatty acids mixture as collector. Powder Technology. 2017;312:159-65. https://doi.org/10.1016/j.powtec.2017.02.032.

225. Tijsseling LT, Dehaine Q, Rollinson GK, Glass HJ. Flotation of mixed oxide sulphide copper-cobalt minerals using xanthate, dithiophosphate, thiocarbamate and blended collectors. Minerals Engineering. 2019;138:246-56. https://doi.org/10.1016/j.mineng.2019.04.022.

226. Luo Y, Zhang G, Mai Q, Liu H, Li C, Feng H. Flotation separation of smithsonite from calcite using depressant sodium alginate and mixed cationic/anionic collectors. Colloids and Surfaces A: Physicochemical and Engineering Aspects. 2020;586:124227. https://doi.org/10.1016/j.colsurfa.2019.124227.

227. Liu Z, Xia Y, Lai Q, An M, Liao Y, Wang Y. Adsorption behavior of mixed dodecane/n-valeric acid collectors on low-rank coal surface: Experimental and molecular dynamics simulation study. Colloids and Surfaces A: Physicochemical and Engineering Aspects. 2019;583:123840. https://doi.org/10.1016/j.colsurfa.2019.123840.

228. Zhang L, Sun X, Li B, Xie Z, Guo J, Liu S. Experimental and molecular dynamics simulation study on the enhancement of low rank coal flotation by mixed collector. Fuel. 2020;266:117046. https://doi.org/10.1016/j.fuel.2020.117046.

229. Dong L, Jiao F, Qin W, Zhu H, Jia W. Effect of acidified water glass on the flotation separation of scheelite from calcite using mixed cationic/anionic collectors. Applied Surface Science. 2018;444:747-56. https://doi.org/10.1016/j.apsusc.2018.03.097.

230. Yang Z, Teng Q, Liu J, Yang W, Hu D, Liu S. Use of NaOL and CTAB mixture as collector in selective flotation separation of enstatite and magnetite. Colloids and Surfaces A: Physicochemical and Engineering Aspects. 2019;570:481-86. https://doi.org/10.1016/j.colsurfa.2019.03.064.

231. El-Midany AA, Arafat Y. Enhancing Phosphate Grade Using Oleic Acid–Sodium Dodecyl Sulfate Mixtures. Chemical Engineering Communications. 2016;203(5):660-65. https://doi.org/10.1080/00986445.2015.1078797.

232. Cao Q, Cheng J, Wen S, Li C, Liu J. Synergistic effect of dodecyl sulfonate on apatite flotation with fatty acid collector. Separation Science and Technology. 2016;51(8):1389-96. https://doi.org/10.1080/01496395.2016.1147467.

233. Li Z, Rao F, Escudero García R, Li H, Song S. Partial replacement of sodium oleate using alcohols with different chain structures in malachite flotation. Minerals Engineering. 2018;127:185-90. https://doi.org/10.1016/j.mineng.2018.08.022.

234. Sis H, Chander S. Improving froth characteristics and flotation recovery of phosphate ores with nonionic surfactants. Minerals Engineering. 2003;16(7):587-95. https://doi.org/10.1016/S0892-6875(03)00137-7.

235. Wang L, Hu G, Sun W, Khoso SA, Liu R, Zhang X. Selective flotation of smithsonite from dolomite by using novel mixed collector system. Transactions of Nonferrous Metals Society of China. 2019;29(5):1082-89. https://doi.org/10.1016/S1003-6326(19)65016-8

236. Xu Y, Xu L, Wu H, Wang Z, Shu K, Fang S, Zhang Z. Flotation and co–adsorption of mixed collectors octanohydroxamic acid/sodium oleate on bastnaesite. Journal of Alloys and Compounds. 2020;819:152948. https://doi.org/10.1016/j.jallcom.2019.152948.

237. Abaka-Wood GB, Zanin M, Addai-Mensah J, Skinner W. The upgrading of rare earth oxides from iron-oxide silicate rich tailings: Flotation performance using sodium oleate and hydroxamic acid as collectors. Advanced Powder Technology. 2018;29(12):3163-72. https://doi.org/10.1016/j.apt.2018.08.019.

238. Filippov LO, Filippova IV, Lafhaj Z, Fornasiero D. The role of a fatty alcohol in improving calcium minerals flotation with oleate. Colloids and Surfaces A: Physicochemical and Engineering Aspects. 2019;560:410-7. https://doi.org/10.1016/j.colsurfa.2018.10.022.

239. Filippov LO, Foucaud Y, Filippova IV, Badawi M. New reagent formulations for selective flotation of scheelite from a skarn ore with complex calcium minerals gangue. Minerals Engineering. 2018;123:85-94. https://doi.org/10.1016/j.mineng.2018.05.001.

240. Somasundaran P. The role of ionomolecular surfactant complexes in flotation. International Journal of Mineral Processing. 1976;3(1):35-40. https://doi.org/10.1016/0301-7516(76)90013-2.

241. Kung HC, Goddard ED. Molecular association in pairs of long-chain compounds. IV. Influence of cation and the hydroxyl position on the alkyl sulfate, alkyl alcohol association. Journal of Colloid Science. 1965;20(7):766-76. https://doi.org/10.1016/0095-8522(65)90050-4.

242. Kung HC, Goddard ED. Studies of molecular association in pairs of long-chain compounds by differential thermal analysis. i. lauryl and myristyl alcohols and sulfates. The Journal of Physical Chemistry. 1963;67(10):1965-69. https://doi.org/10.1021/j100804a601.

243. Kung HC, Goddard ED. Molecular association in fatty acid potassium soap systems. II. Journal of Colloid and Interface Science. 1969;29(2):242-49. https://doi.org/10.1016/0021-9797(69)90193-3.

244. Kulkarni RD, Somasundaran P. Kinects of oleate adsorption at liquid/air interface and its role in hematite flotation. Advances in Interfacial Phenomen. 1975;71(150)124-33.

245. Kung HC, Goddard ED. Interaction of amines and amine hydrochlorides. Kolloid-Zeitschrift und Zeitschrift für Polymere. 1969;232:812-3. https://doi.org/10.1007/BF01500660.

246. Mena CF, Arsel M, Pellegrini L, Orta-Martinez M, Fajardo P, Chavez E, Guevara A, Espín P. Community-Based Monitoring of Oil Extraction: Lessons Learned in the Ecuadorian Amazon. Society and Natural Resources. 2020;33(3):406-17. https://doi.org/10.1080/08941920.2019.1688441.

247. Flores JA, Konrad O, Flores CR, Schroder NT. Inventory data on Brazilian Amazon′s non-wood native biomass sources for bioenergy production. Data in Brief. 2018;20:1935-41. https://doi.org/10.1016/j.dib.2018.09.050.

248. Urzedo DI, Neilson J, Fisher R, Junqueira RGP. A global production network for ecosystem services: The emergent governance of landscape restoration in the Brazilian Amazon. Global Environmental Change. 2020;61:102059. https://doi.org/10.1016/j.gloenvcha.2020.102059.

249. Valdetaro DCOF, Harrington TC, Oliveira LSS, Guimarães LMS, McNew DL, Pimenta LVA, Gonçalves RC, Schurt DA, Alfenas AC. A host specialized form of Ceratocystis fimbriata causes seed and seedling blight on native Carapa guianensis (andiroba) in Amazonian rainforests. Fungal Biology. 2019;123(2):170-82. https://doi.org/10.1016/j.funbio.2018.12.001.

250. Serra JL, Rodrigues AMC, Freitas RA, Meirelles AJA, Darnet SH, Silva LHM. Alternative sources of oils and fats from Amazonian plants: Fatty acids, methyl tocols, total carotenoids and chemical composition. Food Research International. 2019;116:12-9. https://doi.org/10.1016/j.foodres.2018.12.028.

251. Bataglion GA, Silva FMA, Santos JM, Santos FN, Barcia MT, Lourenço CC, Salvador MJ, Godoy HT, Eberlin MN, Koolen HHF. Comprehensive characterization of lipids from Amazonian vegetable oils by mass spectrometry techniques. Food Research International. 2014;64:472-81. https://doi.org/10.1016/j.foodres.2014.07.011.

252. Pereira E, Ferreira MC, Sampaio KA, Grimaldi R, Meirelles AJA, Maximo GJ. Physical properties of Amazonian fats and oils and their blends. Food Chemistry. 2019;278:208-15. https://doi.org/10.1016/j.foodchem.2018.11.016.

253. Shaharum NSN, Shafri HZM, Ghani WAWAK, Samsatli S, Prince HM, Yusuf B, Hamud AM. Mapping the spatial distribution and changes of oil palm land cover using an open source cloud-based mapping platform. International Journal of Remote Sensing. 2019;40(19):7459-76. https://doi.org/10.1080/01431161.2019.1597311.

254. Chendynski LT, Cordeiro T, Messias GB, Mantovani ACG, Spacino KR, Zeraik ML, Borsato D. Evaluation and application of extracts of rosemary leaves, araçá pulp and peel of bacuri in the inhibition of the oxidation reaction of biodiesel. Fuel. 2020;261:116379. https://doi.org/10.1016/j.fuel.2019.116379.

255. Balick MJ, Gershoff SN. Nutritional evaluation of the Jessenia bataua palm: Source of high quality protein and oil from tropical America. Economic Botany. 1981;35(3):261-71. https://doi.org/10.1007/BF02859117.

256. Almeida AS, Vieira ICG, Moura N, Lees AC. Heterogeneity of tree diversity and carbon stocks in Amazonian oil palm landscapes. Plant Ecology and Diversity. 2020;13(1):105-13. https://doi.org/10.1080/17550874.2019.1710616.

257. Montúfar R, Laffargue A, Pintaud J-C, Hamon S, Avallone S, Dussert S. Oenocarpus bataua Mart. (Arecaceae): rediscovering a source of high oleic vegetable oil from Amazonia. Journal of the American Oil Chemists' Society. 2010;87:167-72. https://doi.org/10.1007/s11746-009-1490-4.

258. Hernández PBN, Fregapane G, Moya MDS. Bioactive compounds, volatiles and antioxidant activity of virgin seje oils (Jessenia bataua) from the Amazonas. Journal of Food Lipids. 2009;16(4):629-44. https://doi.org/10.1111/j.1745-4522.2009.01171.x.

259. Tsukamoto Y, Oya H, Kikuchi T, Yamada T, Tanaka R. Guianofruits C–I from fruit oil of andiroba (Carapa guianensis, Meliaceae). Tetrahedron. 2019;75(9):1149-56. https://doi.org/10.1016/j.tet.2018.12.036.

260. Novello Z, Scapinello J, Magro JD, Zin G, Luccio MD, Tres MV, Oliveira JV. Extraction, chemical characterization and antioxidant activity of andiroba seeds oil obtained from pressurized n-butane. Industrial Crops and Products. 2015;76:697-701. https://doi.org/10.1016/j.indcrop.2015.07.075.

261. Amaral LFG, Fierro IM. Profile of medicinal plants utilization through patent documents: The andiroba example. Revista Brasileira de Farmacognosia. 2013;23(4):716-22. https://doi.org/10.1590/S0102-695X2013005000046.

262. Roma GC, Camargo-Mathias MI, Nunes PH, Remédio RN, Faria AU, Bechara GH. Effects of andiroba (Carapa guianensis) oil in ticks: Ultrastructural analysis of the synganglion of Rhipicephalus sanguineus (Latreille, 1806) (Acari: Ixodidae). Acta Tropica. 2015;141(A):7-15. https://doi.org/10.1016/j.actatropica.2014.06.018.

263. Senhorini GA, Zawadzki SF, Farago PV, Zanin SMW, Marques FA. Microparticles of poly(hydroxybutyrate-co-hydroxyvalerate) loaded with andiroba oil: Preparation and characterization. Materials Science and Engineering: C. 2012;32(5):1121-26. https://doi.org/10.1016/j.msec.2012.02.027.

264. Júnior RNCM, Dolabela MF, Silva MN, Póvoa MM, Maia JGS. Antiplasmodial activity of the andiroba (Carapa guianensis Aubl., Meliaceae) oil and its limonoid-rich fraction. Journal of Ethnopharmacology. 2012;142(3):679-83. https://doi.org/10.1016/j.jep.2012.05.037.

265. Gaspar AS, Wagner FE, Amaral VS, Lima SAC, Khomchenko VA, Santos JG, Costa BFO, Durães L. Development of a biocompatible magnetic nanofluid by incorporating SPIONs in Amazonian oils. Spectrochimica Acta Part A: Molecular and Biomolecular Spectroscopy. 2017;172:135-46. https://doi.org/10.1016/j.saa.2016.04.022.

266. Hammer MLA, Johns EA. Tapping an Amazônian plethora: four medicinal plants of Marajó island, Pará (Brazil). Journal of Ethnopharmacology. 1993;40(1):53-75. https://doi.org/10.1016/0378-8741(93)90089-N.

267. Silva JAP, Cardozo NSM, Petzhold CL. Enzymatic synthesis of andiroba oil based polyol for the production of flexible polyurethane foams. Industrial Crops and Products. 2018;113:55-63. https://doi.org/10.1016/j.indcrop.2018.01.020.

268. Costa JS, Almeida AAC, Tomé AR, Citó AMGL, Saffi J, Freitas RM. Evaluation of possible antioxidant and anticonvulsant effects of the ethyl acetate fraction from Platonia insignis Mart. (Bacuri) on epilepsy models. Epilepsy and Behavior. 2011;22(4):678-84. https://doi.org/10.1016/j.yebeh.2011.09.021.

269. Silva BJM, Hage AAP, Silva EO, Rodrigues APD. Medicinal plants from the Brazilian Amazonian region and their antileishmanial activity: a review. Journal of Integrative Medicine. 2018;16(4):211-22. https://doi.org/10.1016/j.joim.2018.04.004.

270. Oliveira P, Oliveira AC, Pinto JKS, Costa DS, Paiva RS. Influência do método de saponificação de óleo vegetal amazônico na flotabilidade da apatita. Holos. 2014;3:284-90. https://doi.org/10.15628/holos.2014.1819.

271. Silva AC, Silva SEM, Rocha TWP. Microflotação de apatita utilizando óleo de castanha de macaúba (Acromia Aculeata) como coletor. Tecnologia em Metalurgia Materiais e Mineração. 2015;12(2):146-52. http://dx.doi.org/10.4322/2176-1523.0836.

3. Coletor de óleo de andiroba

Aplicação do óleo de Andiroba como um novo coletor na flotação de apatita

Nesse estudo, buscou-se avaliar o desempenho do coletor obtido a partir da saponificação do óleo de Andiroba na flotabilidade de apatita e carbonatos (calcita e dolomita), a partir de ensaios de microflotação em tubo de Hallimond modificado. Foram realizadas caracterizações das amostras minerais (DRX, WDXRF, FTIR e XPS) da amostra graxa (FTIR, Cromatografia Gasosa, Índices de acidez, saponificação e iodo) e do coletor obtido (FTIR, CMC), além de ensaios de caracterização da adsorção deste sobre os minerais (Mobilidade eletroforética e FTIR). Os ensaios varreram variáveis como tempo de condicionamento, pH do sistema e concentração da solução de coletor na flotabilidade dos minerais avaliados. Os resultados mostraram que a seletividade da flotação foi alcançada em uma faixa de pH próxima à neutralidade, com recuperação apatita superior a 90%. Na faixa alcalina (acima do pH 10), a queda na flotabilidade de minerais, principalmente apatita, já era esperada devido à adsorção de espécies diméricas. O tempo de condicionamento provou ser um fator importante para a seletividade do sistema, apresentando uma relação direta com a flutuabilidade do apatite, e indicando que a adsorção de AOC ocorreu por meio da quimiossorção. Entre os carbonatos, principalmente para dolomita, a investigação demonstrou uma adsorção menos efetiva do coletor, devido aos picos menos pronunciados nos espectros do FTIR e redução menos significativa no potencial zeta após interação com o coletor.

Application of Andiroba tree oil as novel collector in apatite flotation

Leandro Henrique Santos*, Luciano Fernandes de Magalhães, Gilberto Rodrigues da Silva and Antônio Eduardo Clark Peres

Department of Metallurgical and Materials Engineering
Universidade Federal de Minas Gerais (UFMG), Belo Horizonte, MG, Brazil

Graphical ABSTRACT

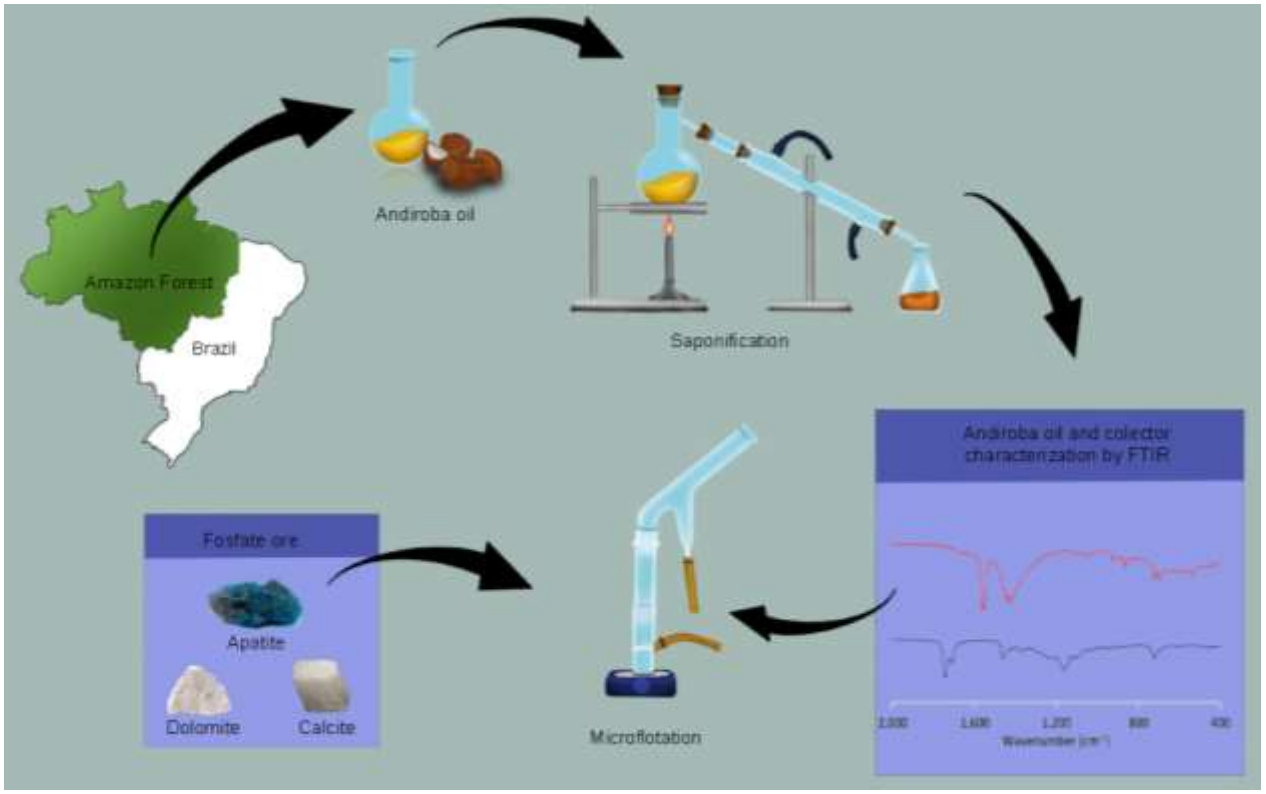

Figura 3.1 – Graphical abstract (Application of Andiroba tree oil as novel collector in apatite flotation)

ABSTRACT

Phosphate ores are highly complex, requiring sophisticated processing steps to meet the specifications of the fertilizer industry. Froth flotation is widely used in several phosphate ore concentration routes, using vegetable-origin fatty acid salts as collectors. In this scenario, the search for alternative sources with high accessibility, efficiency, and availability becomes strategic. In this work, Andiroba oil (Carapas guianensi) was evaluated regarding its physicochemical characteristics (fatty profile, acidity, saponification, and iodine indices) and the performance of its fatty acid salts as a selective apatite collector in the flotation from calcium and magnesium carbonate gangue minerals, commonly found in phosphate ores. The oil sample was found to be mainly composed of oleic and palmitic acid. The best selectivity between apatite and carbonates was obtained at pH 7.5 and 20mg.L^{-1} collector concentration, especially for the apatite-dolomite system. The zeta potential and FTIR results indicated that chemisorption and precipitation of calcium salts were the collector adsorption mechanism responsible for hydrophobization. The selectivity achieved was attributed to the difference in the conformation of the hydrophobic layers formed on the surface of each mineral, being related to the spatial arrangement and density of active sites. Andiroba oil proved to be promising as an apatite collector in flotation systems with carbonate gangue, being an environmentally attractive alternative for the phosphate industry.

Keywords: *apatite flotation; amazon oils; andiroba oil; novel collector*.

3.1 Introduction

The mineral industry is increasingly searching for less polluting processes, either by reducing waste generation or by using sustainable alternatives to petroleum-based inputs, which are in line with the growing environmental demands [1]. Among the different resources which require more sustainable processing, phosphate ores are strategic to the global food security and biodiesel production and can involve sophisticated processing steps to meet the specifications of the fertilizer industry [2].

Froth flotation is widely applied in phosphate ore concentration routes, using fatty acid salts as collectors. Given the high costs, the phosphate industry employs more accessible fatty acids from vegetable oils, with high efficiency at room temperature, in addition to technical and economic availability. Tall oil, widely used in apatite flotation in the past, has been replaced by vegetable sources such as corn, soybean, and rice bran oils [3-5].

Brazil is home to a rich variety of plant species, even though only a small fraction of these species have been investigated, with few applications implemented in the environmental, technological, and food industries. The Amazon is rich in plant resources, such as fruits and oilseeds, whose commercial exploitation is an important tool in the economic and social development of local communities. These resources have fatty acids with high unsaturation levels, typical of palm-like species, being more expressive than the oleic and linoleic acids. Palm trees have demonstrated good adaptation to tropical areas, with more than 150 species in the region, providing various types of oils with high pulp and seed yields, representing the high potential for industrial application [6].

Andiroba (*Carapas guianensi*) is an endemic tree in humid forests in South America, present throughout the Amazon region, which produces round fruits with brown colored seeds, from which its thick oil (60% by weight) is extracted, which solidifies at temperatures below 25°C and quickly reaches rancidity after extraction. This oil is traditionally applied in the cosmetic and pharmaceutical industry due to its febrifugal, analgesic, antibacterial, antiparasitic, insecticidal, and repellent properties, as a function of the limonoids present in its unsaponifiable fraction. The saponifiable fraction is mainly composed of oleic (57%), palmitic (25%), and stearic (10%) acids [7].

Amazonian oils have already been shown to be selective in froth flotation systems [8, 9]. In addition, they are abundant, of low extraction cost, and generators of development

for local communities [10]. Up to date, no study has investigated the potential of andiroba oil as a collector in froth flotation. The present work presents the characterization of andiroba oil, its physicochemical properties, adsorption behavior, and application as an apatite collector in the separation from carbonate minerals in froth flotation systems.

3.2 Methodology

3.2.1 Samples

The andiroba oil (AO) sample was obtained from the Amazon Oil Industry Company (Ananindeua, Brazil). Fruit pulp and seeds were used to extract the sample using cold pressing in absence of solvent. Gas Chromatography (GC) for methyl esters of fatty acids was used to obtain the sample fatty acid profile. The peak identification was performed using the FAME C14-C22 standard (Supelco CAT n°18917). During the GC analysis, a HP7820A gas chromatograph (Agilent, USA) was used. The equipment was equipped with a SGE column and flame ionization detector, using hydrogen gas as a carrier. Sample characterization also involved the determination of the saponification (ASTM D5558-95), acidity (D5555-95), and iodine indexes using the Wijs method (ASTM D5554-15). These analyses aimed to confirm characteristics that can influence the collector's performance, such as unsaturation and the carbon molecule chain length.

The collector was synthesized via saponification of the oil sample at 75°C, using a reaction with sodium hydroxide solution at 2% (w/v) in anhydrous ethanol with reflux for 60 minutes. The product was subjected to filtration, obtaining a fatty acid salt (AOC), in addition to a liquid portion, composed mainly of glycerol and ethanol. Fourier transform infrared spectroscopy (FTIR), using a Nicolet 6700 spectrometer (Thermo Scientific, USA) was used to evaluate the extent of the saponification reaction. The attenuated total reflection (ATR) mode was used in the analyses, which conducted 64 scans in the 4000-675cm^{-1}, with a resolution of 4cm^{-1}. The surface tension of the AOC solution was used to evaluate the critical micellar concentration (CMC) of the collector, using the Du Nouy ring method. During the tests, a K10ST tensiometer (Krüss, Germany) was used. The platinum ring was previously flame-treated to remove any organic contamination. The system temperature and pH were adjusted to 23°C and 7.5, respectively, with the aid of NaOH and HCl solutions.

The present study was conducted using apatite and carbonate mineral samples collected in loco from igneous phosphate deposits. Sample preparation was initially performed by particle size reduction along with hand picking to select the purest crystals. Further pulverizing was performed using an agate mortar and pestle to adjust particle size range to 212-75μm for microflotation tests, following the particle size specifications of the ore currently processed using Brazilian flotation circuits. A portion of this sample was further pulverized below 38μm for mineralogical and chemical characterizations, as well as zeta potential tests.

3.2.2 Methods

Mineralogical characterization of the mineral samples was carried out via powder X-ray diffraction (PXRD) on a PW1710 diffractometer (Philips-PANalytical, UK) equipped with a graphite monochromator crystal and copper X-ray source (λκα=1.54Å). The analyses were conducted at 50kV and 35mA, 2θ varying between 3° and 90°, with 0.06° step (2θ) and 3s as scan time. Rietveld refinement was performed to seni-quantify each crystalline phase. Wavelength dispersive X-ray fluorescence spectroscopy (WDXRF) was used for chemical characterization of the samples using a PW2404 spectrometer (Philips-PANalytical, UK) equipped with a rhodium composite anode tube. For the analysis, 2g samples were used and prepared by fusion with $Li_2B_4O_7$.

Microflotation tests were carried out in a modified Hallimond tube [11] to evaluate the minerals' floatability, previously conditioned with the AOC collector reagent. Then, the extender and the upper part of the tube were coupled, and the volume of the tube (245mL) was completed with the same conditioning solution. The system was kept under agitation from a magnetic bar inserted at the base of the tube, keeping the particles in suspension. After conditioning, nitrogen gas (N_2) was released into the system at a $40cm^3.min^{-1}$ flow rate through the base of the tube, composed of porous glass, and flotation was performed for 1 minute (collection time). After this stage, the operator performed the collection, drying, and weighing of the products obtained in the test. The test performance was evaluated based on floatability, defined as the percentage ratio between the mass of the floated material and the total recalculated mass of the test. The selectivity between pairs was measured using the selectivity coefficient (βA/B), widely used in phase separation in aqueous systems [12], adapted in the present work,

considering the relationship between the partitions of the respective minerals (A and B) between floated and sunken.

The zeta potential of the mineral particles was obtained via electrophoretic mobility tests, using a ZM3-D-G Particle Analyzer (Zeta Meter, USA). The previous preparation of the particles involved their conditioning in a system containing 10mg of mineral sample, with particle size below 38µm, and a 10^{-3}M KNO_3 electrolyte solution (100mL) with pH previously adjusted for the test. Then, based on Stokes' Law, the system was allowed to stand for long enough so that only particles below 2µm remained in the suspension. Then, a portion of the supernatant was collected to be used in the test. Both suspensions and solutions had their pH adjusted using HNO_3 and KOH.

The extent of AOC adsorption onto the mineral particles was evaluated via Fourier transform infrared spectroscopy (FTIR) using 0.2g samples, previously conditioned with the collector, in solution adjusted to the appropriate concentration and pH. The conditioning time used was 30 minutes. After filtering, the solid fraction was dried for 24 hours at 70°C. Then, the products were submitted for analysis via FTIR-ATR considering the range between 4000 to 400cm^{-1}, applying a resolution of 4cm^{-1} and 64 scans.

The surface of mineral samples was investigated using an AMICUS monochromatic X-ray photoelectron spectrometer (Kratos Analytical, UK) with an Mg κα X-ray source (1253.6eV). The elemental surveys were performed from 0 to 1200eV (resolution: 1eV, dwell time: 100ms), whereas high-resolution spectra were obtained using a pass energy of 0.1eV. The samples (-212µm +75µm) were conditioned (0.5g) in 25mL of distilled water at pH 7.5 for 7min. After filtering, the solid was dried in an oven for 24 hours at 50ºC. The samples were then degassed for 6 hours in a forced-air oven at room temperature and kept in a vacuum desiccator, before the experiments. The results were fitted using the software Vision Processing (Kratos Analytical, UK) and the C 1s peak for C-C was used as standard (BE at 284.8 eV) for shift correction [13].

3.3 Results and Discussion

3.3.1 Mineral samples characterization

The diffractograms obtained in the XRD analyses are shown in Figure 3.2. The interpretation was performed using ICDD’s standards (International Diffraction Data

Center) from PDF-2 database published in 2010 to compare the peaks.

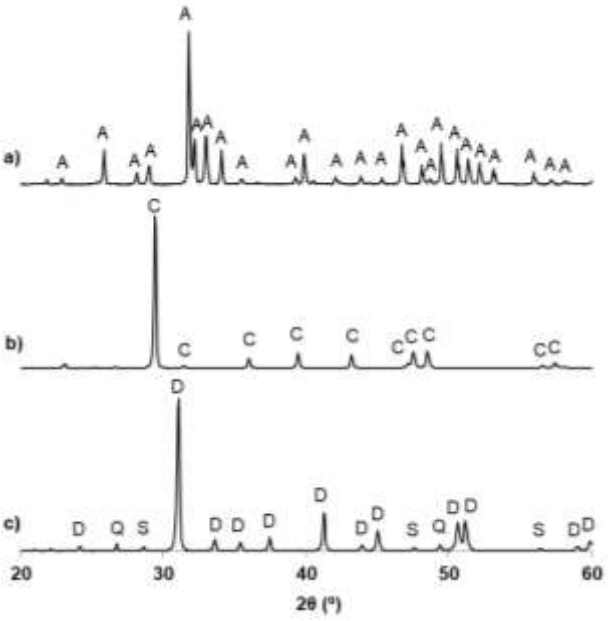

Figure 3.2 – X-Ray diffractograms of the apatite (a), calcite (b) and dolomite (c) samples. ICDD - A: apatite (09-0432), C: calcite (88-1807), D: dolomite (84-2065), Q: quartz (88-2302), S: sphalerite (05-0566)

The refinement by the Rietveld Method showed that the apatite sample was identified as fluorapatite presented a high degree of purity (99%), as well as the calcite (99%) and dolomite (96%) samples, which was confirmed by the analysis of the results via WDXRF. The apatite sample has a major component of P, O, and Ca, in addition to small contamination of Si and Mg, from carbonates and quartz remaining in the sample. Calcite and dolomite showed Ca, Mg and O as major elements, but in different proportions, in addition to the occurrence of traces of Si, relative to the remaining quartz. Dolomite showed lesser purity among the minerals, with traces of Zn and Fe from sphalerite present in the sample, as indicated in the PXRD results. All minerals showed traces of Al, probably from silicates present in minor amounts.

3.3.2 Characterization of andiroba oil and saponification products

The fatty acid profile of the andiroba oil, obtained via GC, is shown in Table 3.1, indicating the predominance of oleic and palmitic acids in its composition. The physical aspect of the sample is defined by the major participation of unsaturated acid (oleic),

ensuring the liquid state of the oil at room temperature. Additionally, the profile is similar to the typical composition recorded in the literature and according to the American Oil Chemist's Society (AOCS) [14]. Some variations found are generally related to the natural characteristics of these resources, such as geographical source, fruit ripeness, and climatic conditions during cultivation [15]. Highly unsaturated molecules like oleic and linoleic acids have been reported to perform well as a collector during flotation [5].

Table 3.1 – Fatty acid composition of Andiroba oil.

	C12:0 lauric	**C14:0 miristic**	**C16:0 palmitic**	**C16:1 palmitoleic**	**C18:0 estearic**	**C18:1 oleic**	**C18:2 linoleic**	**Others**
Test	0.3	0.3	27.1	1.2	8.8	48.2	12.1	2.0
Amazon oil (2021) [16]	-	-	25-32	0.8-1.5	6-13	45-58	6-14	-
Serra *et al.* (2019) [14]	5.35	3.57	28.72	0.82	6.16	44.67	9.3	1.41
Silva *et al.* (2018) [17]	-	-	25.1	0.53	10.11	57.58	5.87	0.81

The oil sample's physicochemical parameters are shown in Table 3.2. The acidity index is related to the proportion of free fatty acids in oil sample composition and, when intended for food, it consists of a parameter to evaluate the quality and conservation of the product [18]. In industrial applications, mainly in flotation, high levels of acidity represent advantages in the saponification stage, used to obtain the collector. This is because a higher proportion of free fatty acids accelerate the reaction kinetics, favoring the breakdown of the triglyceride ester bonds that make up the oil, followed by the neutralization of the released fatty acids. Therefore, the high value observed for this parameter is beneficial to the application [9, 19]. For andiroba oil, the low acidity index (21.1±0.5mg $KOH.g^{-1}$), in relation to other Amazonian oils (between 28 and 43mg $KOH.g^{-1}$) [8], indicates an inferior performance in the saponification reaction. Saponification and iodine index relates to the size of the fatty acid's hydrocarbon chains and the degree of unsaturation of these chains, respectively. The results corroborated with the information provided by the manufacturer [16] and recorded in the literature [14]. The iodine index obtained for andiroba oil (66±2g $I2.g^{-1}$) is related to the high efficiency of the collector in the floatability of apatite, due to the high degree of unsaturation present in its composition, evidenced by the presence of oleic (C18:1) and linoleic (C18:2) acids [20]. The saponification index (194±15 mg $KOH.g^{-1}$), which is considerably high in relation to other Amazonian oils [8], is related to the presence of molecules with long carbon chains, reflecting a higher molecular weight. This collector

characteristic gives greater stability to the hydrophobic film formed on the surface of the particles, due to the greater interaction between the carbon chains and their packing. Furthermore, it promotes greater efficiency in the phenomenon of adhesion to the air bubble, due to the greater drainage capacity of its water film during the induction step [5]. As discussed for the fatty acid profile, discrepancies observed for the saponification index value obtained in other studies for andiroba oil may be related to variations in its composition due to aspects to be considered during the cultivation stage, presenting an irrelevant impact for the synthesis of collectors [15].

Table 3.2 – Chemical characterization of the andiroba oil sample

	Test	Amazon oil (2021) [16]	Serra *et al.* (2019) [14]
Acidity Index (mg KOH.g^{-1})	21.1±0.5	<15	21.70±0.26
Saponification Value (mg KOH.g^{-1})	194±15	190-210	241.43±2.40
Iodine Value (g I_2.g^{-1})	66±2	65-75	63.30±0.21

The ATR-FTIR spectra of the andiroba oil sample and the product of its saponification are shown in Figure 3.3, with emphasis on free fatty acids' specific bands, carboxylates, and alcohols. The success of the saponification reaction is indicated by the disappearance of the 1,744cm^{-1} (triglycerides) and 1,711cm^{-1} (free fatty acids) bands, which were present in the spectra of the oil sample (Figure 3.3a), and the appearance of the 1,558cm^{-1} band (sodium fatty acid salts) in the spectra of the reaction product (Figure 3.3b) [21]. In addition, bands related to alcohol applied in the reaction (879cm^{-1}, 1,047cm^{-1}) can be observed [22]. The results show that a fatty acid salt collector (AOC) can be obtained through a complete (or almost complete) saponification of andiroba oil samples.

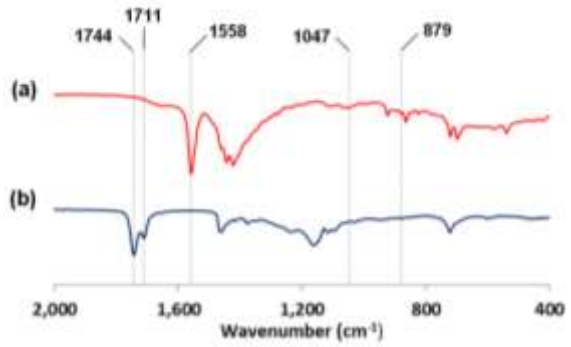

Figure 3.3 – ATR-FTIR spectra of andiroba oil (a) and andiroba oil collector (b).

The surface tension of aqueous AOC solutions, at pH 7.5 and 23°C, was evaluated at

different concentrations, as shown in Figure 3.4. The literature records the influence of the solution's concentration, pH, and temperature on its surface tension [23]. The results show the inverse relationship between concentration and solution surface tension, as a result of the positioning of the molecules at the liquid-gas interface. As highlighted in the graph, the pre-micellar (PCMC) and critical micelle (CMC) concentrations were determined at approximately 25mg.L^{-1} and 175mg.L^{-1}, respectively. In this concentration range, the formation of hemi-micelles is observed, favoring the collection of particles, as it promotes the stability of the hydrophobic film through the immobilization of collecting species at the mineral surface and, consequently, the bubble-particle adhesion [4]. Above 175mg.L^{-1}, the formation of micelles takes place, negatively affecting the process, since they can form clusters or even reverse the hydrophobization of mineral particles [23].

The AOC CMC demonstrates the formation of micelles at a lower concentration than that of sodium oleate solutions, which can present CMC up to 300mg.L^{-1}. This fact can be attributed to the composition of the vegetable oil sample that, although rich in oleic acid, presents a significant contribution of palmitic, stearic, and linoleic acids. This configuration generates a lower packaging than that observed for systems containing pure sodium oleate, since the difference in the vibrational energy of the different carbon chains (size and conformation), due to thermal movement, makes it difficult to pair the collecting species and the stability of the hydrophobic film on the mineral surface [24].

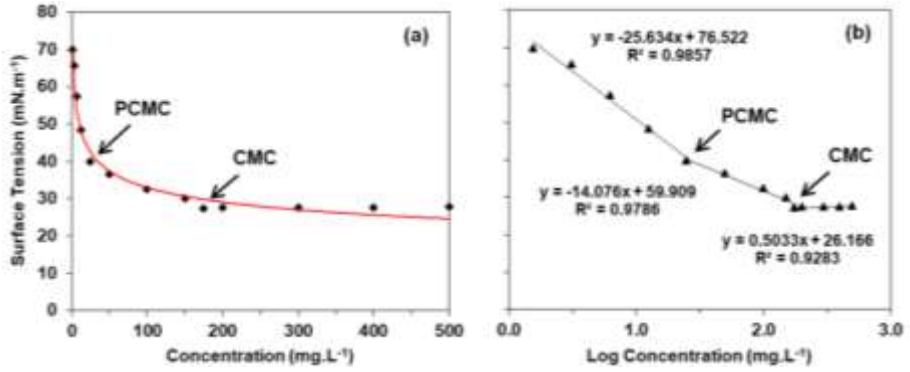

Figure 3.4 – Surface tension of AOC solution as a function of concentration (a) and log of concentration (b), at pH 7.5 and 23ºC.

3.3.3 Microflotation

The results of the microflotation of apatite, calcite, and dolomite at different AOC concentrations and pH conditions are shown in Figure 3.5, respectively. The selectivity between apatite and carbonates can be seen from the analysis of the selectivity coefficient (β) in Figure 3.5, with emphasis on the apatite/dolomite pair. The system conditions which favor this scenario are 20mg.L^{-1} AOC concentration and pH 7.5 for both carbonates, showing expressive floatability for apatite (90.25%), in opposition to low calcite (10.53%) and dolomite (8.18%) recoveries. The results corroborate with the data obtained in the zeta potential analyses as, at the same pH condition, the apatite surface presents a greater negative residual charge when compared to the carbonates, suggesting greater collector adsorption onto apatite.

The increase in the AOC concentration, from 10 to 20mg.L^{-1}, directly affected the floatability of the apatite sample. As for the carbonates, this was not able to make the particles more recoverable, especially dolomite. The increase in the AOC concentration resulted in a subtle increase in the floatability of calcite, in a more alkaline environment, which has also been reported in studies with sodium oleate [25]. Maximum apatite recovery and selectivity in the apatite/carbonate system were obtained at collector concentrations higher than those reported in the literature when evaluating pure sodium oleate (approximately 5mg.L^{-1}) [26], which is the main component of AOC, considering the proportion of oleic acid in the oil sample (48.2%) [27, 28]. The discrepancies among maximum recovery concentrations of minerals recorded for pure sodium oleate and andiroba oil collectors may be related to the difference in the degree of the carbon chain packing of the collector after adsorption on the mineral surface. This is due to the presence of other species in the composition of the AOC, in addition to oleate, with carbon chains that are distinct from each other, due to the fatty profile of andiroba oil. This diversity of carbon chains affects the conformation of the hydrophobic film on mineral particles. As the AOC has a variety of carbon chains from the different fatty acids that make up the oil, the organization of the molecules in the adsorbed layer is less compact compared to the more homogeneous hydrophobic layer formed in the adsorption of sodium oleate, which has a single type of chain. Therefore, flotation using AOC may require a higher collector concentration to form a more cohesive collector layer on the particle surface, ensuring its effective hydrophobization [29].

The high floatability observed for apatite at slightly basic pH is consistent with previous studies in which maximum recovery has been reported at a pH range close to neutrality when using different types of fatty acids [5], including oleic acid, the major component in the andiroba oil sample. This behavior is consistent with AOC adsorption dependent on the speciation of its fatty acids, which present pKa at approximately 4.8 [30]. In systems with a pH below this value, fatty acids are predominantly in the molecular form, favoring low-intensity physical adsorption on the mineral surface, whereas in systems with a pH above the pka, practically all the fatty acid is present in the ionic form, with the polar group, being active for adsorption in Ca2+ sites at the mineral surface through chemical adsorption [31]. For intermediate pH systems, close to neutrality, the formation of ionomolecular complexes can be expected from the combination of molecular and ionic species of fatty acid, favoring mineral hydrophobization due to the increase in the collector concentration [32, 33]. This is the case of the systems evaluated in this study since systems with pH 7.5 showed high selectivity between apatite and carbonates. Under alkaline conditions, the formation of micelles or collecting precipitates in the solution can occur, in addition to the appearance of dimer-type structures, which present stability even under highly alkaline conditions. The adsorption of dimeric species formed in strongly alkaline pH on the particles reduces the hydrophobization of the particles because of the configuration obtained for the polar groups of the collector, directed to the solution, favoring the interaction with the polar groups of the aqueous phase [4, 33]. Also, high pH conditions favor the competition between carboxyl and hydroxyl ions for Ca^{2+} sites on the mineral surface, favoring the high concentration of carboxylate in the solution and the consequent formation of micelles, and impairing the formation of carboxylate on the surface of a mineral, negatively affecting the floatability [31].

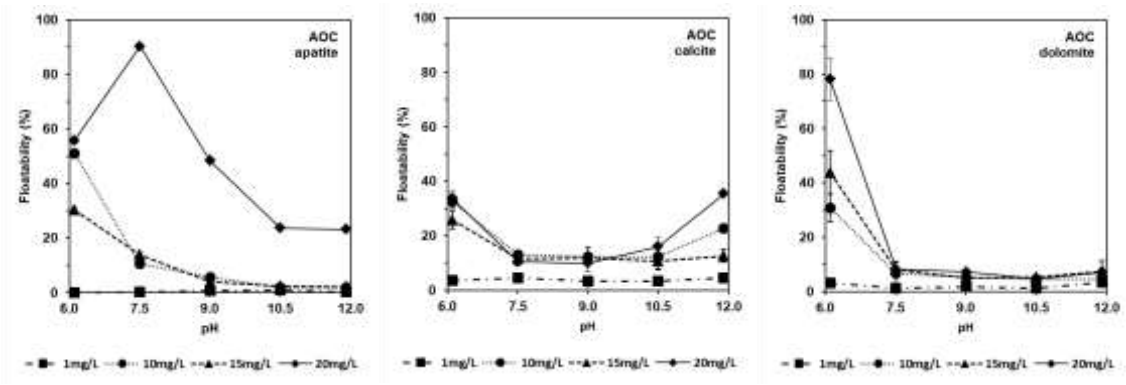

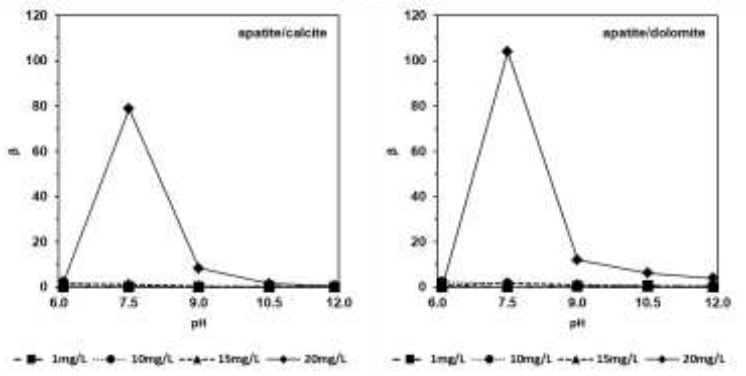

Figure 3.5 – Effect of pH and AOC concentration on apatite, calcite, and dolomite floatability, and the selectivity in apatite/calcite and apatite/dolomite systems.

In the second step of this study, floatability curves were drawn up to evaluate the impact of conditioning time on the minerals recovery using AOC, focusing on the most selective conditions to separate apatite from calcite and dolomite. Until then, all microflotation tests were performed using 7 minutes of conditioning. The results with 3 and also 5 minutes of conditioning are shown in Figure 3.6.

The collector adsorption on the investigated mineral system can be considered chemical in nature, as discussed and previously demonstrated [34]. Therefore, because of the nature of the collector/particle interaction, its intensity relates to the reaction time between species in the flotation system. The tests with apatite showed a direct relationship between flotation performance and conditioning time. The hydrophobization mechanism by the adsorption of the collector on their surface through the precipitation of oleate in calcium sites (chemical nature) agrees with the results obtained since the floatability of minerals has been directly related to the occurrence of Ca2+ sites in the apatite surface [35]. Semi-soluble minerals, such as apatite and carbonates, show a partial solubility depending on the system conditions. Due to its slow kinetics, the conditioning time is directly related to the solubilization of these minerals. This solubility favors the formation of active sites on its surface containing Ca^{2+}, in addition to increasing the concentration of this ion in the liquid phase. This phenomenon can be promoted by the decomposition of the CO_3^{-2} ions to an acidic medium, in the case of carbonates, or the solubilization of the PO_4^{-3} ions, in the conditioning of apatite. This scenario favors the formation of calcium dioleate in the system and its subsequent precipitation on the mineral surface, reinforcing its hydrophobization [27]. The

solubility balance of these semi-soluble minerals is related to their crystallinity, surface area, porosity, and presence of impurities or substitutions in their composition [28].

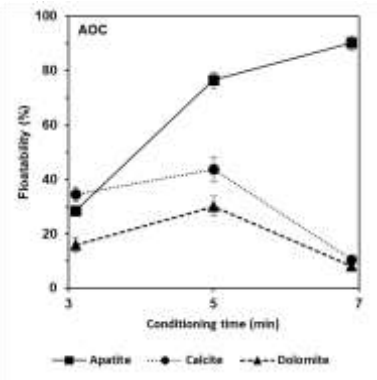

Figure 3.6 – Effect of conditioning time on the recovery of apatite, calcite and dolomite.

3.3.4 X-ray photoelectron spectroscopy (XPS)

The surface analyses of the minerals used in this study, after conditioning in distilled water at pH 7.5, were performed XPS, generating the elemental composition shown in Table 3.3 and the high-resolution spectra presented in Figures 3.7, 3.8 and 3.9. The technique is widely discussed, revised, and applied on the surface characterization of particles when subjected to specific conditions, even conditioned with flotation reagents [36].

The surface atomic composition of the samples, obtained via XPS, confirms their purity, being identified only as the constituent elements of the minerals, without traces of contaminants. The exception was registered in the compositional analysis of apatite, for which a small percentage of carbon (C), from carbonates, was detected, without compromising the purity of the samples used in this study. This characterization is important for understanding the available sites for reagent adsorption in flotation systems [37].

The collector chemisorption mechanism, suggested by results of previous studies, would be related to the interaction between Ca^{2+} sites on the mineral surface and the COO^{-} anion present in the reagent, precipitating calcium carboxylate at these sites [35, 38]. The presence of significant amounts of Ca on the surface of apatite and carbonates obtained via XPS, suggests that Ca^{2+} sites might have been available for AOC adsorption in all minerals. The dolomite sample showed a lower percentage of Ca on its

surface, reflecting its chemical composition, possibly negatively affecting the collector adsorption and reducing its floatability. The higher percentage of surface Ca on the calcite surface did not result in greater floatability, as seen in the microflotation results. Another factor that may have contributed to the low intensity of collector adsorption on carbonates is related to the test pH, close to neutrality. Under these conditions, the solubility of carbonates is lower, making it difficult to form free Ca^{2+} sites on the particle surface. The expressive adsorption of the collector on apatite may suggest the influence of the conformation of this Ca-collector interaction on the mineral surface. The arrangement of the Ca^{2+} sites on the apatite surface could be organized in such a way that it would fit more appropriately with the spatial deformation of the carboxylate groups in the collector, promoting greater interaction between them.

Table 3.3 – Atomic composition at apatite, calcite, and dolomite surface conditioned at pH 7.5.

	Elemental Content (%)					
	C	O	Ca	P	F	Mg
Apatite	2,8	70,1	14,0	11,2	1,9	-
Calcite	18,7	63,9	17,4	-	-	-
Dolomite	13,3	66,4	8,8	-	-	11,5

The apatite high-resolution XPS spectra (Figure 3.7) indicated the presence of other sites different from those of apatite. The Ca 2p, P 2p and F 1s spectra were fitted with peaks assigned for apatite at 347.56eV (Ca $2p_{3/2}$) and 350.77eV (Ca $2p_{1/2}$), 133.44eV, and 684.76eV, respectively [39]. The C 1s spectrum showed the presence of adventitious C-C [40] at 284.80eV, which is possibly due to the presence of organic contaminants, and the presence of carbonate sites, due to the required fitting of a peak at 288.94eV [41], identified by characterization via WDXRF. Besides the apatite peak in the O 1s spectra, at 531.42eV [42], the presence of metal oxide sites was also indicated by a peak fitted at 529.60eV [43]. Both contaminants identified on the apatite surface (carbonate and metal oxide) can act as active sites for the adsorption of carboxylates, favoring particle hydrophobization.

The calcite high-resolution XPS spectra (Figure 3.8) indicated the mineral surface presented no other contamination besides the adventitious C-C, at 284.80eV, as the others samples. The calcite peak was observed at 289.42eV in the C 1s spectrum, according to the previous studies [41]. The Ca $2p_{3/2}$ and Ca $2p_{1/2}$ spectra were properly

fitted with calcite peaks at 346.98eV and 350.31eV, respectively [41]. The O 1s spectrum was fitted with a peak at 531.48eV, attributed to the CO_3^{2-} in the calcite composition [44].

The dolomite C 1s XPS spectrum indicated the presence of adventitious C-C as contamination at the mineral surface, a peak at around 284.81eV (Figure 3.9), whereas a second peak was identified at around 289.71eV, which was assigned to CO_3^{2-} from the dolomite composition [45]. The fitting of the O 1s spectrum showed the presence of oxygen as dolomite [46], with a peak at 531.86eV, and the presence of metal oxide sites [43], because of the presence of a peak at around 530.01eV. This result indicates the oxidation of Zn and Fe in the minor percentage of sphalerite indicated by the PXRD and WDXRF results. The Ca 2p spectrum was properly fitted with the doublets for dolomite (Ca $2p_{3/2}$ and Ca$2p_{1/2}$ at around 347.30eV and 350.75eV, respectively), whereas the Mg 2p spectrum was fitted with a dolomite peak at 50.06eV [46]. Although the Ca 2p and Mg 2p spectra indicated no other species than dolomite at the sample surface, the presence of a metal oxide can be expected, as shown in the O 1s spectrum. As discussed for apatite, the presence of Fe sites on the surface of dolomite could corroborate for the adsorption of the carboxylate-type collector and may explain the floatability exhibited by the sample at pH 6 (Figure 3.5), which would be expected to be low because of to the low proportion of Fe sites on the mineral surface.

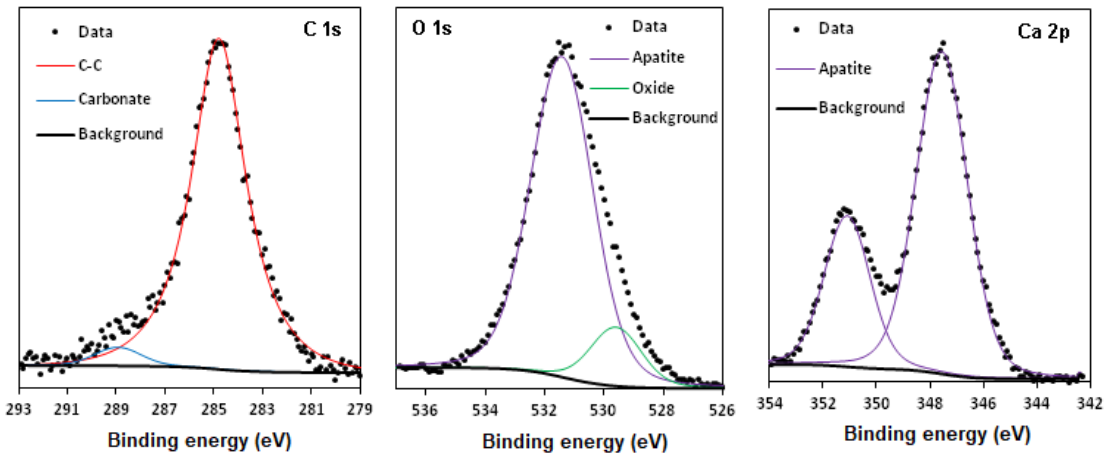

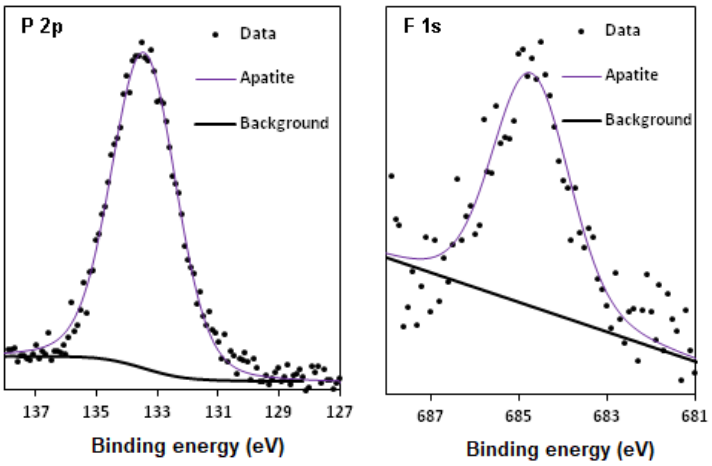

Figure 3.7 – Fitted peaks in the C 1s, O 1s, Ca 2p, P 2p e F 1s XPS high-resolution spectra of the apatite sample.

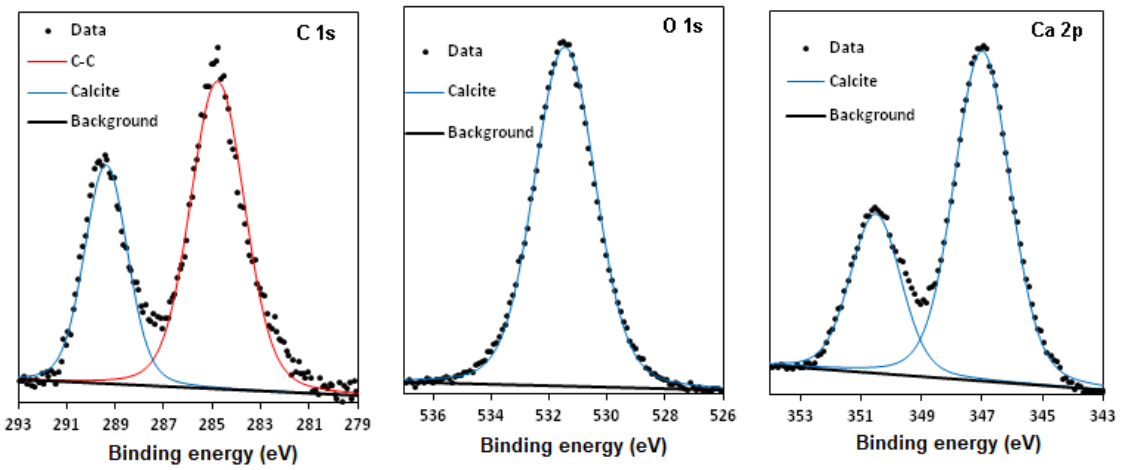

Figure 3.8 – Fitted peaks in the C 1s, O 1s, and Ca 2p high-resolution XPS spectra of the calcite sample.

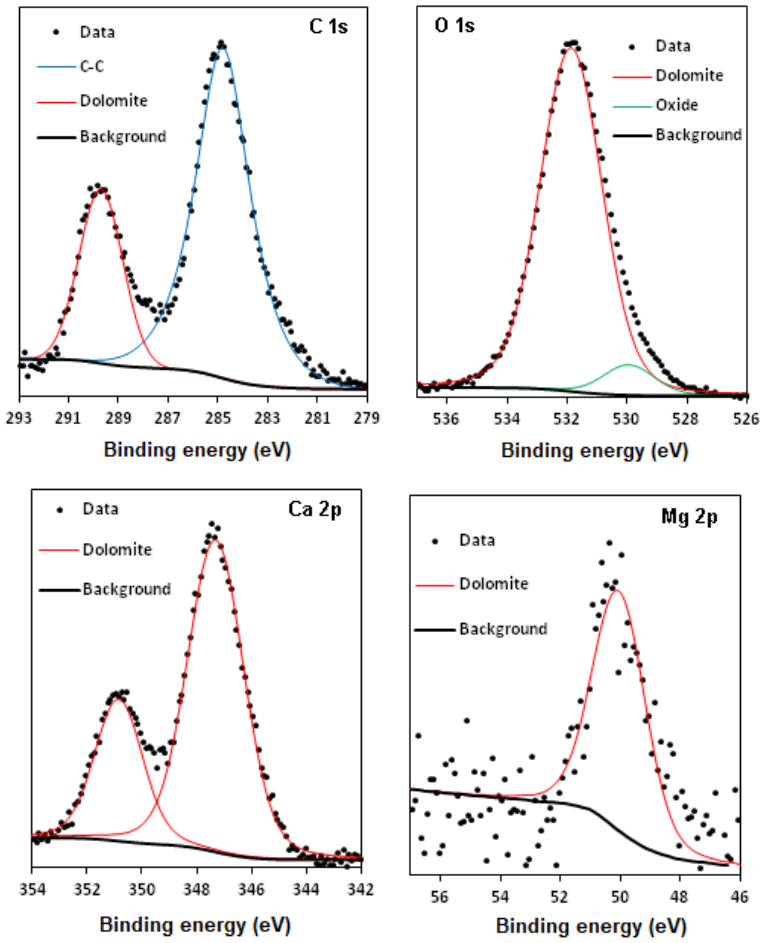

Figure 3.9 – Fitted peaks in the C 1s, O 1s, Ca 2p e Mg 2p high-resolution XPS spectra of the dolomite sample.

3.3.5 Zeta Potential

The zeta potential of minerals used in this study, obtained in the presence and absence of a collector, are shown in Figure 3.10. The tests were performed using KCl solution (10^{-3} M) as an inert electrolyte, with the objective of providing sufficient amounts of ions in the system to promote compression of the electric double layer and facilitate diffusion through it, without affecting the electrokinetic behavior of the particles [47]. The apatite zeta potential can vary significantly as a function of the mineral composition, as a result of the presence of different elements in their crystalline structure due to ionic substitutions, reflecting in different isoelectric points (IEP) [48]. The fluorapatite sample evaluated in this work presented a negative zeta potential in the entire pH range investigated, indicating the possible occurrence of an isoelectric point at pH below 4, corroborating with IEP values found for other fluorapatite samples [49].

The zeta potentials of calcite and dolomite demonstrated IEP values at pH close to 7 and 11, respectively, corroborating previous studies [25].

The electrokinetic behavior of semi-soluble minerals is influenced by the partial solubilization of the particles, since the main cations and anions in their composition, in addition to their hydrolysis products, behave as potential determining ions (PDI) [50]. For apatite, the Ca^{2+} and PO_4^{3-} ions and their hydrolysis products behave like PDI. Under conditions below the IEP, H^+ and $CaH_2PO_4^+$ present in the solution can give a positive charge to the apatite surface. The negative surface charge observed under pH conditions above IEP is caused by the adsorption of OH^- and HPO_4^{2-} ions on positive sites (Ca^{2+} and HPO_4Ca^+) of the particle [33].

After conditioning with the AOC, the zeta potential curve of apatite showed a shift to more negative values, over the entire pH range evaluated. This fact can be attributed to the increase in the net negative charge of the mineral surface because of the adsorption of the anionic collector on the Ca^{2+} sites [38]. As this behavior was observed even under repulsive conditions, in which the minerals already had a negative surface charge, it can be deduced that the collector adsorption mechanism followed the specific adsorption model. The collector speciation, which is a function of pH, affects its interaction with the mineral surface, according to its pKa and the conditions of the system [25]. The major presence of the collector in the molecular form in acidic conditions would affect the surface charge of the particle less significantly. Under neutral and slightly alkaline conditions, the coexistence of ionic and molecular species is observed, providing the formation of compounds known as iono-molecular compounds. Such species favor the stability of the hydrophobic film on the particle surface and the reduction of its surface charge. For highly alkaline conditions, the formation of dimeric species of the collector and their subsequent adsorption on the mineral surface is responsible for altering the mineral surface properties. In the structure of this type of compound, pairs of carboxylate ions are oriented in the opposite direction. Therefore, when the polar portion of one of these ions that make up the dimer interacts with the mineral surface, the opposite position of the other ion present in the structure provides the orientation of its polar group to the aqueous phase, causing a contact angle reduction and, consequently, impairing mineral hydrophobization [4, 33].

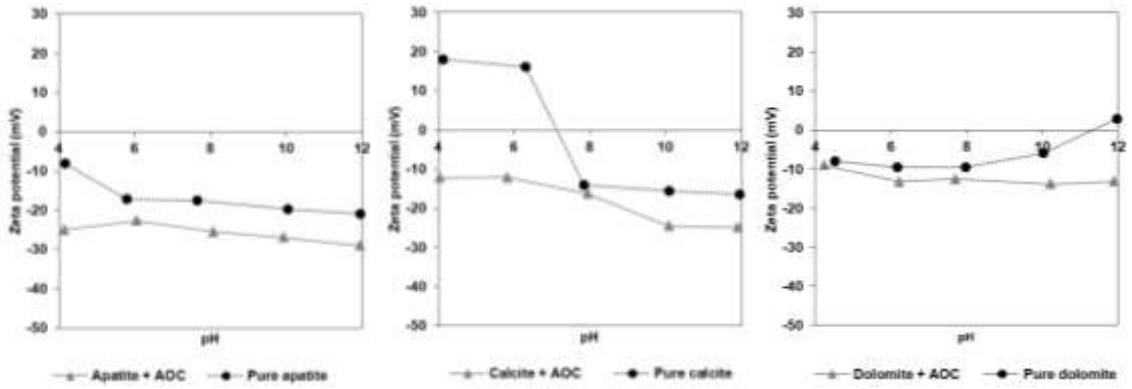

Figure 3.10 – Zeta potential of apatite, calcite, and dolomite as a function of pH, natural and conditioned with AOC.

3.3.6 Fourier-transform infrared spectroscopy (FTIR)

The minerals samples ATR-FTIR spectra were obtained before and after conditioning at pH 7.5 shows peaks characteristic of hydrocarbon chains present in the collector such as 2,852cm^{-1} and 2,922cm^{-1} (CH_2), and 2,958cm^{-1} (CH_3) [3, 22].

Figure 3.11, with the wavenumber range between 2,000cm^{-1} and 400cm^{-1}, shows the AOC carboxylate group, characterized by the peak at 1,558cm^{-1} [21], can be associated with the collector chemical adsorption at the Ca^{2+} sites on the mineral surface, forming a monolayer, or with the formation of sodium dicarboxylate salt in solution and its subsequent precipitation on the mineral surface [51]. The adsorption on Ca^{2+} sites can be identified by the characteristic peaks of calcium dicarboxylate, depending on the coordination of the calcium carboxylate complex. The results shown in Figure 3.11 indicate the formation of a monodentate complex with a peak at 1.540cm^{-1}, formed with a single Ca^{2+} ion on the mineral surface, and a bidentate complex characterized by a peak at 1.575cm^{-1} [52]. The presence of the adsorbed collector on the mineral surface, related to the intensity of the peaks identified in the FTIR-ATR spectrum, was more expressive for apatite and calcite. The selectivity detected between apatite and calcite, even when observing the adsorption in both samples, can be attributed to the high proportion of calcium in the surface composition (Table 3.3), favoring the wide adsorption of the collector on the calcite particles. This scenario may favor the formation of the bilayer, making it difficult for the bubble to adhere to the mineral particle and, consequently, affecting its collection and reducing floatability. For dolomite, considering the lower participation of calcium in its composition, the

adsorption of the collector may have been compromised, affecting its floatability. However, even with lesser active Ca^{2+} sites on its surface, the effective collector adsorption on the apatite particle can be suggested by the high flotability observed, together with the indication of collector adsorption, according to its characterization via FTIR.

The discrepancy observed in the hydrophobization of the evaluated minerals, even though the collector adsorption was identified in all of them, can be associated with the synergistic effect of the salts present in the collector and the spacing of the adsorption sites on the surface of the mineral. Thus, the resulting structure of the reagent layer formed on the apatite particles is more stable, favoring their effective hydrophobization. For calcite, and especially dolomite, the layer should be less stable, with a predominance of the hydrophilic character on the mineral surface.

Collectors obtained from the saponification of vegetable oils can experience synergy when applied to flotation, due to their varied fatty profile [53]. The behavior of mixed collector systems varies according to the reagent nature, type of collector-particle interaction, structure, and proportion between the reagents [54].

The mechanism of action of these reagents is based on the speciation observed as a function of the system conditions, supported by the premise of the existence of ionic and non-ionic species in the system and the synergy between them [30]. The discussion on the formation of ionomolecular compounds in flotation systems, resulting from the synergy between ionic and non-ionic species, was initiated considering systems composed of a single fatty acid [32]. So far, few studies have explored this discussion, mainly considering complex systems, employing collectors of mixed fatty acid salts composition from plant sources [4].

The synergistic action observed in mixed collectors promotes improvements in the flotation process, when compared to the use of pure fatty acid salts, such as oleate. Among these, the reduced consumption of reagents, increased recovery and concentrate content, improved stability of the hydrophobic coating on the mineral surface, and greater stability of the foam formed [55]. Furthermore, they can cause the critical micellar concentration and surface tension reduction in the solution [56], in addition to an increase in angle contact [57] and mitigation of the deleterious effect of Ca^{2+} ions, reducing collector loss by precipitation [58].

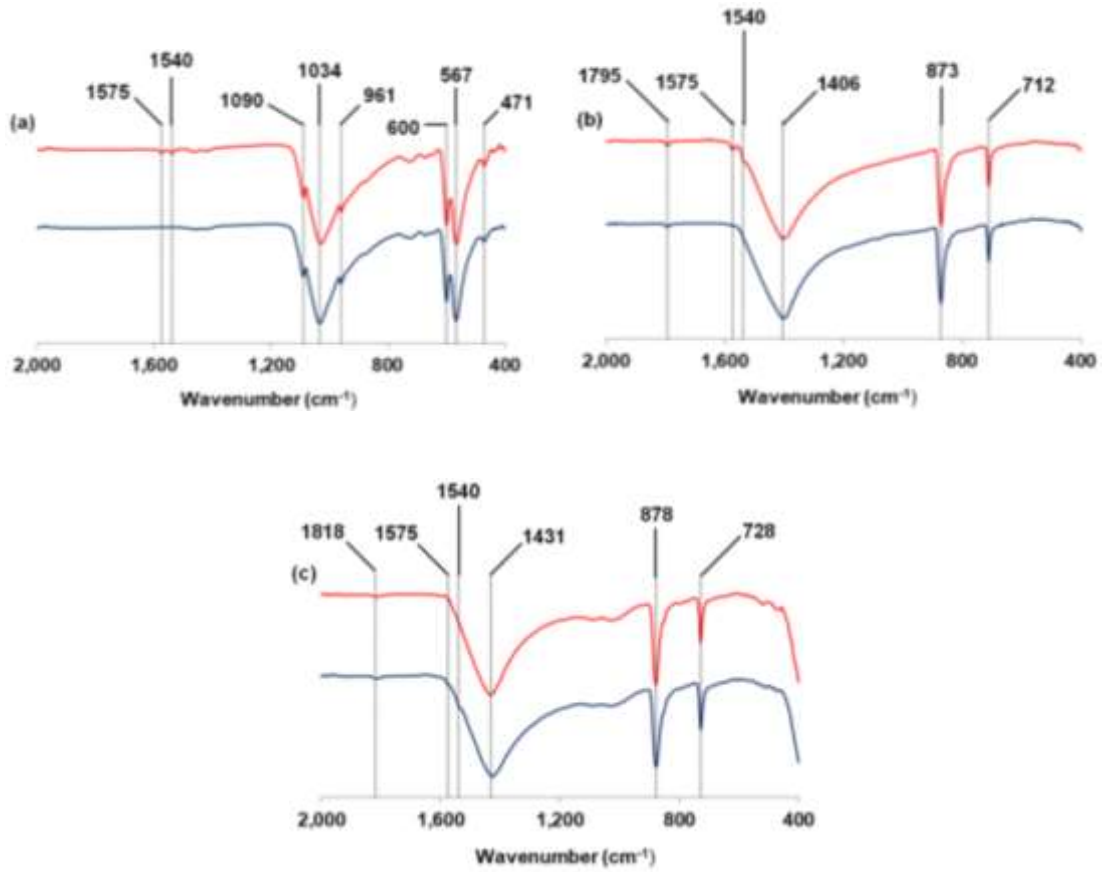

Figure 3.11 – ATR-FTIR spectra of pure minerals (top) and conditioned with 20mg.L^{-1} AOC solution at pH 7.5 (bottom) [apatite (a), calcite (b) and dolomite (c)].

3.4 Conclusion

The discrepancies in relation to the packaging of the molecules present in AOC, in relation to the sodium oleate, reflected in a reduction in the CMC and the collector concentration of maximum selectivity between apatite and dolomite, and calcite. The composition of the vegetable sample, rich in oleic, palmitic, stearic, and linoleic acids, promotes inferior packaging, due to differences in size and conformation of the hydrocarbon chains of fatty acids present in the oil, making it difficult to pair close molecules because of the difference in the chains' vibrational energy.

The best selectivity of the andiroba oil collector was obtained at a pH range close to neutrality, with apatite recovery greater than 90%. In the alkaline range (above pH 10), the drop in floatability, main apatite, was already expected due to the adsorption of dimeric species. The conditioning time proved to be an important factor for the selectivity of the system, presenting a direct relation to apatite floatability, and

indicating that AOC adsorption occurred via chemisorption, as shown in the FTIR results. Among the carbonates, mainly for dolomite, the investigation demonstrated poorer collector adsorption, due to the less pronounced peaks in the FTIR spectra and less significant zeta potential reduction after interaction with the collector.

Andiroba oil does not yet have an application in the mineral industry, even in view of the high production potential, in addition to a composition favorable to application in froth flotation, due to its fatty acid profile. As well as other sources from palm trees, Andiroba shows good adaptation to tropical areas, supplying various types of oils with high pulp and seed yields. The results obtained and the scenario presented in this study indicate that andiroba oil has a high potential as a renewable resource for the production of selective flotation collectors as alternatives to those traditionally used in phosphate concentration circuits.

3.5 Acknowledgements

The authors thank the financial support from CNPq, FAPEMIG, CAPES and PROEX CAPES for the support to PPGEM. This study was financed in part by Coordenação de Aperfeiçoamento de Pessoal de Nível Superior – Brasil (CAPES) – Finance Code 001.

3.6 References

1. Geissler B, Mew MC, Matschullat J, Steiner G. Innovation potential along the phosphorus supply chain: A micro and macro perspective on the mining phase. Science of The Total Environment. 2020;714:136701. https://doi.org/10.1016/j.scitotenv.2020.136701.

2. Zhang P. Comprehensive Recovery and Sustainable Development of Phosphate Resources. Procedia Engineering. 2014;83:37-51. https://doi.org/10.1016/j.proeng.2014.09.010.

3. Kou J, Tao D, Xu G. Fatty acid collectors for phosphate flotation and their adsorption behavior using QCM-D. International Journal of Mineral Processing. 2010;95(1-4):1-9. https://doi.org/10.1016/j.minpro.2010.03.001.

4. Cao Q, Cheng J, Wen S, Li C, Bai S, Liu D. A mixed collector system for phosphate flotation. Minerals Engineering. 2015;78:114-21. https://doi.org/10.1016/j.mineng.2015.04.020.

5. Brandao PRG, Caires LG, Queiroz DSB. Vegetable lipid oil-based collectors in the flotation of apatite ores. Minerals Engineering. 1994;7(7):917-25. https://doi.org/10.1016/0892-6875(94)90133-3.

6. Urzedo DI, Neilson J, Fisher R, Junqueira RGP. A global production network for ecosystem services: The emergent governance of landscape restoration in the Brazilian Amazon. Global Environmental Change. 2020;61:102059. https://doi.org/10.1016/j.gloenvcha.2020.102059.

7. Tsukamoto Y, Oya H, Kikuchi T, Yamada T, Tanaka R. Guianofruits C–I from fruit oil of andiroba (Carapa guianensis, Meliaceae). Tetrahedron. 2019;75(9):1149-56. https://doi.org/10.1016/j.tet.2018.12.036.

8. Oliveira P, Mansur H, Mansur A, Silva Gd, Peres AEC. Apatite flotation using pataua palm tree oil as collector. Journal of Materials Research and Technology. 2019;8(5):4612-19. https://doi.org/10.1016/j.jmrt.2019.08.005.

9. Carvalho JAE, Brandão PRG, Henriques AB, Oliveira PS, Cançado RZL, Silva GR. Selective flotation of apatite from micaceous minerals using patauá palm tree oil collector. Minerals Engineering. 2020;156:106474. https://doi.org/10.1016/j.mineng.2020.106474.

10. Teixeira N, Melo JCS, Batista LF, Paula-Souza J, Fronza P, Brandão MGL. Edible fruits from Brazilian biodiversity: A review on their sensorial characteristics versus bioactivity as tool to select research. Food Research International. 2019;119:325-48. https://doi.org/10.1016/j.foodres.2019.01.058.

11. Silva GR, Espiritu ERL, Mohammadi-Jam S, Waters KE. Surface characterization of microwave-treated chalcopyrite. Colloids and Surfaces A: Physicochemical and Engineering Aspects. 2018;555:407-17. https://doi.org/10.1016/j.colsurfa.2018.06.078.

12. Santos LH, Carvalho PLG, Rodrigues GD, Mansur MB. Selective removal of calcium from sulfate solutions containing magnesium and nickel using aqueous two phase systems (ATPS). Hydrometallurgy. 2015;156:259-63. https://doi.org/10.1016/j.hydromet.2015.06.010.

13. Yang B, Yin W, Zhu Z, Sun H, Sheng Q, Fu Y, Yao J, Zhao K. Differential adsorption of hydrolytic polymaleic anhydride as an eco-friendly depressant for the selective flotation of apatite from dolomite. Separation and Purification Technology. 2021;256:117803. https://doi.org/10.1016/j.seppur.2020.117803.

14. Serra JL, Rodrigues AMC, Freitas RA, Meirelles AJA, Darnet SH, Silva LHM. Alternative sources of oils and fats from Amazonian plants: Fatty acids, methyl tocols, total carotenoids and chemical composition. Food Research International. 2019;116:12-9. https://doi.org/10.1016/j.foodres.2018.12.028.

15. Cheesbrough TM. Changes in the enzymes for fatty acidsynthesis and desaturation during acclimation of developingsoybean seeds to altered growth temperature. Plant Physiology. 1989;90(2):760-4. https://doi.org/10.1104/pp.90.2.760.

16.Amazon oil. Andiroba (Carapas guianensis). Disponível em https://www.amazonoil.com.br/pt/andiroba/. 2021. Acessado em 25/03/2021.

17. Silva JAP, Cardozo NSM, Petzhold CL. Enzymatic synthesis of andiroba oil based polyol for the production of flexible polyurethane foams. Industrial Crops and Products. 2018;113:55-63. https://doi.org/10.1016/j.indcrop.2018.01.020.

18. ANVISA. Resolução RDC n°270. Regulamento técnico para óleos vegetais, gorduras vegetais e creme vegetal. Brasília. 2005, 7p.

19. Poulenat G, Sentenac S, Mouloungui Z. Fourier-transform infrared spectra of fatty acid salts - kinetics of high-oleic sunflower oil saponification. Journal of Surfactants and Detergents. 2003;6(4):305-10. https://doi.org/10.1007/s11743-003-0274-1.

20. Wang Y, Feng Y, Zhang Q, Lu D, Hu Y. Flotation separation of diaspore from aluminosilicates using commercial oleic acids of different iodine values. International Journal of Mineral Processing. 2017;168:98-101. https://doi.org/10.1016/j.minpro.2017.09.013.

21. Schulz H, Baranska M. Identification and quantification of valuable plant substances by IR and Raman spectroscopy. Vibrational Spectroscopy. 2007;43(1):13-25. https://doi.org/10.1016/j.vibspec.2006.06.001.

22. Zhang Q, Liu C, Sun Z, Hu X, Shen Q, Wu J. Authentication of edible vegetable oils adulterated with used frying oil by Fourier Transform Infrared Spectroscopy. Food Chemistry. 2012;132(3):1607-13. https://doi.org/10.1016/j.foodchem.2011.11.129.

23. Leja, J. Adsorption of flotation collectors. In: P. Press, Editor. Surfuce Chemistry Froth Flotation. New York: 1982, p. 493-548.

24. Kanicky J, Shah D. Effect of Premicellar Aggregation on the p K a of Fatty Acid Soap Solutions. Langmuir. 2003;19(6):2034-8. https://doi.org/10.1021/la020672y.

25. Pugh R, Stenius P. Solution chemistry studies and flotation behaviour of apatite, calcite and fluorite minerals with sodium oleate collector. International Journal of Mineral Processing. 1985;15(3):193-218. https://doi.org/10.1016/0301-7516(85)90035-3.

26. Barros LAF, Ferreira EE, Peres AEC. Floatability of apatites and gangue minerals of an igneous phosphate ore. Minerals Engineering. 2008;21(12-14):994-99. https://doi.org/10.1016/j.mineng.2008.04.012.

27. Filippova IV, Filippov LO, Lafhaj Z, Barres O, Fornasiero D. Effect of calcium minerals reactivity on fatty acids adsorption and flotation. Colloids and Surfaces A: Physicochemical and Engineering Aspects. 2018;545:157-66. https://doi.org/10.1016/j.colsurfa.2018.02.059.

28. Zhong K, Vasudevan TV, Somasundaran P. Floatability of apatites of different type and origin: role of surface area and porosity. International Journal of Mineral Processing. 1993;38(3-4):177-88. https://doi.org/10.1016/0301-7516(93)90074-K.

29. Lu Y, Miller JD. Carboxyl Stretching Vibrations of Spontaneously Adsorbed and LB-Transferred Calcium Carboxylates as Determined by FTIR Internal Reflection Spectroscopy. Journal of Colloid and Interface Science. 2002;256(1):41-52. https://doi.org/10.1006/jcis.2001.8112.

30. Kung HC, Goddard ED. Molecular association in fatty acid potassium soap systems. II. Journal of Colloid and Interface Science. 1969;29(2):242-49. https://doi.org/10.1016/0021-9797(69)90193-3.

31. Quast K. The use of zeta potential to investigate the pKa of saturated fatty acids. Advanced Powder Technology. 2016;27(1):207-14. https://doi.org/10.1016/j.apt.2015.12.003.

32. Somasundaran P. The role of ionomolecular surfactant complexes in flotation. International Journal of Mineral Processing. 1976;3(1):35-40. https://doi.org/10.1016/0301-7516(76)90013-2.

33. Vučinić DR, Radulović DS, Deušić SĐ. Electrokinetic properties of hydroxyapatite under flotation conditions. Journal of Colloid and Interface Science. 2010;343(1):239-45. https://doi.org/10.1016/j.jcis.2009.11.024.

34. Pan Z, Wang Y, Wei Q, Chen X, Jiao F, Qin W. Effect of sodium pyrophosphate on the flotation separation of calcite from apatite. Separation and Purification Technology. 2020;242:116408. https://doi.org/10.1016/j.seppur.2019.116408.

35. Horta D, Monte MBM, Leal Filho LS. The effect of dissolution kinetics on flotation response of apatite with sodium oleate. International Journal of Mineral Processing. 2016;146:97-104. https://doi.org/10.1016/j.minpro.2015.12.003.

36. Wang Z, Wu H, Xu Y, Shu K, Yang J, Luo L, Xu L. Effect of dissolved fluorite and barite species on the flotation and adsorption behavior of bastnaesite. Separation and Purification Technology. 2020;237:116387. https://doi.org/10.1016/j.seppur.2019.116387.

37. Shoaib M, Quadri SMR, Wani OB, Bobicki E, Garrido GI, Elkamel A, Abdala A. Adsorption of enhanced oil recovery polymer, schizophyllan, over carbonate minerals. Carbohydrate Polymers. 2020;240:116263. https://doi.org/10.1016/j.carbpol.2020.116263.

38. Rao KH, Antti B-M, Forssberg E. Mechanism of oleate interaction on salt-type minerals, Part II. Adsorption and electrokinetic studies of apatite in the presence of sodium oleate and sodium metasilicate. International Journal of Mineral Processing. 1990;28(1-2):59-79. https://doi.org/10.1016/0301-7516(90)90027-V.

39. Zhong C, Feng B, Zhang W, Zhang L, Guo Y, Wang T, Wang H. The role of sodium alginate in the flotation separation of apatite and dolomite. Powder Technology. 2020;373:620-6. https://doi.org/10.1016/j.powtec.2020.07.007.

40. Chu DH, Vinoba M, Bhagiyalakshmi M, Baek IH, Nam SC, Yoon Y, Kim SH, Jeong SK. CO2 mineralization into different polymorphs of CaCO3 using an aqueous-CO2 system. RSC Advances. 2013;3:21722-9. https://doi.org/10.1039/C3RA44007A.

41. Baer DR, Marmorstein AM, Williford RE, Blanchard DL. Comparison Spectra for Calcite by XPS. Surface Science Spectra. 1992;1(1):80-6. https://doi.org/10.1116/1.1247674.

42. Layrolle P, Lebugle A. Synthesis in Pure Ethanol and Characterization of Nanosized Calcium Phosphate Fluoroapatite. Chemistry of Materials. 1996;8(1):134-44. https://doi.org/10.1021/cm950326k.

43.Thermo Scientific XPS. Magnesium, Alkaline Earth Metal. Disponível em http://xpssimplified.com/elements/magnesium.php. Acessado em 25/04/2021.

44. Dong L, Wei Q, Qin W, Jiao F. Selective adsorption of sodium polyacrylate on calcite surface: Implications for flotation separation of apatite from calcite. Separation and Purification Technology. 2020;241:116415. https://doi.org/10.1016/j.seppur.2019.116415.

45. Zeng M, Yang B, Guan Z, Zeng L, Luo H, Deng B. The selective adsorption of xanthan gum on dolomite and its implication in the flotation separation of dolomite from apatite. Applied Surface Science. 2021;551:149301. https://doi.org/10.1016/j.apsusc.2021.149301.

46. Hu X, Joshi P, Mukhopadhyay SM, Higgins SR. X-ray photoelectron spectroscopic studies of dolomite surfaces exposed to undersaturated and supersaturated aqueous solutions. Geochimica et Cosmochimica Acta. 2006;70(13):3342-50. https://doi.org/10.1016/j.gca.2006.04.022.

47. Fuerstenau DW, Pradip. Zeta potentials in the flotation of oxide and silicate minerals. Advances in Colloid and Interface Science. 2005;114-115:9-26. https://doi.org/10.1016/j.cis.2004.08.006.

48. Filippova IV, Filippov LO, Duverger A, Severov VV. Synergetic effect of a mixture of anionic and nonionic reagents: Ca mineral contrast separation by flotation at neutral pH. Minerals Engineering. 2014;66-68:135-44. https://doi.org/10.1016/j.mineng.2014.05.009.

49. Filippov LO, Duverger A, Filippova IV, Kasaini H and Thiry J. Selective flotation of silicates and Ca-bearing minerals: The role of non-ionic reagent on cationic flotation. Minerals Engineering. 2012;36-38:314-23. https://doi.org/10.1016/j.mineng.2012.07.013.

50. Parks GA. Adsorption in the Marine Environment. In: Academic Press. Chemical Oceanography. Londres: 1975, p. 241-308.

51. Lu Y, Drelich J, Miller JD. Oleate Adsorption at an Apatite Surface Studied by Ex-Situ FTIR Internal Reflection Spectroscopy. Journal of Colloid and Interface Science. 1998;202(2):462-76. https://doi.org/10.1006/jcis.1998.5466.

52. Mielczarski JA, Cases JM, Bouquet E, Barres O, Delon JF. Nature and structure of adsorption layer on apatite contacted with oleate solution. 1. Adsorption and Fourier transform infrared reflection studies. Langmuir. 1993;9(9):2370-82. https://doi.org/10.1021/la00033a020.

53. Silva KLC, Silva MMC, Moraes MM, Camara CAG, Santos ML, Fagg CW. Chemical composition and acaricidal activity of essential oils from two species of the genus Bauhinia that occur in the Cerrado biome in Brazil. Journal of Essential Oil Research. 2020;32(1):23-31. https://doi.org/10.1080/10412905.2019.1662338.

54. Wang Z, Wang L, Wang J, Xiao J, Liu J, Xu L, Fu K. Strengthened floatation of molybdite using oleate with suitable co-collector. Minerals Engineering. 2018;122:99-105. https://doi.org/10.1016/j.mineng.2018.03.042.

55. Xu L, Jiao F, Jia W, Pan Z, Hu C, Qin W. Selective flotation separation of spodumene from feldspar using mixed anionic/nonionic collector. Colloids and Surfaces A: Physicochemical and Engineering Aspects. 2020;594:124605. https://doi.org/10.1016/j.colsurfa.2020.124605.

56. Zhang H, Han C, Liu W, Hou D, Wei D. The chain length and isomeric effects of monohydric alcohols on the flotation of magnesite and dolomite by sodium oleate. Journal of Molecular Liquids. 2019;276:471-79. https://doi.org/10.1016/j.molliq.2018.11.143.

57. Sis H, Chander S. Adsorption and contact angle of single and binary mixtures of surfactants on apatite. Minerals Engineering. 2003;16(9):839-48. https://doi.org/10.1016/S0892-6875(03)00202-4.

58. Cao Q, Cheng J, Wen S, Li C, Liu J. Synergistic effect of dodecyl sulfonate on apatite flotation with fatty acid collector. Separation Science and Technology. 2016;51(8):1389-96. https://doi.org/10.1080/01496395.2016.1147467.

4. Sinergia entre coletores em sistema de flotação

Aplicação do óleo de Andiroba como um novo coletor na flotação de apatita

Nesse estudo, buscou-se avaliar o efeito da composição de coletores alternativos, obtidos a partir da saponificação de óleos de Andiroba e Patauá, além de gordura de Bacuri, todos de origem amazônica, na flotabilidade de apatita e carbonatos (calcita e dolomita), a partir de ensaios de microflotação em tubo de Hallimond modificado. Foram realizadas caracterizações das amostras minerais (DRX, WDXRF, FTIR e XPS) e graxas (FTIR, Cromatografia Gasosa, Índices de acidez, saponificação e iodo), além dos coletores obtidos (FTIR, CMC). A adsorção deste sobre os minerais foi caracterizada a partir de ensaios de Mobilidade eletroforética e FTIR. Os ensaios varreram variáveis como tempo de condicionamento, pH do sistema e concentração da solução de coletor na flotabilidade dos minerais avaliados. Os resultados apontaram o melhor desempenho do coletor de óleo de Andiroba na seletividade do sistema apatita/carbonatos, em concentração 20mg.L^{-1} e pH 7,5. Em geral, coletores com alta proporção de insaturação (Andiroba, Patauá e Oleato) apresentaram afinidade pelos minerais com maior proporção de Ca na sua superfície, sendo estes a apatita e a calcita. Dentre eles, os obtidos a partir de amostras graxas amazônicas apresentaram menor CMC que o oleato (majoritário na composição destes), demonstrando o impacto da presença de compostos com cadeias carbônicas diferentes em um mesmo sistema. Já os coletores com alta proporção de saturação (Bacuri e Palmitato) apresentaram maior adsorção sobre a dolomita, com menor incidência de sítios Ca na sua superfície. Tal fenômeno pode ser atribuído às características morfológicas da dolomita avaliada (alto diâmetro médio de poros e baixa área superficial específica) e à maior facilidade de conformação de cadeias saturadas (lineares) em um filme hidrofóbico recobrindo a partícula mineral. O tempo de condicionamento afetou positivamente o desempenho dos coletores, corroborando com a hipótese de que a adsorção destes sobre as partículas minerais se estabelece a partir de quimissorção. Entretanto, em alguns casos, longos tempos de condicionamento se mostraram capazes de reverter esse cenário, provavelmente formando uma bicamada sobre essas partículas.

Synergetic effects of fatty acids in amazon oil-based collectors for phosphate flotation

Leandro Henrique Santos*, Adriele Mércia Alves Santos, Luciano Fernandes de Magalhães, Gilberto Rodrigues da Silva and Antônio Eduardo Clark Peres

Department of Metallurgical and Materials Engineering,
Universidade Federal de Minas Gerais (UFMG), Belo Horizonte, MG, Brazil

ABSTRACT

The mineral industry seeks less polluting processes, including by replacing inputs with sustainable options, in line with growing environmental demands. Alternative sources of fatty acids for the synthesis of phosphate collectors is a great example of this challenge, as their fatty acid profile affects flotation performance. In this work, Amazonian oils (pataua - *Oenocarpus bataua* / andiroba - *Carapas guianensi*) and fat (bacuri - *Platonia insiginis*), of various composition, were studied to evaluate the relation between their physicochemical properties (acid profile, acidity, saponification and iodine indexes) and their performance as apatite, calcite and dolomite collector. Andiroba oil collector, with a high proportion of unsaturation in its composition, promoted greater selectivity between apatite/carbonates (pH 7.5), among the evaluated collectors, including those obtained from pure fatty acid. Bacuri fat collector, with a high proportion of saturation in its composition, showed high performance in the hydrophobization of dolomite, due to the lower incidence of Ca^{+2} sites available for interaction, in relation to the other minerals, and greater stability achieved for the layer hydrophobic, due to the alignment of the linear chains and synergistic action of fatty acid salts. The understanding of the effect of the acid profile of oils and fats on their performance in flotation systems is fundamental in the search for alternative sources in the synthesis of collectors for the mineral industry.

Keywords: *fatty acids; collectors; synergy; flotation; phosphate ore.*

4.1 Introduction

The complexity of phosphate ores, with association apatite with silicates and carbonates, requires sophisticated processing steps to meet the specifications of the fertilizer industry [1]. Froth flotation is efficient in several phosphate concentration routes using fatty acid salts from plant sources as collectors [2], with high accessibility, efficiency and availability [3].

Vegetable oils are systems composed of different fatty acids in varying proportions. The collector molecules obtained from the saponification of these oils can experience synergy when applied to flotation [4]. The behavior of mixed collector systems depends on the nature of the reagents, type of collector-particle interaction, structure and proportion between the reagents [5]. Studies on mixtures of collectors indicated that their synergistic action has advantages such as reduced reagent consumption, improved recovery and content, greater mineral surface coverage and froth stability [6, 7]. Non-ionic reagents, when used together with oleate, provided a reduction in the critical micellar concentration and surface tension of the solution, demonstrating that the surfactants are concentrated at the liquid/gas interface [8], in addition to increased contact angle [9], reduction of reagent consumption and mitigation of the deleterious effect of Ca^{2+} ions, which cause the collector to precipitate [10].

The interaction between the collectors obtained from vegetable oils can be discussed from the perspective of an anionic / anionic or anionic / nonionic synergy, depending on their speciation under the system conditions [11]. The first discussions on the synergistic effect of fatty acid collectors were based on the formation of ionomolecular complexes, although it was elaborated by analyzing systems containing a single acid, and has been underdeveloped until then [12]. Records regarding the synergy of fatty acids present in vegetable oils in ore flotation are scarce, especially discussions on stability, configuration and hydrophobicity of the formed film [13].

Brazil has several sources of oils and fats with great potential for application in the synthesis of fatty acid salts due to the high yield in the production of oils and fats containing fatty acids with a high level of unsaturation, typical of palm-like species, oleic and linoleic acids being the most expressive [14].

The pataua (Oenocarpus bataua), andiroba (Carapas guianensi) and bacuri (Platonia insiginis) oils are examples of these sources, being extracted from fruits or seeds of

species native to the Amazon (Oenocarpus bataua, Carapas guianensi and Platonia insiginis, respectively). While pataua oil has a major composition represented by oleic (80%) and palmitic (15%) acids, with small proportions of steric, lauric and myristic [15], andiroba oil is composed of oleic (57%), palmitic (25%) and stearic (10%) acids [16]. Bacuri fat, on the other hand, presents a major profile of saturated acids, as palmitic (65%) and oleic acid (25%), resulting in its solid appearance at room temperature [17, 18].

Amazonian oils have already been shown to be selective in froth flotation systems [19, 20], including pataua [21], besides being abundant, of low extraction cost and generators development for the local communities. The synergy in collector of mixed fatty acid composition is still not well studied, leaving a gap in the understanding of its mechanism of action during adsorption and floatability of mineral particles. The present work evaluates the synergistic effect of the fatty acid composition of pataua and andiroba oils, and of bacuri fat in the adsorption and flotation of apatite, calcite and dolomite particles, seeking selectivity in relation to common carbonates found in phosphate ores.

4.2 Methodology

4.2.1 Samples

The apatite, calcite and dolomite samples used in this study were collected from outcrops of the Araxá igneous phosphate deposit (Araxá, Brazil), being prepared via fragmentation with a hammer and an agate mortar and pestle to achieve the size range between 212µm and 75µm, which is based on traditional particle size specifications applied to ore flotation circuits in Brazil. The thin portion (-38µm) was submitted to chemical and mineralogical characterization, in addition to zeta potential and FTIR tests. The andiroba oil (AO), pataua oil (PO) and bacuri fat (BF) were provided by the Amazon Oil Industry Company (Ananindeua, Brazil), being obtained via cold pressing in the absence of pulp solvents and seeds of the respective fruits. Analytical grade acid samples were also use in the study. The oleic acid (OA) sample was purchased from LabSynth (Diadema, Brazil), while the palmitic acid (PA) sample was provided by Clariant (Belo Horizonte, Brazil).

4.2.2 Methods

X-ray powder diffraction was performed in a PW1710 diffractometer (Philips-PANalytical, United Kingdom) equipped with a graphite monochromator crystal and copper X-ray source ($\lambda\kappa\alpha$ = 1.54Å), which analyzes performed at 50kV and 35mA, 2θ ranging from 3° to 90°, step size of 0.06° and 3s scan time. Rietveld refinement was performed for all mineral samples to verity their purity. Wavelength dispersive X-ray fluorescence (WDXRF) was conducted on a PW2404 spectrometer (Philips-PANalytical, UK) equipped with a rhodium anode tube. Sample preparation followed the bead method using Li2B4O7, and 2g of each mineral.

The characterization of the oil samples was initially performed via Gas Chromatography (GC) using an HP7820A gas chromatograph (Agilent, USA), equipped with a flame ionization detector and SGE column, using hydrogen gas as a carrier. The FAME C14-C22 standard (Supelco CAT No.18917) was used for peak identification. The determination of the samples physicochemical properties was investigated via the following procedures: saponification index (ASTM D5558-95), acidity index (D5555-95) and iodine index by the Wijs method (ASTM D5554-15).

Each oil, fat and acid sample was submitted to the alcoholic saponification step (NaOH 2%w/v in anhydrous ethanol) at 75°C under reflux for 60 minutes. The solid product obtained in each reaction, after filtration, was dried in an oven at 70ºC for 24 hours, being stored for later use as a collector. Each fatty acid salt was identified according to the related sample as andiroba oil collector (AOC), pataua oil collector (POC), bacuri fat collector (BFC), sodium oleate (SO), and sodium palmitate (SP). The extent of the saponification reaction was characterized via Fourier Transform Infrared Spectroscopy (FTIR) tests, comparing the fatty sample to its respective collector. A Nicolet 6700 spectrometer (Thermo Scientific, USA) was used in the attenuated total reflectance (ATR) mode, with 64 scans in the 4000-675cm^{-1} range, with a resolution of 4cm^{-1}.

The Du Nouy ring method was used to obtain the surface tension of collector solutions and determine the critical micelle concentration (CMC), using a K10ST tensiometer (Krüss, Germany). The methodology involved the preparation of 20mL collector solutions, at approximately 21°C and pH 7.5, adjusted using NaOH and HCl solutions. At each test, the platinum ring was flame treated prior to each test to remove contamination.

Microflotation tests were performed in a modified Hallimond tube [22], using 0.5g of pure mineral sample (-212µm +75µm). Previously, minerals were conditioned for 7 minutes in 25mL of pH-adjusted collector solution at the base of the tube, with the aid of a magnetic stirring bar. Then, the extender and the upper part of the tube were attached, and the useful volume of the tube (245mL) filled with the same conditioning solution and nitrogen gas (N_2) was injected through the porous plate at the base of the tube at a flow rate of $40cm^3.min^{-1}$, and flotation was carried out for 1 minute. The floated and sunken products were collected, filtered, dried and weighed, and the floatability was calculated as the percentage of floated mass. The selectivity between pairs was obtained using the selectivity coefficient ($\beta_{A/B}$), widely used in phase separation in aqueous systems, adapted in the present work, considering the relationship between the partitions of the respective minerals (A and B) between floated and sunken [23].

Electrophoresis was used to measure the electrophoretic mobility of the samples using the ZM3-D-G Particle Analyzer (Zeta Meter, USA), with later calculation of the zeta potential. The sample preparation step involved the production of suspensions using 10mg of mineral sample below 38µm and 100mL of a 10^{-3}M pH-adjusted KNO_3 solution (supporting electrolyte). Based on Stokes' law, the rest time for each suspension was determined, seeking to obtain particles finer than 2µm in the final sample collected for the tests. HNO^3 and KOH were used as pH regulators.

The adsorption mechanism in the mineral-collector interaction was characterized via Fourier Transform Infrared Spectroscopy (FTIR). During sample preparation, 0.2g of each mineral was conditioned with 100mL of concentrated collector solution for 30min. The adsorption density of the collectors on the mineral particles was obtained indirectly, using the quantification of the remaining collector concentration in the supernatant after conditioning. This quantification was performed using a TOC-L Total Organic Carbon (TOC) analyzer (Shimadzu, Japan). The supernatant was prepared by conditioning of 0.5g of mineral sample with 25mL of collector solution at $20mg.L^{-1}$ for 7 minutes, followed by filtration and separation of the supernatant for analysis.

The surface of apatite, calcite, and dolomite were investigated using an AMICUS monochromatic X-ray photoelectron spectrometer (Kratos Analytical, UK) equipped with an Mg κα X-ray source (1253.6eV). The elemental surveys were performed from 0 to 1200eV (resolution: 1eV, dwell time: 100ms), whereas high resolution spectra were

obtained using a pass energy of 0.1eV. The samples (-212µm +75µm) were conditioned (0.5g) in 25mL of distilled water at pH 7.5 for 7min. After filtering, the solid was dried in an oven at 50ºC for 24 hours. Prior to the analyzes, the samples were degassed for 6 hours in an oven with forced air flow at room temperature and kept in a vacuum desiccator, prior to the experiments. The results were fitted using the software Vision Processing (Kratos Analytical, UK) and the C 1s peak for C-C was used as standard (BE at 284.8eV) for shift correction [24].

The determination of the specific surface area and porosimetry of apatite, calcite and dolomite was performed using a BK200C N2 adsorption porosimeter (Beijing JWGB Sci & Tech Co., China). The mineral samples were previously dried for 12 hours and submitted to degassing. The analysis was performed from 37 points of P/P0 (ratio between applied pressure (P) and saturation vapor pressure of the adsorbed gas (P0), in this case N2), with 24 points in the adsorption and 13 points on desorption. In all tests, specific surface area data was calculated by the BET equation (Brunauer, Emmett and Teller), and average pore diameter, average pore volume and total pore volume in the adsorption and desorption step were obtained using the BJH (Barrett, Joyner and Halenda) method.

4.3 Results and Discussion

4.3.1 Characterization of mineral samples

The XRD analysis resulted in the diffractograms shown in Figure 4.1, interpreted using the PDF-2 database, provided by the International Diffraction Data Center (ICDD, 2010). The data was submitted to a crystallographic refinement using the Rietveld Method, confirming the purity of the samples. For apatite, identified as fluorapatite, and calcite, the results indicated purity above 99%, while the dolomite sample showed 96% purity. These results were confirmed by the WDXRF analyzes, which showed that the apatite sample presented P, O and Ca as major elements, in addition to a small Si and Mg contamination, while the calcite and dolomite samples presented Ca, Mg and O as major elements, but in different proportions, in addition to the presence of traces of Si. Dolomite had the lowest purity among the minerals, with the presence of quartz and traces of Zn and Fe, which were identified as sphalerite in the XRD results. Al was detected in a minimal amount in all samples, probably coming from silicates present in minor amounts.

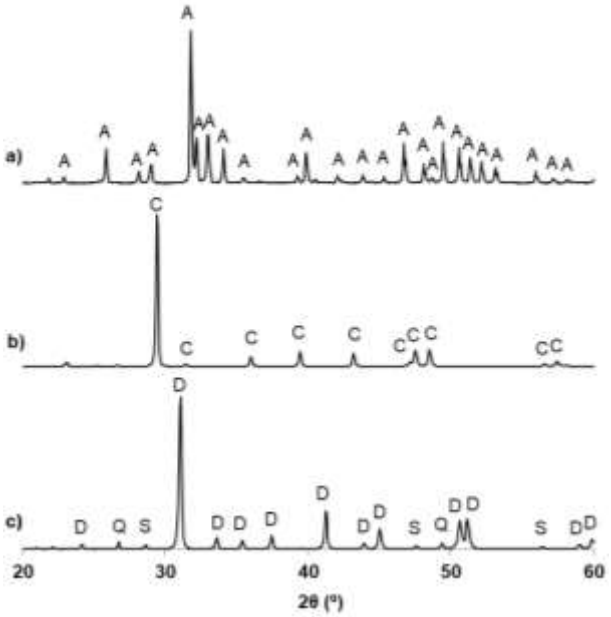

Figure 4.1 – X-Ray diffractograms of the apatite (a), calcite (b) and dolomite (c) samples. ICDD - A: apatite (09-0432), C: calcite (88-1807), D: dolomite (84-2065), Q: quartz (88-2302), S: sphalerite (05-0566)

The BET (specific surface area) and BJH (porosimetry) results, presented in Table 4.1, show that apatite presents an intermediate surface area and average pore diameter, in relation to the calcite and dolomite. The significant specific surface area of calcite, related to its low porosity, may indicate the easy to fragment, since all samples were submitted to the same preparation procedure, being in the same size range. The dolomite presented pores with larger diameters than the apatite, corroborating its smaller specific surface area. This characteristic facilitates the adsorption of reagents in the active sites inside the pores, but can hinder the adhesion of the hydrophobized particle to the N_2 bubbles and, consequently, its floatability.

Table 4.1 – Surface area and porosity of minerals samples.

Sample	Specific Surface Area ($m^2.g^{-1}$)	Total Pore Volume ($cm^3.g^{-1}$)	Average Pore Diameter (nm)
Apatite	0.91349	0.002	9.502
Calcite	2.17631	0.000	0.206
Dolomite	0.31321	0.002	26.805

4.3.2 Characterization of oil, fat and acid samples and saponification products.

The results of the characterization of oils, fats and fatty acids by GC are shown in Table 4.2. The analysis of oleic acid (OA) and palmitic acid (PA) confirmed their purity, in agreement with the manufacturers' specifications. The fatty acid profiles of the oils of pataua (PO) and andiroba (AO), in addition to the bacuri fat (BF), show the majority proportion of oleic and palmitic acids in their composition. PO presents majority composition in oleic acid and BF, in palmitic acid. AO presents an intermediate proportion of these fatty acids in its composition.

Table 4.2 – PO, BF, AO, OA, PA fatty acid profiles.

Fatty acid		C12:0 lauric	C14:0 Miristic	C16:0 Palmític	C16:1 palmitoleic	C18:0 esteáric	C18:1 oleic	C18:2 linoleic	Others
OA	Test	0.0	0.0	1.6	0.0	2.7	88.7	6.6	0.4
	Labsynth (2021) [29]	-	-	-	-	-	90	-	10
PA	Test	-	-	95,5	-	-	-	-	4,5
	Clariant (2021) [30]	-	-	98	-	-	-	-	2
PO	Test	0.7	0.5	11.5	0.7	4.4	75.0	5.9	1.3
	Amazon oil (2021) [26]	-	-	6-15	< 2	2-9.5	68-83	2-9	-
	Serra *et al.* (2019) [17]	0.20	0.09	13.59	0.41	2.75	78.46	3.49	1.01
AO	Test	0.3	0.3	27.1	1.2	8.8	48.2	12.1	2.0
	Amazon oil (2021) [25]	-	-	25-32	0.8-1.5	6-13	45-58	6-14	-
	Serra *et al.* (2019) [17]	5.35	3.57	28.72	0.82	6.16	44.67	9.3	1.41
	Silva *et al.* (2018) [16]	-	-	25.1	0.53	10.11	57.58	5.87	0.81
BF	Test	0.9	0.7	56.8	8.3	1.7	28.1	3.1	0.4
	Amazon oil (2021) [27]	-	-	67-75	3-7	-	22-27	-	-
	Serra *et al.* (2019) [17]	0.03	0.16	63.09	6.56	1.24	26.16	2.63	0.13

The physical aspect of PO (84% unsaturation) and AO (60% unsaturation) is characterized by the majority participation of unsaturated chain acid (oleic), ensuring the liquid state of oils at room temperature. On the other hand, the predominance of saturated fatty acid (palmitic) in BF (25% unsaturation) provides its solid appearance at room temperature, characteristic of fats [3, 25-27]. Additionally, the profile of PO, AO and BF are similar to the typical composition of these vegetable oils and fats reported in the literature and according to the American Oil Chemist's Society (AOCS) [16-18]. Small variations observed can be attributed to the natural characteristics of these resources such as geographic origin, age of the fruits and climatic conditions during their cultivation [28]. Unsaturated fatty acids such as oleic and linoleic, present in the evaluated plant samples, show good performance in floatability during flotation [3]. The presence of these fatty acids is also observed in vegetable oils traditionally used in

flotation routes for phosphate ore, such as tall oil, rice bran and soybean [13].

The chemical parameters of PO, AO e BF are shown in Table 4.3. The acidity index (AI) indicates the proportion of free fatty acids in the composition of oil and fat samples. When intended for the food industry, it represents a parameter of product quality and conservation, with strict control [31]. In industrial applications, mainly in flotation, high acidity indexes represent advantages in the saponification step, used to obtain the collector. This is because a greater proportion of free fatty acids in the system accelerate the reaction kinetics, breaking the triglyceride ester bonds that make up the oil/fat, followed by the neutralization of the released fatty acids [32]. Therefore, the high values observed for this parameter in AO and BF are beneficial to collector synthesis. For AO, the value obtained for saponification index (SI) corroborates the manufacturer's indication, while, for BF and PO, the results were slightly lower than the manufacturer's indication. This parameter provides information on the size of the hydrocarbon chains of the fatty acids that make up the fatty samples. Therefore, these small variations observed in BF and PO may be related to some changes suffered by the samples between the period of analysis carried out by the company and in the laboratory, or by the difference in precision between the analyzes carried out. Finally, the iodine index (II) is indicative of the degree of unsaturation of the carbon chain of fatty acids present in the sample. The values obtained for all samples corroborate the manufacturer's indication. As discussed for the fatty acid profile, discrepancies observed for the saponification index value reported in the literature for andiroba oil may be related to variations in its composition due to aspects to be considered during the cultivation stage, with an impact irrelevant for obtaining collecting reagents [28].

Table 4.3 – Chemical parameters of oils and fat.

	AO			**BF**			**PO**		
	Test	Amazon oil (2021) [25]	Serra *et al.* (2019) [17]	Test	Amazon oil (2021) [25]	Serra *et al.* (2019) [17]	Test	Amazon oil (2021) [25]	Serra *et al.* (2019) [17]
AI (mg KOH.g^{-1})	21.1±0.5	<15	21.70±0.26	16,0±0,3	<7.5	16.78±0.26	7.5±0,2	<10	7.52±0.06
SI (mg KOH.g^{-1})	194±15	190-210	241.43±2.40	179±4	200-220	242.39±0.69	179±3	192-209	181.522±0.13
II (g I_2.g^{-1})	66±2	65-75	63.30±0.21	53±3	50-65	76.29±0.49	75±2	70-83	73.18±1.57

From the saponification reaction of the oils and fat samples (AO, BF and PO), their respective collectors were obtained in the form of sodium salts. They are the andiroba oil collector (AOC), bacuri fat collector (BFC) and pataua oil collector (POC). Also, from the neutralization reaction of the fatty acids, sodium salts were obtained as

collectors: sodium oleate (SO) and sodium palmitate (SP). The extension of the saponification reaction can be evaluated based on the ATR- FTIR spectra of the oil/fat sample and its respect to sodium salt (Figure 4.2). The 1,744cm^{-1} and 1,711cm^{-1} bands are characteristic of triglycerides and free fatty acids present in the oils/fat, while the 1,558cm^{-1} band is characteristic of sodium fatty acid salts, confirming that the saponification was complete [33]. Also, minor bands related to the alcohol used in the reaction (879cm^{-1} and 1.047cm^{-1}) were highlighted [34].

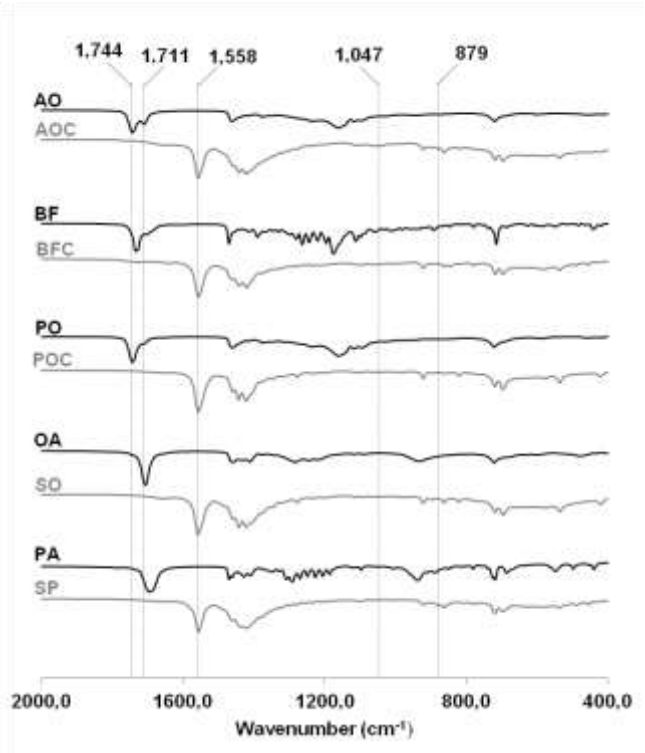

Figure 4.2 – ATR-FTIR spectra of oils, fat and acids (in bold) and its salt collectors (gray).

The surface tension curves and critical micelle concentration (CMC) of each collector are available in Figure 4.3. Factors such as temperature, solution concentration and medium pH affect the CMC of aqueous solutions. The positioning of molecules at the liquid/gas interface provides an inverse relationship between the concentration of collectors in the solutions and their respective surface tension. The analysis of the curves provides the concentration values characterized as critical premicellar concentration (PCMC) and critical micelle concentration (CMC). For concentrations comprised between these parameters, there is the formation of species that promote

greater floatability of particles, known as hemi-micelles. These structures favor the immobilization of collecting species on the mineral surface, enhancing bubble-particle adhesion [13]. From the CMC, it is observed the formation of species that negatively affect the process, known as micelles. These structures agglomerate or reverse the hydrophobization of mineral particles. The values obtained for PCMC and CMC of the evaluated collectors are shown in Table 4.4.

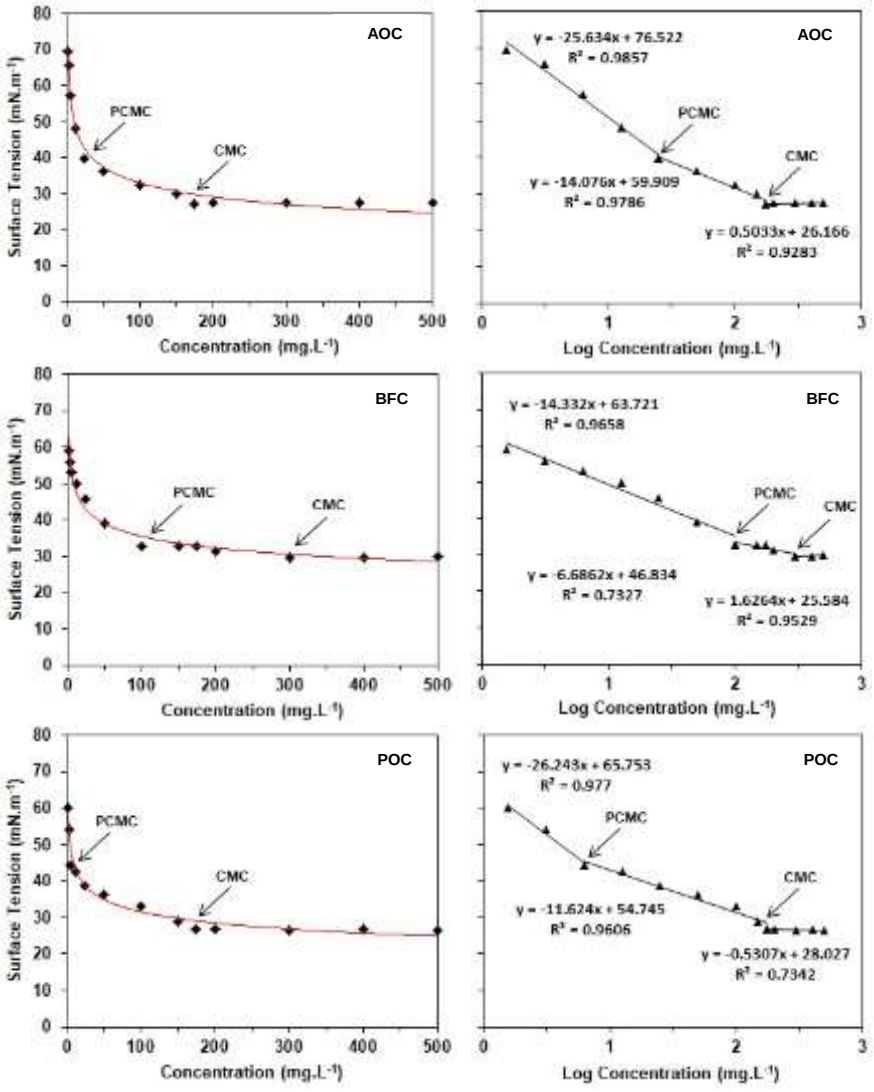

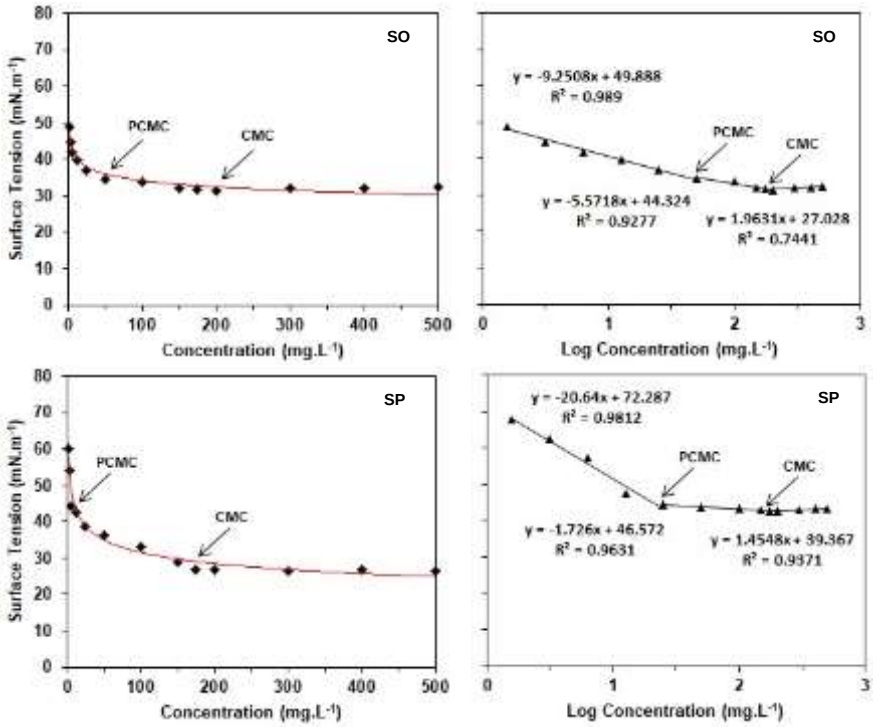

Figure 4.3 – Surface tension of collector solutions as a function of concentration (a) and log of concentration (b), at pH 7.5.

Table 4.4. PCMC and CMC of the collectors.

	AOC	BFC	POC	SO	SP
PCMC ($mg.L^{-1}$)	25	100	6,25	50	25
CMC ($mg.L^{-1}$)	175	300	175	200	200

The CMC values obtained for sodium oleate were consistent with those reported in the literature (up to 300$mg.L^{-1}$). No references were found for sodium palmitate in the literature that would allow such a comparison. The BFC showed a discrepant CMC in relation to other collectors from Amazonian oils, indicating the formation of micelles at higher concentrations. Such discrepancy can be attributed to the high proportion of palmitic acid in its composition, while AOC and POC are mainly composed of oleic acid. The configuration of the angular carbon chains of oleic acid provides a distinct configuration in relation to the linear chains of palmitic acid, favoring the interaction between them and the formation of micelles at even low concentrations in the aqueous solution. Also, the composition of the vegetable oil sample, represented by the mixture of fatty acids present in its fatty profile, generates a less dense packing than that

observed for the system containing pure fatty acid salt, since the differences in size and conformation of the carbon chains of the fatty acids present in the oil make it difficult to match close molecules due to the difference in vibrational energy caused by the thermal movement of currents [8].

4.3.3 Microflotation

The floatability of apatite, calcite and dolomite (Figure 4.4) was evaluated as a function of collector concentration, pH, and conditioning time. These analyzes aimed to compare the performance of high purity fatty acid salts (sodium oleate and sodium palmitate) to that of the mixtures present in the oil-based collectors, in different proportions.

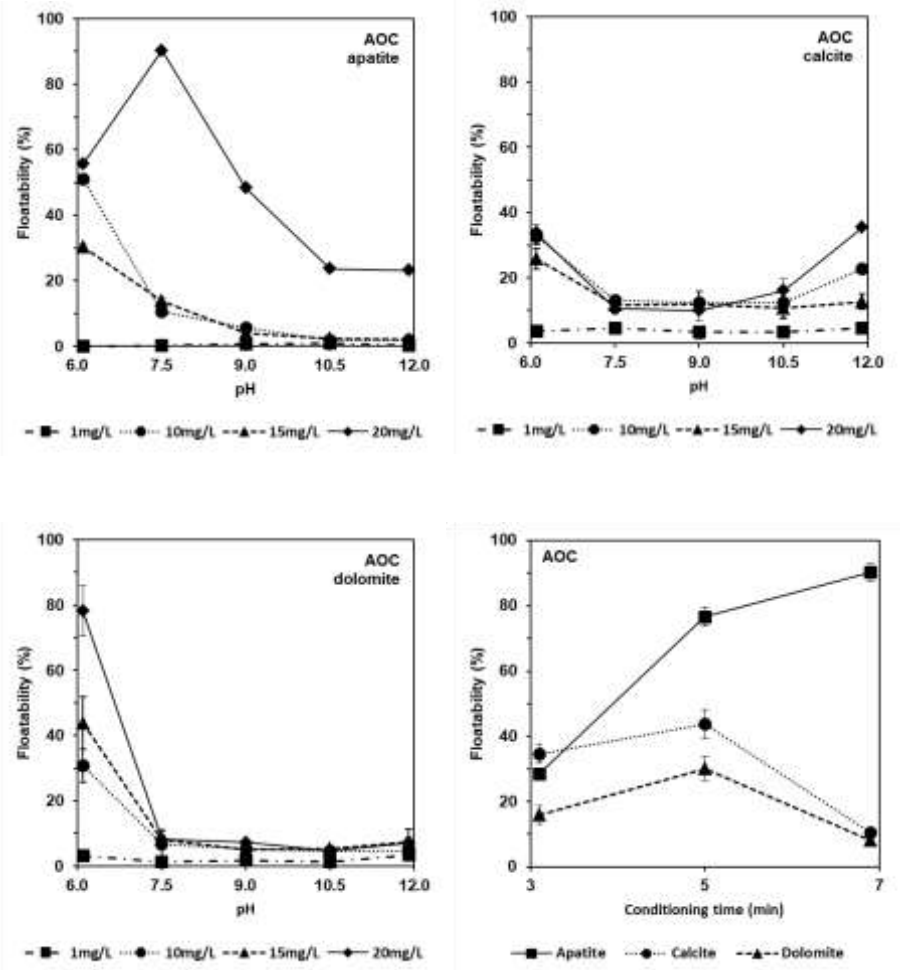

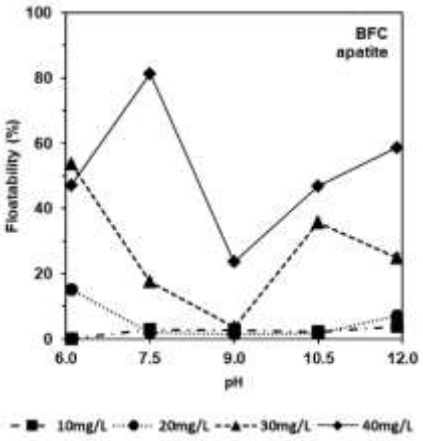
BFC
apatite
Floatability (%)
pH
10mg/L
20mg/L
30mg/L
40mg/L

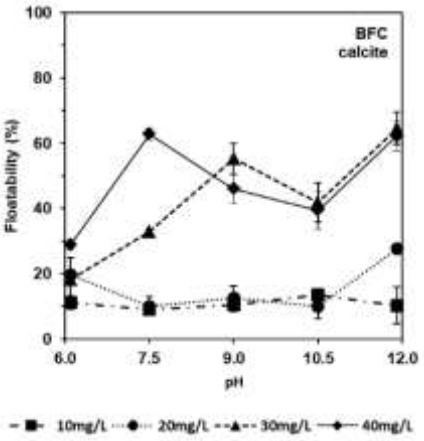
BFC
calcite
Floatability (%)
pH
10mg/L
20mg/L
30mg/L
40mg/L

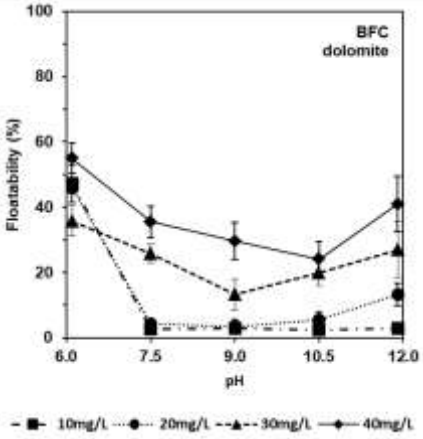
BFC
dolomite
Floatability (%)
pH
10mg/L
20mg/L
30mg/L
40mg/L

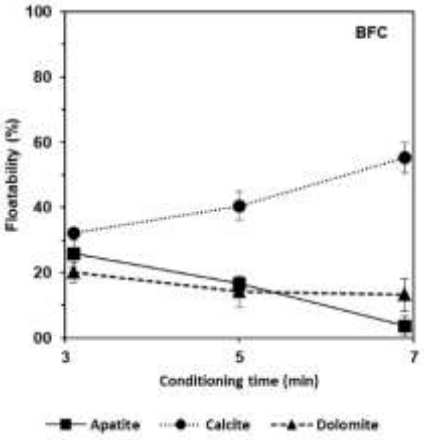
BFC
Floatability (%)
Conditioning time (min)
Apatite
Calcite
Dolomite

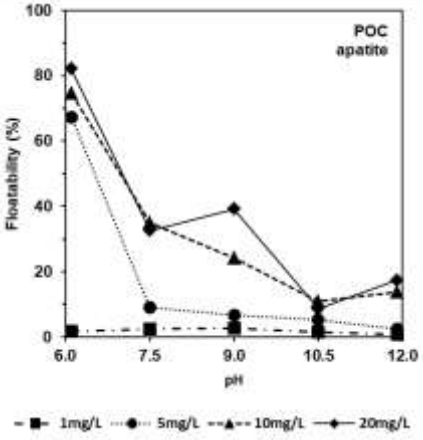
POC
apatite
Floatability (%)
pH
1mg/L
5mg/L
10mg/L
20mg/L

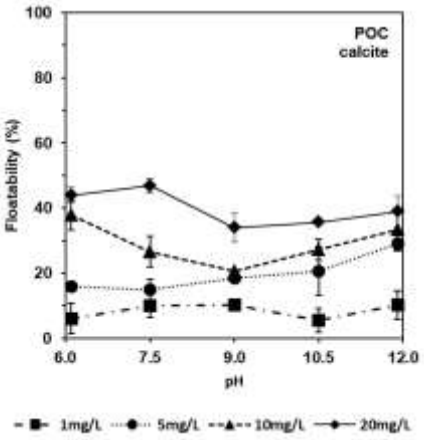
POC
calcite
Floatability (%)
pH
1mg/L
5mg/L
10mg/L
20mg/L

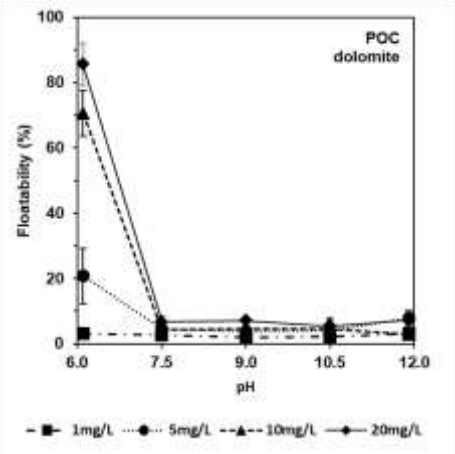
POC
dolomite
Floatability (%)
pH
1mg/L
5mg/L
10mg/L
20mg/L

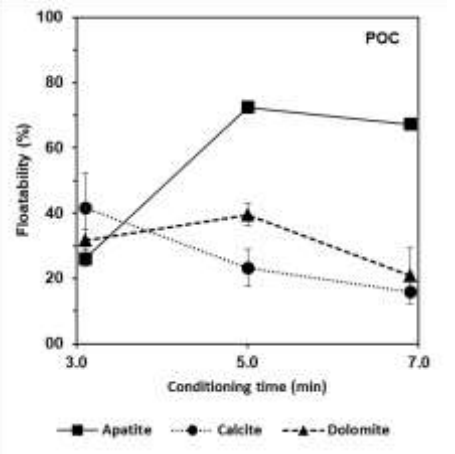
POC
Floatability (%)
Conditioning time (min)
Apatite
Calcite
Dolomite

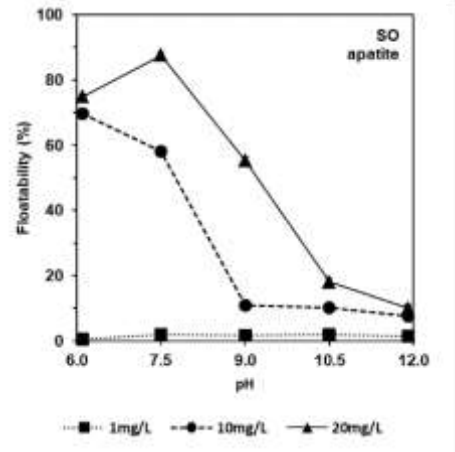
SO
apatite
Floatability (%)
pH
1mg/L
10mg/L
20mg/L

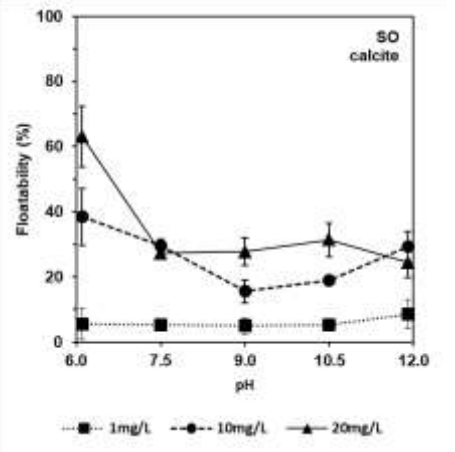
SO
calcite
Floatability (%)
pH
1mg/L
10mg/L
20mg/L

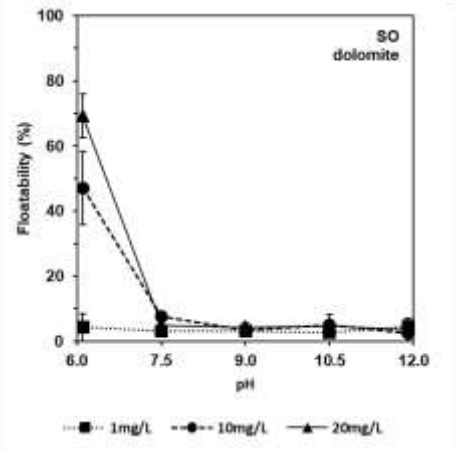
SO
dolomite
Floatability (%)
pH
1mg/L
10mg/L
20mg/L

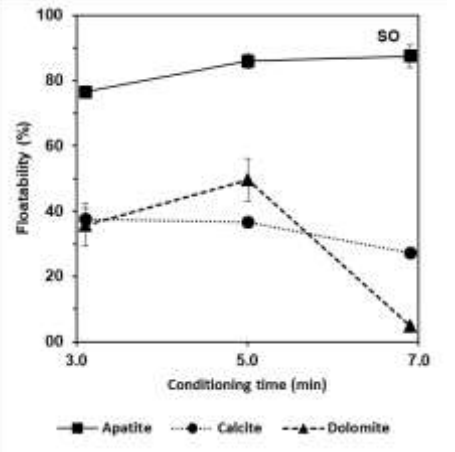
SO
Floatability (%)
Conditioning time (min)
Apatite
Calcite
Dolomite

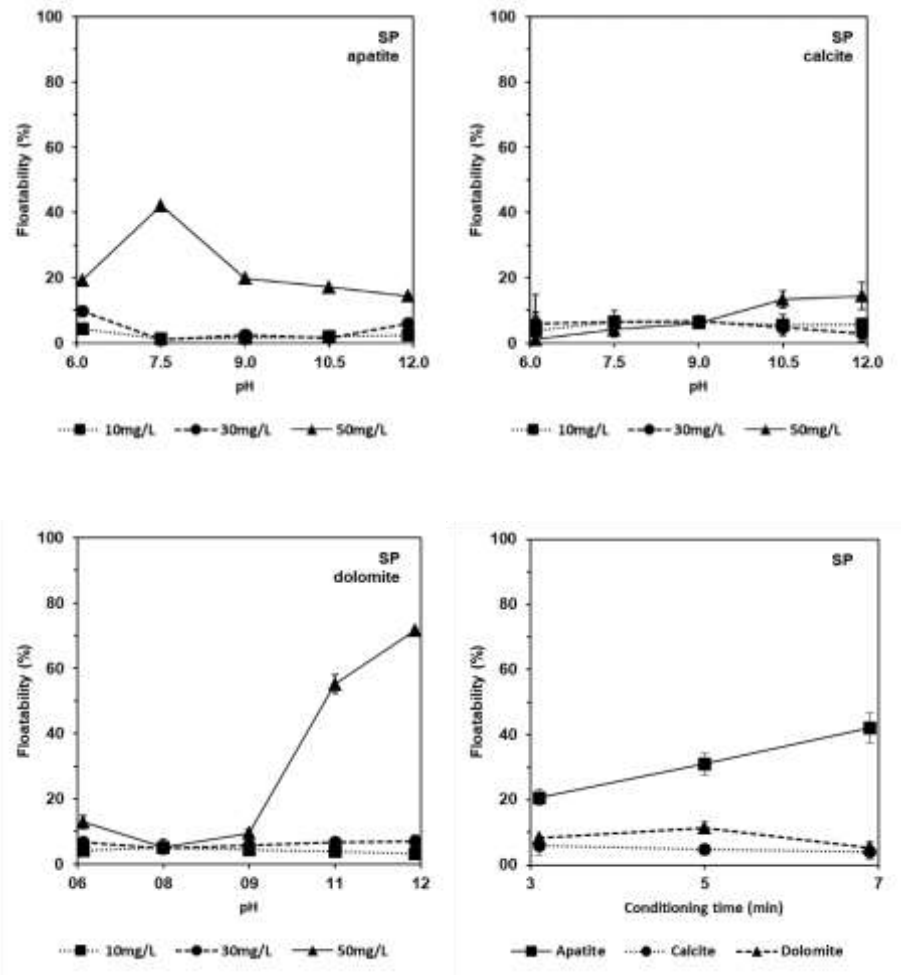

Figure 4.4 – Effect of collector concentration, pH and conditioning time on apatite, calcite and dolomite floatability.

The tests using SO demonstrated selectivity under conditions of pH 7.5 and collector concentration equal to 20mg.L^{-1}. Under these conditions, the high floatability of apatite (88±7%), compared to both calcite (27±1%) and dolomite (5±1%), provide this selective condition. The performance of sodium oleate as a collector for systems containing apatite and carbonates has been extensively investigated, with the results reported in the literature [3, 35, 36]. The high selectivity observed for the apatite/dolomite pair corroborates the characterization obtained for the zeta potential of mineral particles. This is because, after conditioning with oleate, a greater reduction in the residual surface charge of the particles for apatite was observed, indicating greater adsorption of oleate at the Ca^{2+} sites. This oleate adsorption mechanism on Ca-bearing minerals is known and reported in the literature [35, 37-39]. The selectivity between the apatite/calcite pair can be due to the discrepancy between the spacing and distribution of the Ca^{2+} sites on

the surface of each mineral, since they showed similar reduction in zeta potential after oleate adsorption. The incidence and spacing between these sites on the mineral surface differ for apatite and carbonates, giving different configurations to the hydrophobic film. The increase in collector concentration directly affected the SO performance on apatite floatability. As for carbonates, this parameter showed a low or negligible relationship with the performance of the collector, especially for dolomite above pH 7.5 as for calcite, above medium pH, the mineral's floatability remained stable in the plateau between 20% and 30%. The selectivity between apatite and carbonates, in systems employing sodium oleate, can be achieved using collector concentrations lower than those obtained in the present study (approximately 5mg.L^{-1}) [36-38].

For the system using SP collector, the most selective scenario was obtained at pH 7.5 and 50mg.L^{-1}collector concentration. Under these conditions, higher floatability was obtained for apatite (42±9%) in comparison to calcite (4±5%) and dolomite (5±4%), which indicates a lower selectivity for direct phosphate flotation if compared to SO collector. The structural difference between the carbon chains of the species, linear for SP and angular for SO, may result in discrepancies in the electronegativity of the polar portion of the collectors, affecting their interaction with active sites on the mineral surface. Furthermore, the interaction between carbon chains, which promotes the stability of the hydrophobic film on the particles, is related to the configuration of these chains. The angularity observed in the SO structure can favor the interaction between the chains, establishing a more stable hydrophobic layer, which favors the hydrophobization and floatability of particles. By analyzing the results, an alternative scenario of selectivity for reverse flotation was observed for highly alkaline conditions, above pH 10.5. In this scenario, dolomite presented high floatability (72±1%), compared to calcite (14±8%) and apatite (14±3%). However, it is important to note that high consumption of pH regulating reagents, in addition to the formation of hydroxycomplexes in the medium, can make the operation unfeasible. Calcite recovery was not significantly affected by the collector concentration or pH of the medium.

The higher floatability observed for apatite at pH 7.5 corroborates with previous studies reported in the literature to oleate, which point to high mineral recovery in conditions close to neutrality [3]. The speciation of fatty acids as a function of pH (pKa around 4.8) reinforces this behavior [11, 40]. In other words, for systems with pH conditions below pKa, fatty acids predominate in their molecular form, promoting physical adsorption, of

low intensity, on mineral particles. In systems with pH conditions above the pKa, the fatty acid is mostly in the ionic form, able to adsorb on the Ca^{2+} sites at the mineral surface through chemical adsorption [36, 40, 41]. The formation of ionomolecular complexes, from the combination of molecular and ionic species of the fatty acid, is predicted for intermediate pH conditions, close to neutrality. The occurrence of this type of species in the system favors the hydrophobization of particles, as their structure is more stable due to the presence of collecting (ionic group) and stabilizing (molecular group) characteristics of the hydrophobic film [12, 39]. For the conditions defined as selective for SO, the pH (7.5) favors the formation of this type of species in the medium, enhancing the apatite flotation. In addition, there may be the formation of micelles or collector precipitates in the solution, as well as the appearance of dimer-type structures, which present stability even under highly alkaline conditions. The adsorption of dimeric species formed at strongly alkaline pH reduces the hydrophobization of the particles due to the exposure of the polar groups of the collector to the solution, favoring the interaction with the polar groups of the aqueous phase [13, 39]. Furthermore, the high pH scenario favors the competition between hydroxyl and carboxylate ions for the Ca2+ sites on the surface of apatite, promoting an increase in the concentration of carboxylate in solution and the formation of micelles, instead of calcium carboxylate at the mineral surface, impairing recovery [40, 41].

The nature of the adsorption of the collector onto the mineral particle affects the time required for the establishment of this interaction. Chemical adsorption, such as that observed between sodium oleate and apatite/carbonates, requires more time for the process to be effectively established. For apatite, the collector showed an increased recovery at longer conditioning time. Even though it is a semi-soluble mineral, the mineral's dissolution kinetics has not been shown to affect the balance of the system. The chemical nature of collector adsorption on calcium-bearing mineral particles, via surface precipitation of oleate, corroborates the direct relationship between flotation performance and the increase in surface Ca^{2+} sites [42]. The partial solubility of the minerals (apatite and carbonates) provides the formation of new Ca^{2+} sites, shifting the adsorption balance towards the formation of calcium dioleate, which can precipitate on the mineral surface [35, 43]. The solubility balance of these semi-soluble minerals is related to their crystallinity, surface area, porosity and presence of impurities or substitutions in their composition. [37]. Due to higher solubility, carbonates showed

worse flotation performance with increasing conditioning time for both SO and SP collectors.

The discrepancies found between the selectivity conditions obtained for AOC, BFC and POC, in relation to SO and SP, presented in Table 4.5, can be related to the difference in the degree of packing of the carbon chains of the adsorbed collector molecules at the mineral surface. As fatty samples present a variety of carbon chains from the different fatty acids that make up the oil/fat, this can result in a less compact hydrophobic film compared to the hydrophobic layer formed in the adsorption of the pure fatty acid salt collector, which has the predominance of sodium oleate or palmitate. Therefore, the oil-based collectors may require different concentrations capable of providing the formation of a cohesive film, ensuring its effective hydrophobization [36]. For all oil-based collectors, the beneficial effect of increasing the concentration, up to a specific level, is evident from the results obtained. Regarding pH, the effects are more evident for systems containing AOC and POC.

Table 4.5 – Selective conditions to separate apatite from carbonates.

		AOC	BFC	POC	SO	SP
Collector concentration ($mg.L^{-1}$)		20	30	5	20	50
pH		7.5	9.0	6.0	7.5	7.5
Floatability	apatite	90±5	7±6	67±3	88±7	42±9
	calcite	11±2	55±9	16±3	27±1	4±5
	dolomite	8±3	13±10	21±17	5±1	5±4

The performance of AOC, including the behavior regarding the conditioning time, was similar to that observed for SO, which can be directly linked to the andiroba oil composition, with major participation of oleic acid (48.2%), followed by the presence of palmitic acid (27.1%). The synergy between the sodium salts of the two fatty acids present in the sample may explain the observed reduction in calcite floatability in a system employing AOC, in comparison to the use of SO. The poor calcite floatability observed for SP in microflotation may have affected the SO action mechanism, when together in the AOC.

The BFC, which presents a major participation of sodium palmitate, based from the presence of palmitic acid in the oil sample (56.8%), in addition to sodium oleate (28.1%) demonstrated affinity for carbonates, similarly SP, which displays an alternative selective scenario for separating dolomite from apatite in alkaline conditions.

In the case of BFC, under these conditions, its affinity is more pronounced for calcite. However, it is evident the poorer performance observed for BFC in the selective flotation of apatite and carbonates at different concentrations and pH, contrasting with the behavior of SO and SP collectors. Such behavior can also indicate the synergistic effect in the adsorption of different sodium fatty acid salts present in an oil-based collector [6, 7, 9]. Still, differing from all other collectors, the BFC conditioning time directly affected the floatability of calcite, reinforcing the discussion about the collector affinity for calcite.

Regarding the POC, collector obtained from patauá oil, a sample with greater participation of oleic acid in its fatty profile (75.0%), in addition to a lower proportion of palmitic acid (11.5%), the results showed a relationship with those obtained for SO, including the effects of the conditioning time, despite lesser similarity with it when compared to AOC. The selectivity observed in the tests agrees with the literature records, despite being inferior than previous studies with POC as apatite and carbonate collector [21]. Regardless of the high production potential, in addition to the favorable composition for application in froth flotation, due to its fatty acid profile [16, 17], no records of studies using andiroba and bacuri oil-based collectors are found in the literature.

4.3.4 X-ray photoelectron spectroscopy (XPS)

The XPS surface characterization of the mineral particles, previously conditioned at pH 7.5, is presented in Table 4.6 and Figures 4.5, 4.6 and 4.7. The technique is generally employed in the field of mineral flotation, providing information about the surface characteristics of the particles, prior to conditioning with reagents or after their adsorption, and can contribute to the understanding and identification of the active sites available for reagent adsorption in flotation systems [24].

The results obtained demonstrate, from the surface atomic composition of the particles, the presence of a small contamination by carbonates, evidenced by the detection of a subtle peak with binding energy of carbonates in the apatite sample (Figure 4.5). This contamination does not compromise the already discussed purity of the mineral sample, from the results obtained by XRD and WDXRF. For calcite and dolomite, the high purity of the samples is confirmed, without the detection of elements other than those present in their chemical composition.

Previous studies report the chemisorption mechanism as the protagonist in the adsorption of fatty acid salt-type collectors on calcium-bearing minerals. The interaction between Ca^{2+} surface sites and COO^- anions from the chemical structure of the collector leads to the formation and precipitation of calcium carboxylate on the minerals. This phenomenon guarantees the hydrofobization of the particles during conditioning with the reagents [42, 44]. The presence of significant amounts of Ca on the surface of apatite, calcite and dolomite, obtained via XPS, suggests that Ca^{2+} sites might have been available for collector adsorption in all minerals. The dolomite sample showed a lower percentage Ca on its surface, reflecting its chemical composition, which may have influenced in a lower adsorption of the collector, minimizing its floatability. The higher percentage of surface Ca on the calcite surface did not result in greater floatability, as seen in the microflotation results. Another factor that may have contributed to the low intensity of collector adsorption on carbonates is related to the test pH, close to neutrality. Under these conditions, the solubility of carbonates is lower, making it difficult to form free Ca^{2+} sites on the mineral surface. The expressive adsorption of high proportion of unsaturation collectors on the apatite suggests the influence of a factor related to the conformation of this Ca-collector interaction on the mineral surface. The arrangement of the Ca^{2+} sites on the apatite surface could be organized in such a way that it would fit more appropriately with the spatial deformation of the carboxylate groups in the collector, promoting greater interaction between them.

Table 4.6 – Atomic composition at the surface of apatite, calcite and dolomite conditioned at pH 7.5.

	Elemental Content (%)					
	C	O	Ca	P	F	Mg
Apatite	2,8	70,1	14,0	11,2	1,9	-
Calcite	18,7	63,9	17,4	-	-	-
Dolomite	13,3	66,4	8,8	-	-	11,5

The apatite high resolution XPS spectra (Figure 4.5) indicated the presence of other sites different from those of apatite in the surface of the particles. The Ca 2p, P 2p and F 1s spectra were fitted with peaks assigned for apatite at 347.56eV (Ca $2p_{3/2}$) and 350.77eV (Ca $2p_{1/2}$), 133.44eV, and 684.76eV, respectively [45]. The C 1s spectrum showed the presence of adventitious C-C [46] at 284.80eV, possibly due to the presence of organic contaminants, and the presence of carbonate sites, due to the required fitting of a peak at

288.94eV [47], identified by characterization via WDXRF. Besides the apatite peak in the O 1s spectra, at 531.42eV [48], the presence of metal oxide sites were also indicated by a peak fitted at 529.60eV [49]. Both contaminants identified on the apatite surface (carbonate and metal oxide) can act as active sites for the adsorption of carboxylates, favoring the hydrophobization of the particles.

The calcite high resolution XPS spectra (Figure 4.6) indicated the mineral surface presented no other contamination besides the adventitious C-C, at 284.80eV, as the others samples. The calcite peak was observed at 289.42eV in the C 1s spectrum, in agreement with previous studies [47]. The Ca $2p_{3/2}$ and Ca $2p_{1/2}$ spectra were properly fitted with calcite peaks at 346.98eV and 350.31eV, respectively [47]. The O 1s spectrum was fitted with a peak at 531.48eV, attributed to the CO_3^{2-} in the calcite composition [50, 51].

The C 1s XPS spectrum indicated the presence of adventitious C-C as a contamination at the dolomite surface, with peak at around 284.81eV (Figure 4.7), whereas a second peak was identified at around 289.71eV, which was assigned to CO_3^{2-} from the dolomite composition [52]. The fitting of the O 1s spectrum showed the presence of oxygen as dolomite [53], with a peak at 531.86eV, and the presence of a metal oxide sites [49], due to the presence of a peak at around 530.01eV. This result indicates the oxidation of Zn and Fe in the minor percentage of sphalerite indicated by the PXRD and WDXRF results. The Ca 2p spectrum was properly fitted with the doublets for dolomite (Ca $2p_{3/2}$ and Ca$2p_{1/2}$ at around 347.30eV and 350.75eV, respectively), whereas the Mg 2p spectrum was fitted with a dolomite peak at 50.06eV [53]. Although the Ca 2p and Mg 2p spectra indicated no other species than dolomite at the sample surface, the presence of a metal oxide can be expected, as shown in the O 1s spectrum. As discussed for apatite, the presence of Fe sites on the surface of dolomite could corroborate for the adsorption of the carboxylate-type collector. This behavior did not favor the hydrophobization of the particles with high proportion of unsaturation collectors, as observed by the results of microflotation (Figure 4.4).

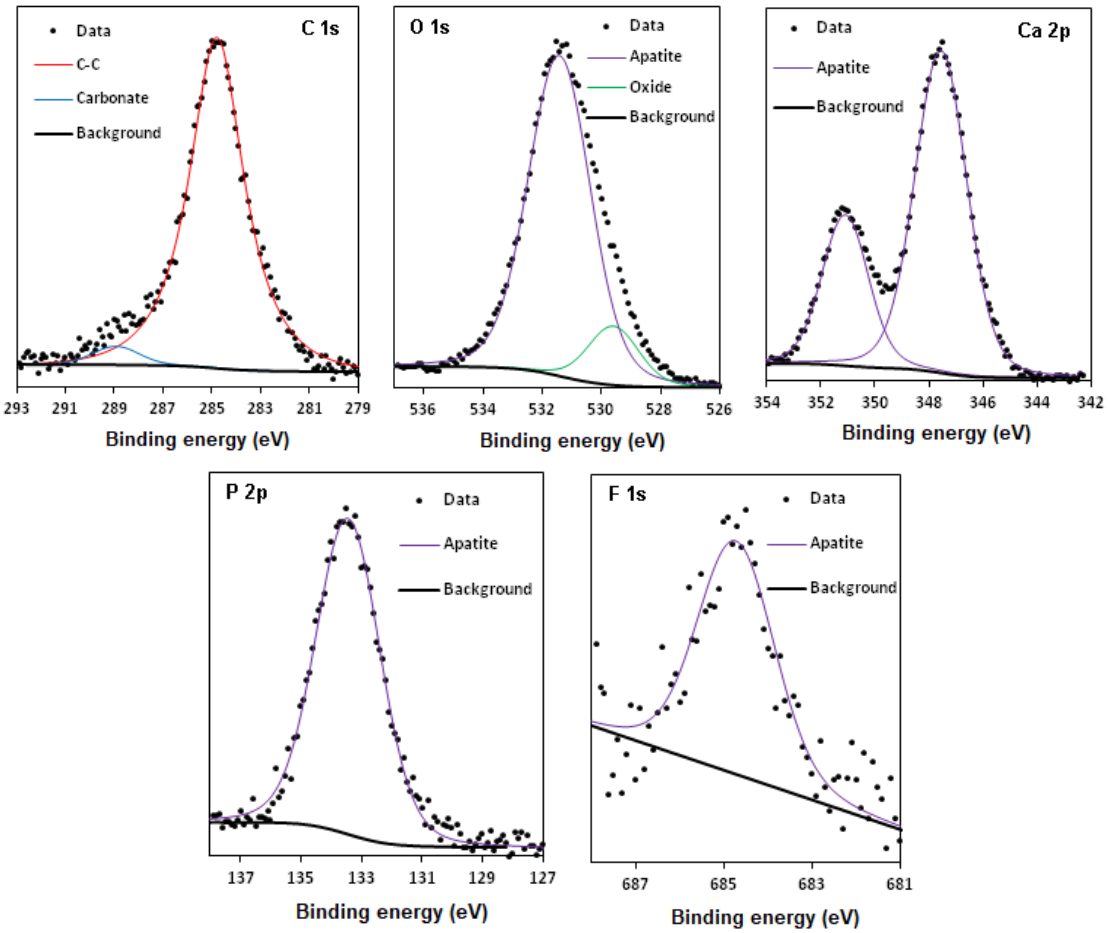

Figure 4.5 – Fitted peaks in the C 1s, O 1s, Ca 2p, P 2p e F 1s XPS high resolution spectra of the apatite sample.

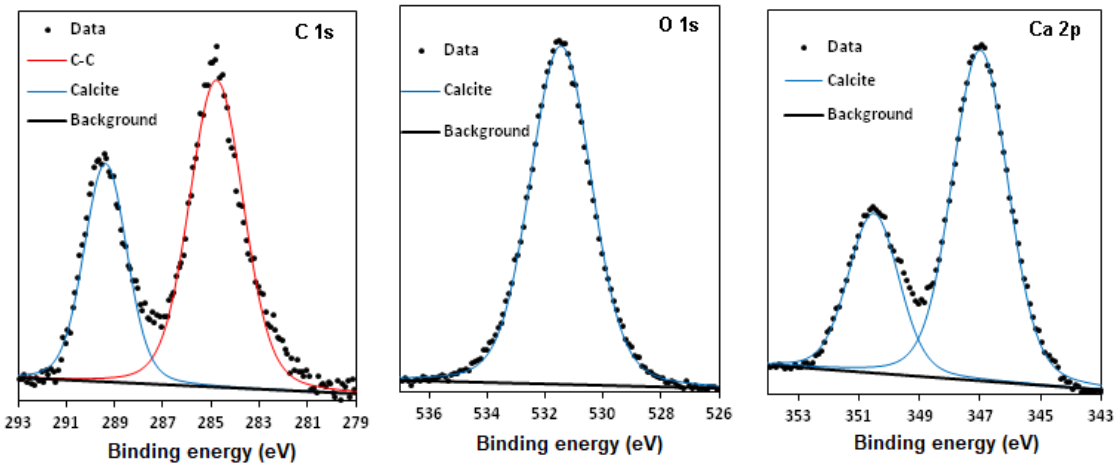

Figure 4.6 – Fitted peaks in the C 1s, O 1s and Ca 2p high resolution XPS spectra of the calcite sample.

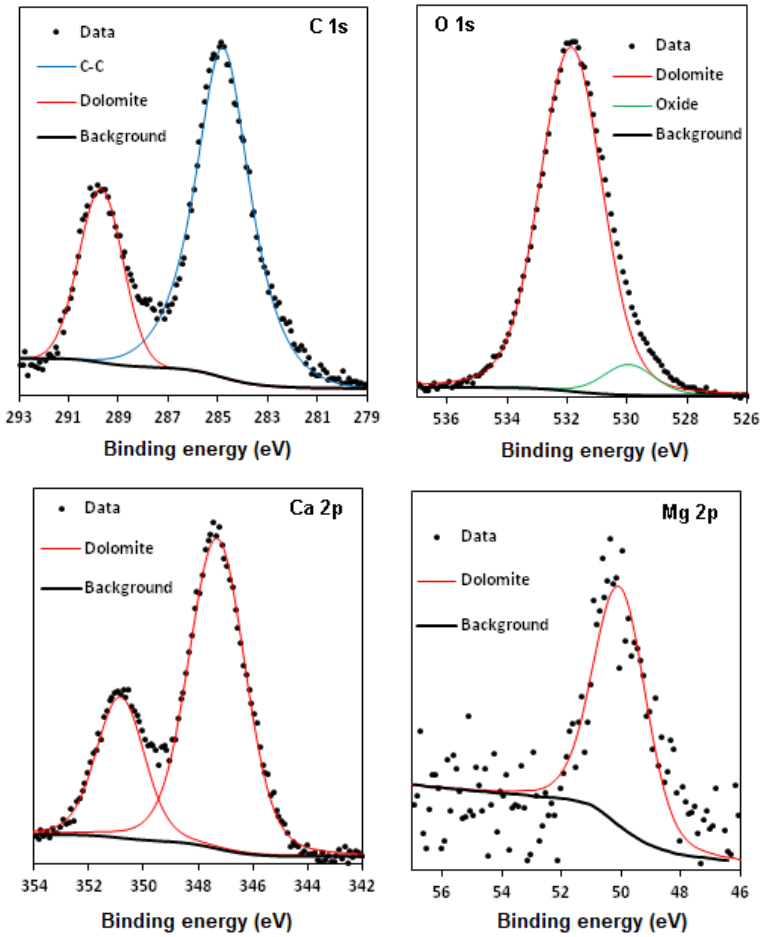

Figure 4.7 – Fitted peaks in the C 1s, O 1s, Ca 2p e Mg 2p high resolution XPS spectra of the dolomite sample.

4.3.5 Total Organic Carbon (TOC) and Collector Adsorption Density (CAD)

The collectors' adsorption density (CAD) on the apatite, calcite and dolomite particles are presented in Figure 4.8. Collectors from both Amazonian oils/fat samples (mixed fatty acid salts) and those obtained from high purity fatty acids were evaluated. For calcite, reduced CAD values can be observed for all collectors, which reflects the low floatability of this mineral. The characteristics of the calcite sample (high proportion of fines due to its high moability, along with low porosity) contributes to low CAD values, indicating a possible sensitivity of the collectors to the presence of fines. This behavior is common to cationic collectors, which establish interactions of the non-specific type with the mineral surface, and this scenario is quite discrepant in relation to the collectors used in the present study (anionic, with a tendency to establish specific type interactions with minerals bearing Ca). The exception in relation to the low floatability of this

mineral is the calcite/BFC system, which showed significant values of floatability at high collector concentrations. This phenomenon may be related to the synergistic action of the fatty acids present in the BF composition, evidenced by the discrepancy between CAD values obtained for BFC and the systems containing SO and SP. A positive reinforcement between the action of pure fatty acid salt collectors can be proposed, when simultaneously present in the system, with higher proportion of PA, reflecting in the better performance of BFC as calcite collector. The conformation of the hydrophobic film proved to be more effective for BFC, indicating the structural positioning of the carbon chains of the fatty acids with greater packing, favoring the CAD for this collector.

The CAD for dolomite presented high values, reflecting the morphological characteristics of its particles (low surface area, with large pores), which may have favored the adsorption of the collectors. However, this higher CAD observed may not reflect in higher floatability of the mineral, since, even hydrophobic, the pore internal surface should present difficulties of interaction with the N2 bubbles, compromising the effectiveness of the attachment phenomenon, impairing the floatability of particles. Furthermore, the CAD for dolomite was favored by the higher proportion of saturated carbon chains in the collectors evaluated (BFC and SP). For the other collectors evaluated, all with higher unsaturation index, lower CAD values were obtained. The configuration acquired by the hydrophobic film composed mainly by saturated chains favors the adsorption of the collector inside the pores, with higher intensity, corroborating with significant CAD values for BFC and SP, especially for the latter, with higher proportion of saturation.

The morphological characteristics of the apatite particles (intermediate specific surface area with the presence of pores with reduced diameters) favored the achievement of coherent CAD values, since they reflect the performance of the adsorbed collectors in collecting the mineral particles. The discrepancy between the high CAD values for SP (high saturation) and its low performance in the floatability of apatite particles demonstrates the formation of a hydrophobic dense film but of low stability for this collector, due to its morphological configuration by the structure of the (saturated) chains that compose it. This discussion corroborates with the results obtained for BFC, showing lower CAD values, but high values of floatability. This phenomenon can be attributed to the synergistic action between the majority composition of saturated chains

and a small proportion of unsaturated chains, which may have stabilized the hydrophobic film, favoring surface coverage, bubble attachment and, consequently, the floatability. The synergy between the fatty acid salts can also be discussed regarding the discrepancy between the CAD values and the performance of SO and POC as apatite collector. For the pure unsaturated SO collector, values close to those presented in the POC fatty profile are observed, which presents a majority proportion of oleic acid in its initial oil sample (75.0%). However, POC performance was poorer compared to that presented by SO. This low performance can be attributed to the minority share of other fatty acids, especially saturated ones, compromising the stability of the hydrophobic film formed by unsaturated oleate chains. The behavior presented by the AOC, with high efficiency in making apatite particles hydrophobic, similar to the SO, even with an intermediate proportion of oleic acid in its composition (48.2%) reinforces the discussion about an ideal proportion between saturation/unsaturation in the configuration of carbon chains present in oil-based collectors with mixed fatty acid composition [6, 7].

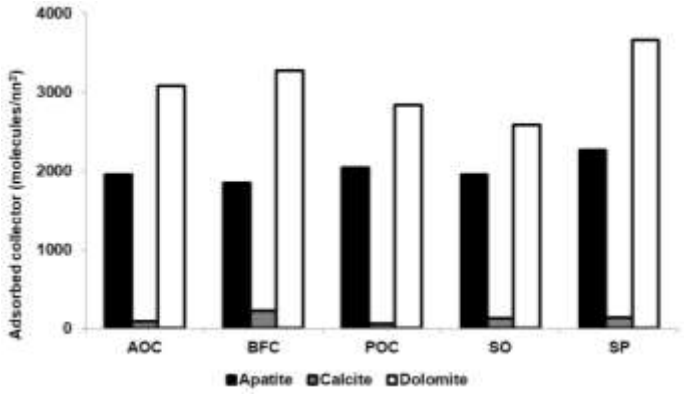

Figure 4.8 – Collector adsorption density.

4.3.6 Zeta Potential

The zeta potential results, obtained in the presence and absence of collectors, are shown in Figure 4.4. Minerals from the apatite group may present relevant variations in their electrokinetic behavior depending on their composition. Such discrepancy is related to the presence of distinct elements in its crystal structure due to ionic substitutions, providing different isoelectric points (IEP) [54-56]. In the case of the apatite used in this study, for the entire pH range evaluated, its zeta potential was negative, indicating an

isoelectric point at pH below 4. According to previous studies, fluorapatite samples, as identified in the XRD data (Figure 4.1), are expected to present this type of behavior, which agrees with the zeta potential results [57].

The partial solubility of semi-soluble minerals affects their electrokinetic behavior. During this process, cations and anions released into the system, in addition to the hydrolysis product of the minerals, can affect the surface characteristics of the minerals, behaving as potential determining ions (PDI) [58]. For apatite, Ca^{2+} and PO_4^{3-}, in addition to their hydrolysis products, affect the surface characteristic of the mineral, if it behaves as PDI. In a system with pH below the IEP, the particles acquire a positive surface charge, due to the adsorption of H^+ and $CaH_2PO_4^+$ ions present in solution, on the particles. Under pH conditions above the IEP, the adsorption of OH- and HPO_4^{2-} ions in positive sites of apatite (Ca^{2+} and HPO_4Ca^+) promotes the occurrence of negative residual charge on the surface of the mineral particles [39].

The zeta potential curve obtained for apatite after conditioning with each collector showed an increase in the negative residual charge on the surface of the particles for the entire pH range evaluated, considering all collectors used in the study. This behavior is evidenced by the displacement of the curves, obtained after conditioning, to more negative regions. This phenomenon can be attributed to the specific adsorption of collectors, all anionic, on the positive sites (Ca^{2+}) present on the apatite surface [44]. Speciation of the collector as a function of pH, according to the respective pKa, affects its interaction with the mineral surface, which occurs differently depending on the system conditions [36]. The major presence of the molecular form of the collector in acidic medium would affect the surface charge of the particle less significantly. The coexistence of ionic and molecular species (including the formation of iono-molecular compounds) in neutral and slightly alkaline conditions enhances the adsorption of the collector and the reduction of the surface charge of the particle. For highly alkaline conditions, the formation of dimeric species of the collector and their subsequent adsorption on the surface of the particles is responsible for altering the mineral surface [13].

The zeta potential values of calcite and dolomite demonstrated IEP at pH close to 7 and 11, respectively, corroborating with the literature [36]. Considering all evaluated collectors, the behavior observed for apatite is repeated for carbonates, i.e., the residual negative charge on the mineral surface is increased after conditioning with anionic

reagents. For conditions above the carbonate IEP, all anionic collectors employed were capable of reversing the residual charge on the surface of the particles. Under these conditions, the electrostatic interaction between the positive residual charge of the pure mineral particles and the negative active group of the anionic collector can contribute to a more intense adsorption of this on the mineral.

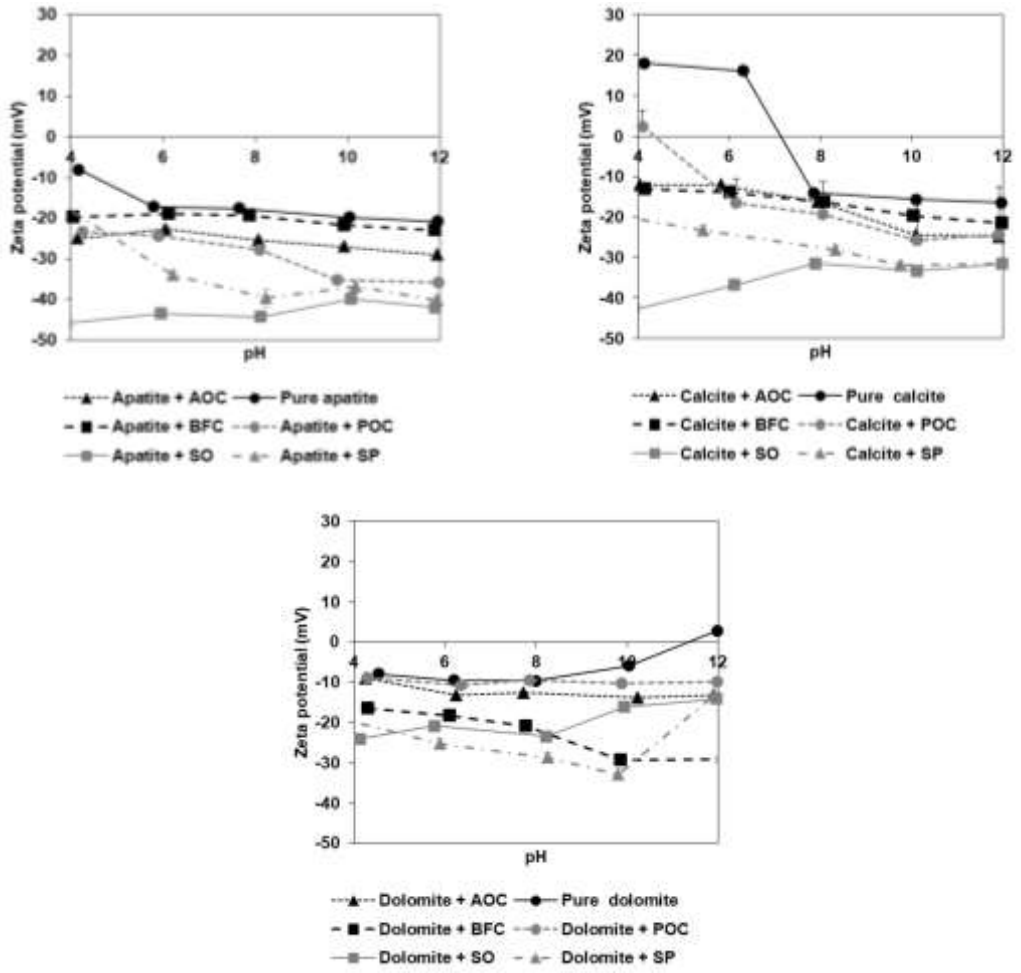

Figure 4.9 – Zeta potential of apatite, calcite and dolomite, as a function of pH, in the presence and absence of collectors.

AOC and POC showed greater affinity for the surface of apatite and calcite, promoting greater reduction in the residual charge on the surface of the particles. As for dolomite, this afinity was less pronounced, reflecting less influence on the surface characteristics of the particles. Such behavior can be attributed to the distinct configuration of the Ca2+ sites, in addition to the surface density of these sites. The composition of the oil samples (AO and PO) that gave rise to these collectors contributes to this behavior, since the SO

presented similar behavior to the AOC and POC. The discrepancies observed between pure fatty acid salt collectors and Amazonian oil-based ones can be attributed to the profile of the latter, which includes other fatty acids, changing the conformational configuration of the hydrophobic film layer formed on the mineral surface. On the other hand, BFC showed high affinity for the surface of dolomite, as well as SP, which is the collector obtained from the major fatty acid in the composition of the Amazon fatty sample that gave rise to this collector. As for apatite and calcite, BFC showed low adsorption on the surface of the particles. Again, the discussion about the influence of the fat profile of the Amazonian sample that gave rise to the collector on its performance in relation to adsorption on the particles can be considered.

4.3.7 Fourier-transform infrared spectroscopy (FTIR)

The ATR-FTIR spectra for apatite, calcite, and dolomite, pure and after conditioning with the evaluated collectors, are presented in Figure 4.10, comprising the wavelength range between 2,000cm^{-1} and 400cm^{-1}. The characteristic bands of each mineral were highlighted in the respective spectra [19]. The procedure involved the preparation of mineral samples, subjected to conditioning with each collectors under previously defined selectivity conditions (Table 4.4).

The proposed mechanism for the adsorption of carboxylate-type collectors on Ca-bearing minerals involves the possibility of formation of hydrophobic monolayer from the anchoring of the reagent molecules on the surface Ca^{2+} sites of the mineral particle and/or the chemical interaction between the carboxylates and Ca^{2+} of the system, followed by the formation and surface precipitation of the calcium dicarboxylate compound. For both scenarios, the phenomena comprise interactions of chemical nature, requiring longer conditioning time and higher reaction energy, resulting in a more stable hydrophobic film on the particles, due to the irreversible nature of the interaction [43].

Previous to the interaction, the presence of the carboxylate group in the structure of the collector is evidenced by the characteristic band at 1,558cm^{-1}, as observed in Figure 4.2 [33]. After the adsorption of the collector on the Ca^{2+} sites at the mineral surface, the occurrence of the compound formed between collector and Ca^{2+} in the system is characterized by the presence of the bands at 1.540cm^{-1} and 1.575cm^{-1}. They differ according to the coordination of the calcium carboxylate complex formed, which can be

monodentate (from the chemical interaction between a single Ca^{2+} ion) or bidentate (formed from two Ca^{2+} ions), respectively [19]. The occurrence of both characteristic bands is observed for all mineral/collector systems evaluated, but with distinct intensities. These bands are more pronounced for the BFC and SP collectors, with a greater proportion of saturation in the carbon chains of the carboxylates that compose them, suggesting the possibility of building a more organized hydrophobic film from a system containing carboxylates with predominantly linear chains, favoring the conformational structure of the latter. Also, for apatite and calcite, these bands were larger than for dolomite. This phenomenon can be attributed to the morphological characteristics of the particles of this mineral, previously discussed. That is, the occurrence of high pore diameter may favor the adsorption of the collector on the internal surface of these, corroborating the results of CAD and floatability achieved. Also, the proportion of Ca in the particle surface chemical composition, higher for calcite and apatite (Table 4.6), may favor the adsorption of the collector on the particles of these minerals. Due to the lower proportion of Ca in their surface composition, the adsorption of the collector on the dolomite particles may have been impaired. The high intensity of the characteristic bands of calcium carboxylate complexes observed in the ATR-FTIR spectra of apatite, even with a lower proportion of Ca in its surface composition compared to calcite, reinforces the adsorption of the collectors on its particles, corroborating with the floatability results of the phosphate mineral.

The relationship between the results obtained for floatability, CAD and adsorption of collectors (ATR-FTIR) demonstrates the effect of different factors on the hydrophobization phenomenon. For dolomite, for example, the positive effect of high saturation in the carbonic chains of the carboxylates present in the collector is evident, since, as a result of the lower indication of surface Ca^{2+} sites, the structural conformation of the layer provided by the majority presence of linear carbonic chains favors the interaction between them, providing greater stability to the hydrophobic film. Moreover, carboxylates with long linear carbon chains may have greater difficulty in interacting with the Ca^{2+} surface sites inside the pores (due to the morphological characteristics of the particles), concentrating on the outer surface of the dolomite, being identified in the ATR-FTIR spectra. Also, the performance of the AOC in the hydrophobization of the particles (mainly for apatite) indicated the positive contribution of the synergistic effect of the fatty acids present in its composition, demonstrating the

existence of an optimal ratio between saturation/unsaturation in the composition of the collector, as previously discussed.

Thus, the theory about the formation of ionomolecular compounds in flotation systems, from the speciation of collectors according to the system conditions and interaction between ionic and non-ionic species, suggests greater stability of the hydrophobic film formed on the mineral particles [11, 12]. All the collectors evaluated in the present work fit in this discussion due to their similar characteristics regarding speciation, representing more complex and little explored systems [13].

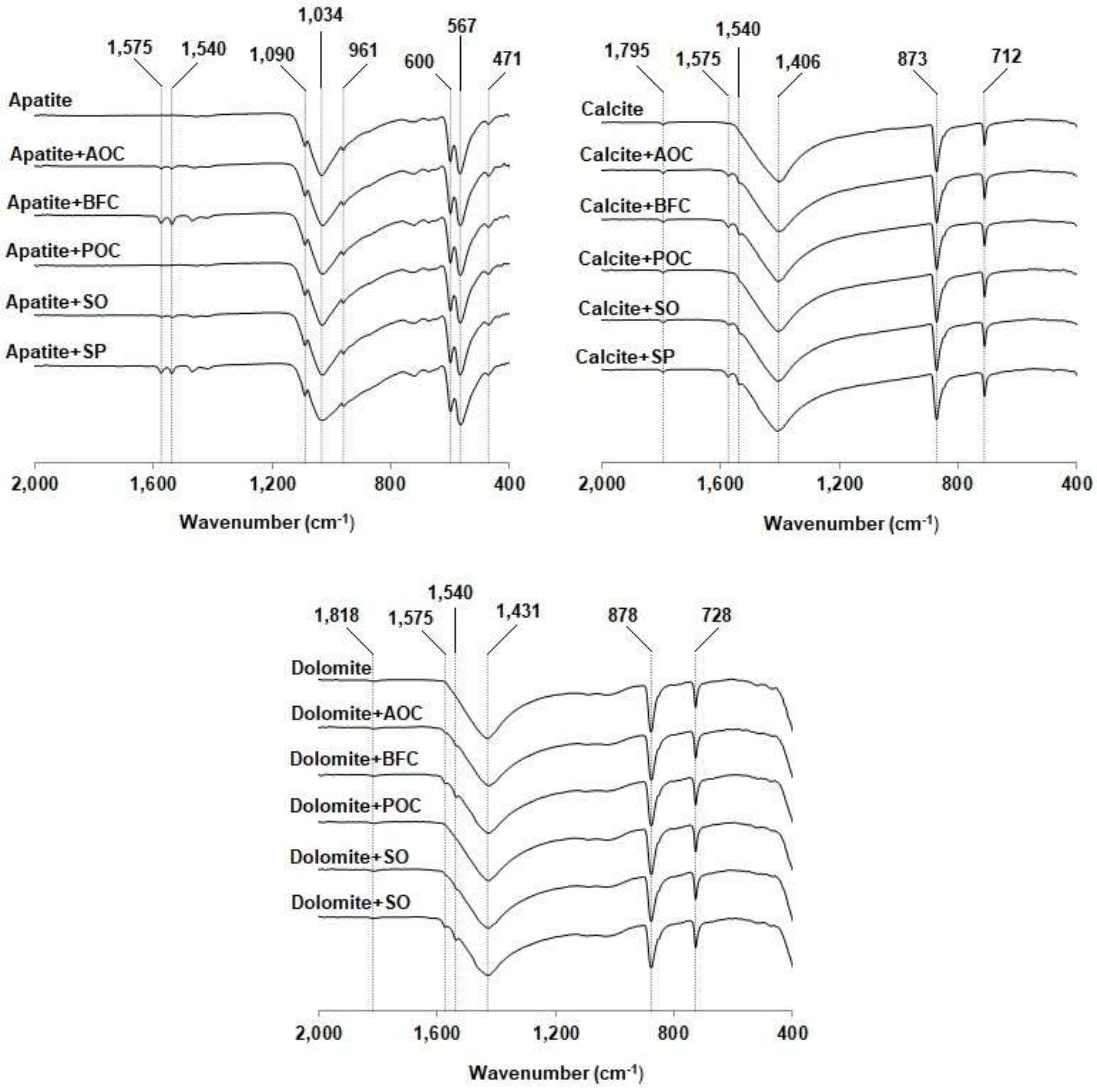

Figure 4.10 – ATR-FTIR spectra of pure minerals, before and after conditioning with collectors under the conditions of maximum selectivity.

4.4 Conclusion

The search for alternative sources for flotation reagents involves their characterization and the study on the effect of composition on performance in real operating systems. The mixed composition in oil-based Amazonian collectors, majorly composed of oleate and palmitate, affected the CMC, adsorption density and selective conditions for the apatite/carbonate separation. The collectors originated from andiroba and pataua oils showed a reduction in CMC values, as expected, due to the conformational discrepancies of the packing of their molecules, in comparison to pure fatty acid collectors (oleate and palmitate). The bacuri fatty collector, on the other hand, showed conflicting performance with previous reports, with greater CMC than oleate and palmitate.

Morphological characteristics of dolomite particles ensured their high collector adsorption density, especially for those with high saturation ratio. The adsorption of the collectors, identified by ATR-FTIR analysis, proved to be more effective for apatite and calcite, attributed to the higher proportion of Ca in their surface composition, provided by XPS analysis, reinforcing the collector-particle interaction hypothesis based on chemical mechanisms.

The andiroba oil collector showed superior performance on selectivity, in relation to oleate and palmitate, evidencing the importance of this parameter in stabilizing the hydrophobic film at the mineral surface. The bacuri fatty collector, with high proportion of saturation in its composition showed high affinity for the dolomite mineral surface, a phenomenon attributed to the lower incidence of Ca^{+2} sites available for interaction, in relation to the other minerals, and greater stability achieved for the hydrophobic layer, due to the alignment of the linear chains.

Given the results obtained and the discussion presented, it is evident the relevance of understanding the effect of the composition of vegetable oils on their performance in flotation systems. All of the Amazonian oil/fat samples evaluated showed a high potential for industrial application as a resource for the production of flotation reagents, proving to be an outstanding alternative source compared to the oils traditionally used in concentration circuits, being environmentally safe and with great availability, important characteristics in the search for new industrial reagents.

4.5 Acknowledgements

The authors thank the financial support from CNPq, FAPEMIG, CAPES and PROEX CAPES for the support to PPGEM. This study was financed in part by Coordenação de Aperfeiçoamento de Pessoal de Nível Superior – Brasil (CAPES) – Finance Code 001.

4.6 References

1. Abouzeid AZM, Negm AT, Elgillani DA. Upgrading of calcareous phosphate ores by flotation: Effect of ore characteristics. International Journal of Mineral Processing. 2009;90(1-4):81-89. https://doi.org/10.1016/j.minpro.2008.10.005.

2. Pereira E, Meirelles AJA, Maximo GJ. Predictive models for physical properties of fats, oils, and biodiesel fuels. Fluid Phase Equilibria. 2020;508:112440. https://doi.org/10.1016/j.fluid.2019.112440.

3. Brandao PRG, Caires LG, Queiroz DSB. Vegetable lipid oil-based collectors in the flotation of apatite ores. Minerals Engineering. 1994;7(7):917-25. https://doi.org/10.1016/0892-6875(94)90133-3.

4. Albuquerque RO, Peres AEC, Aquino JA, Praes PE, Pereira CA. Pilot Scale Direct Flotation of a Phosphate Ore with Silicate-Carbonate Gangue. Procedia Engineering. 2012;46:105-10. https://doi.org/10.1016/j.proeng.2012.09.452.

5. Wang Z, Wang L, Wang J, Xiao J, Liu J, Xu L, Fu K. Strengthened floatation of molybdite using oleate with suitable co-collector. Minerals Engineering. 2018;122:99-105. https://doi.org/10.1016/j.mineng.2018.03.042.

6. Xu L, Jiao F, Jia W, Pan Z, Hu C, Qin W. Selective flotation separation of spodumene from feldspar using mixed anionic/nonionic collector. Colloids and Surfaces A: Physicochemical and Engineering Aspects. 2020;594:124605. https://doi.org/10.1016/j.colsurfa.2020.124605.

7. Buckley AN, Hope GA, Parker GK, Steyn J, Woods R. Mechanism of mixed dithiophosphate and mercaptobenzothiazole collectors for Cu sulfide ore minerals. Minerals Engineering. 2017;109:80-97. https://doi.org/10.1016/j.mineng.2017.03.002.

8. Zhang H, Han C, Liu W, Hou D, Wei D. The chain length and isomeric effects of monohydric alcohols on the flotation of magnesite and dolomite by sodium oleate. Journal of Molecular Liquids. 2019;276:471-79. https://doi.org/10.1016/j.molliq.2018.11.143.

9. Sis H, Chander S. Adsorption and contact angle of single and binary mixtures of surfactants on apatite. Minerals Engineering. 2003;16(9):839-48. https://doi.org/10.1016/S0892-6875(03)00202-4.

10. Cao Q, Cheng J, Wen S, Li C, Liu J. Synergistic effect of dodecyl sulfonate on apatite flotation with fatty acid collector. Separation Science and Technology. 2016;51(8):1389-96. https://doi.org/10.1080/01496395.2016.1147467.

11. Kung HC, Goddard ED. Molecular association in fatty acid potassium soap systems. II. Journal of Colloid and Interface Science. 1969;29(2):242-49. https://doi.org/10.1016/0021-9797(69)90193-3.

12. Somasundaran P. The role of ionomolecular surfactant complexes in flotation. International Journal of Mineral Processing. 1976;3(1):35-40. https://doi.org/10.1016/0301-7516(76)90013-2.

13. Cao Q, Cheng J, Wen S, Li C, Bai S, Liu D. A mixed collector system for phosphate flotation. Minerals Engineering. 2015;78:114-21. https://doi.org/10.1016/j.mineng.2015.04.020.

14. Almeida AS, Vieira ICG, Moura N, Lees AC. Heterogeneity of tree diversity and carbon stocks in Amazonian oil palm landscapes. Plant Ecology and Diversity. 2020;13(1):105-13. https://doi.org/10.1080/17550874.2019.1710616.

15. Hernández PBN, Fregapane G, Moya MDS. Bioactive compounds, volatiles and antioxidant activity of virgin seje oils (Jessenia bataua) from the Amazonas. Journal of Food Lipids. 2009;16(4):629-44. https://doi.org/10.1111/j.1745-4522.2009.01171.x.

16. Silva JAP, Cardozo NSM, Petzhold CL. Enzymatic synthesis of andiroba oil based polyol for the production of flexible polyurethane foams. Industrial Crops and Products. 2018;113:55-63. https://doi.org/10.1016/j.indcrop.2018.01.020.

17. Serra JL, Rodrigues AMC, Freitas RA, Meirelles AJA, Darnet SH, Silva LHM. Alternative sources of oils and fats from Amazonian plants: Fatty acids, methyl tocols, total carotenoids and chemical composition. Food Research International. 2019;116:12-9. https://doi.org/10.1016/j.foodres.2018.12.028.

18. Pereira E, Ferreira MC, Sampaio KA, Grimaldi R, Meirelles AJA, Maximo GJ. Physical properties of Amazonian fats and oils and their blends. Food Chemistry. 2019;278:208-15. https://doi.org/10.1016/j.foodchem.2018.11.016.

19. Kou J, Tao D, Xu G. Fatty acid collectors for phosphate flotation and their adsorption behavior using QCM-D. International Journal of Mineral Processing. 2010;95(1-4):1-9. https://doi.org/10.1016/j.minpro.2010.03.001.

20. Silva AC, Silva SEM, Rocha TWP. Microflotação de apatita utilizando óleo de castanha de macaúba (Acromia Aculeata) como coletor. Tecnologia em Metalurgia Materiais e Mineração. 2015;12(2):146-52. http://dx.doi.org/10.4322/2176-1523.0836.

21. Oliveira P, Mansur H, Mansur A, Silva Gd, Peres AEC. Apatite flotation using pataua palm tree oil as collector. Journal of Materials Research and Technology. 2019;8(5):4612-19. https://doi.org/10.1016/j.jmrt.2019.08.005.

22. Silva GR, Espiritu ERL, Mohammadi-Jam S, Waters KE. Surface characterization of microwave-treated chalcopyrite. Colloids and Surfaces A: Physicochemical and Engineering Aspects. 2018;555:407-17. https://doi.org/10.1016/j.colsurfa.2018.06.078.

23. Santos LH, Carvalho PLG, Rodrigues GD, Mansur MB. Selective removal of calcium from sulfate solutions containing magnesium and nickel using aqueous two phase systems (ATPS). Hydrometallurgy. 2015;156:259-63. https://doi.org/10.1016/j.hydromet.2015.06.010.

24. Wang Z, Wu H, Xu Y, Shu K, Yang J, Luo L, Xu L. Effect of dissolved fluorite and barite species on the flotation and adsorption behavior of bastnaesite. Separation and Purification Technology. 2020;237:116387. https://doi.org/10.1016/j.seppur.2019.116387.

25. Amazon oil. Andiroba (Carapas guianensis). Available from https://www.amazonoil.com.br/pt/andiroba/. 2021. Acessed in 25/03/2021.

26. Amazon oil. Pataua (Oenocarpus bataua). Available from https://www.amazonoil.com.br/pt/pataua/. 2021. Acessed in 25/03/2021.

27. Amazon oil. Bacuri (Platonia insignis). Available from https://www.amazonoil.com.br/pt/bacuri/. 2021. Acessed in 25/03/2021.

28. Cheesbrough TM. Changes in the enzymes for fatty acidsynthesis and desaturation during acclimation of developingsoybean seeds to altered growth temperature. Plant Physiology. 1989;90(2):760-4. https://doi.org/10.1104/pp.90.2.760.

29. Labsynth. Ácido Oleico. Available from https://www.labsynth.com.br/fispq/FISPQ-%20Acido%20Oleico.pdf. Acessed in 09/10/2021.

30. Clariant. Ácido Palmítico. Available from https://www.clariant.com/pt/Business-Units/Oil-and-Mining-Services/Mining-Solutions. Acessed in 09/10/2021.

31. ANVISA. Resolução RDC n°270. Regulamento técnico para óleos vegetais, gorduras vegetais e creme vegetal. Brasília. 2005, 7p.

32. Poulenat G, Sentenac S, Mouloungui Z. Fourier-transform infrared spectra of fatty acid salts - kinetics of high-oleic sunflower oil saponification. Journal of Surfactants and Detergents. 2003;6(4):305-10. https://doi.org/10.1007/s11743-003-0274-1.

33. Schulz H, Baranska M. Identification and quantification of valuable plant substances by IR and Raman spectroscopy. Vibrational Spectroscopy. 2007;43(1):13-25. https://doi.org/10.1016/j.vibspec.2006.06.001.

34. Calvino-Casilda V, Mul G, Fernandez JF, Rubio-Marcos F, Bañares MA. Monitoring the catalytic synthesis of glycerol carbonate by real-time attenuated total reflection FTIR spectroscopy. Applied Catalysis A: General. 2011; 409-410:106-12. https://doi.org/10.1016/j.apcata.2011.09.036.

35. Filippova IV, Filippov LO, Lafhaj Z, Barres O, Fornasiero D. Effect of calcium minerals reactivity on fatty acids adsorption and flotation. Colloids and Surfaces A: Physicochemical and Engineering Aspects. 2018;545:157-66. https://doi.org/10.1016/j.colsurfa.2018.02.059.

36. Pugh R, Stenius P. Solution chemistry studies and flotation behaviour of apatite, calcite and fluorite minerals with sodium oleate collector. International Journal of Mineral Processing. 1985;15(3):193-218. https://doi.org/10.1016/0301-7516(85)90035-3.

37. Barros LAF, Ferreira EE, Peres AEC. Floatability of apatites and gangue minerals of an igneous phosphate ore. Minerals Engineering. 2008;21(12-14):994-99. https://doi.org/10.1016/j.mineng.2008.04.012.

38. Pan Z, Wang Y, Wei Q, Chen X, Jiao F, Qin W. Effect of sodium pyrophosphate on the flotation separation of calcite from apatite. Separation and Purification Technology. 2020;242:116408. https://doi.org/10.1016/j.seppur.2019.116408.

39. Vučinić DR, Radulović DS, Deušić SĐ. Electrokinetic properties of hydroxyapatite under flotation conditions. Journal of Colloid and Interface Science. 2010;343(1):239-45. https://doi.org/10.1016/j.jcis.2009.11.024.

40. Joseph-Soly S, Quast K, Connor JN. Effects of Eh and pH on the oleate flotation of iron oxides. Minerals Engineering. 2015;83:97-104. https://doi.org/10.1016/j.mineng.2015.08.014.

41. Quast K. The use of zeta potential to investigate the pKa of saturated fatty acids. Advanced Powder Technology. 2016;27(1):207-14. https://doi.org/10.1016/j.apt.2015.12.003.

42. Horta D, Monte MBM, Leal Filho LS. The effect of dissolution kinetics on flotation response of apatite with sodium oleate. International Journal of Mineral Processing. 2016;146:97-104. https://doi.org/10.1016/j.minpro.2015.12.003.

43. Lu Y, Drelich J, Miller JD. Oleate Adsorption at an Apatite Surface Studied by Ex-Situ FTIR Internal Reflection Spectroscopy. Journal of Colloid and Interface Science. 1998;202(2):462-76. https://doi.org/10.1006/jcis.1998.5466.

44. Rao KH, Antti B-M, Forssberg E. Mechanism of oleate interaction on salt-type minerals, Part II. Adsorption and electrokinetic studies of apatite in the presence of sodium oleate and sodium metasilicate. International Journal of Mineral Processing. 1990;28(1-2):59-79. https://doi.org/10.1016/0301-7516(90)90027-V.

45. Zhong C, Feng B, Zhang W, Zhang L, Guo Y, Wang T, Wang H. The role of sodium alginate in the flotation separation of apatite and dolomite. Powder Technology. 2020;373:620-6. https://doi.org/10.1016/j.powtec.2020.07.007.

46. Chu DH, Vinoba M, Bhagiyalakshmi M, Baek IH, Nam SC, Yoon Y, Kim SH, Jeong SK. CO2 mineralization into different polymorphs of CaCO3 using an aqueous-CO2 system. RSC Advances. 2013;3:21722-9. https://doi.org/10.1039/C3RA44007A.

47. Baer DR, Marmorstein AM, Williford RE, Blanchard DL. Comparison Spectra for Calcite by XPS. Surface Science Spectra. 1992;1(1):80-6. https://doi.org/10.1116/1.1247674.

48. Layrolle P, Lebugle A. Synthesis in Pure Ethanol and Characterization of Nanosized Calcium Phosphate Fluoroapatite. Chemistry of Materials. 1996;8(1):134-44. https://doi.org/10.1021/cm950326k.

49. Thermo Scientific XPS. Magnesium, Alkaline Earth Metal. Disponível em http://xpssimplified.com/elements/magnesium.php. Acessado em 25/04/2021.

50. Dong L, Wei Q, Qin W, Jiao F. Selective adsorption of sodium polyacrylate on calcite surface: Implications for flotation separation of apatite from calcite. Separation and Purification Technology. 2020;241:116415. https://doi.org/10.1016/j.seppur.2019.116415.

51. Wang T, Feng B, Guo Y, Zhang W, Rao Y, Zhong C, Zhang L, Cheng C, Wang H, Luo X. The flotation separation behavior of apatite from calcite using carboxymethyl chitosan as depressant. Minerals Engineering. 2020;159:106635. https://doi.org/10.1016/j.mineng.2020.106635.

52. Zeng M, Yang B, Guan Z, Zeng L, Luo H, Deng B. The selective adsorption of xanthan gum on dolomite and its implication in the flotation separation of dolomite from apatite. Applied Surface Science. 2021;551:149301. https://doi.org/10.1016/j.apsusc.2021.149301.

53. Hu X, Joshi P, Mukhopadhyay SM, Higgins SR. X-ray photoelectron spectroscopic studies of dolomite surfaces exposed to undersaturated and supersaturated aqueous solutions. Geochimica et Cosmochimica Acta. 2006;70(13):3342-50. https://doi.org/10.1016/j.gca.2006.04.022.

54. Fuerstenau DW, Pradip. Zeta potentials in the flotation of oxide and silicate minerals. Advances in Colloid and Interface Science. 2005;114-115:9-26. https://doi.org/10.1016/j.cis.2004.08.006.

55. Amankonah JO, Somasundaran P. Effects of dissolved mineral species on the electrokinetic behavior of calcite and apatite. Colloids and Surfaces. 1985;15:335-53. https://doi.org/10.1016/0166-6622(85)80082-2.

56. Mishra SK. The electrokinetics of apatite and calcite in inorganic electrolyte environment. International Journal of Mineral Processing. 1978;5(1):69-83. https://doi.org/10.1016/0301-7516(78)90006-6.

57. Filippov LO, Duverger A, Filippova IV, Kasaini H and Thiry J. Selective flotation of silicates and Ca-bearing minerals: The role of non-ionic reagent on cationic flotation. Minerals Engineering. 2012;36-38:314-23. https://doi.org/10.1016/j.mineng.2012.07.013.

58. Parks GA. Adsorption in the Marine Environment. In: Academic Press. Chemical Oceanography. Londres: 1975, p. 241-308.

5. Considerações Finais

5.1 Conclusões

Neste trabalho, coletores aniônicos obtidos a partir de fontes graxas alternativas de origem amazônica foram avaliados em sistemas de flotação apatita/carbonatos, tendo como objetivo atingir condições operacionais que promovam a seletividade entre fosfatos e carbonatos, sendo estes, minerais de ganga problemáticos para os processos químicos aos quais o concentrado fosfático são submetidos, durante a produção de fertilizantes fosfatados. Com base nos resultados desta pesquisa, as seguintes conclusões principais são destacadas:

- A saponificação alcóolica a quente com NaOH, empregando refluxo, demostrou ser eficiente para a obtenção de coletores aniônicos a partir de amostras graxas amazônicas, confirmada através de análises de ATR-FTIR dos óleos/gordura e dos produtos sólidos obtidos. Ainda, o processo garante a reprodutibilidade dos ensaios de microflotação com o mesmo lote de coletor obtido, minimizando erros de variação composicional na obtenção deste;
- A composição mista dos coletores aniônicos obtidos, maioritariamente compostos por oleato e palmitato, afetou a CMC, a densidade de adsorção e as condições seletivas para a separação apatita/carbonato;
- Coletores obtidos a partir de óleos de andiroba e patauá, com composição majoritária em oleato (insaturado), apresentaram menor CMC em relação aos coletores obtidos a partir dos ácidos graxos puros (oléico e palmítico). Tal comportamento pode ser atribuído às diferenças de tamanho e conformação das cadeias de hidrocarbonetos de ácidos graxos presentes no óleo, dificultando o emparelhamento de moléculas durante a formação das micelas em função da diferença na energia vibracional das cadeias. O coletor aniônico obtido a partir da gordura de bacuri demonstrou comportamento discrepante, apresentando maior CMC em relação ao coletor obtido a partir do ácido palmítico (saturado), majoritário em sua composição.
- Coletores com alta proporção de saturação em suas cadeias carbônicas demostraram melhor desempenho na adsorção sobre a dolomita, favorecido pelas características morfológicas de suas partículas (elevado diâmetro médio de

poros e baixa área superficial específica) e maior facilidade de alinhamento entre cadeias carbônicas lineares, com conformação mais estável do filme hidrofóbico;

- Coletores com baixa proporção de saturação demonstraram melhor desempenho na adsorção sobre a apatita e calcita, favorecido pela maior proporção de Ca em sua composição superficial, fornecida pela análise XPS, reforçando a hipótese de interação coletor-partícula baseada em mecanismos químicos.
- O coletor obtido a partir do óleo de andiroba alcançou maior seletividade para o sistema apatita/carbonatos, em relação ao oleato e palmitato, evidenciando a importância da sinergia entre os carboxilatos, em especial a configuração espacial de suas cadeias carbônicas, na estabilização do filme hidrofóbico na superfície mineral. Máxima seletividade foi obtida para concentração de 20mg.L^{-1} do coletor em pH 7,5;

Diante dos resultados obtidos, fica evidente a relevância de compreender o efeito da composição dos óleos vegetais sobre seu desempenho em sistemas de flotação. Todas as amostras de óleo/gordura amazônica avaliadas mostraram um alto potencial de aplicação industrial como recurso para a produção de reagentes de flotação, provando ser uma promissora fonte alternativa em relação aos óleos tradicionalmente utilizados em circuitos de concentração, sendo ambientalmente seguros e com grande disponibilidade, características importantes na busca de novos reagentes industriais.

5.2 Sugestões para trabalhos futuros

Óleos e gorduras de origem amazônica apresentam alto potencial de aplicação industrial em sistemas de flotação. O presente estudo avaliou o desempenho de três representantes destes. Para ampliar o entendimento dessas fontes promissoras, novos estudos devem ser desenvolvidos com outras fontes endêmicas de amostras graxas de origem amazônica.

Para as fontes amazônicas alternativas avaliadas, sugere-se o estudo, em escala de flotação em bancada e/ou coluna, do desempenho destes coletores sobre a flotação de minérios fosfáticos, de preferência, empregando planejamento fatorial para melhor interpretação dos resultados. Cabe, ainda, uma avaliação econômica do emprego destes reagentes alternativos, envolvendo logística, disponibilidade e possíveis adequações de

instalações e consumo.

Visando a aplicação industrial destes coletores, sugere-se também o estudo de otimização da saponificação de óleos/gordura, uma vez que, durante o trabalho, foi empregada a saponificação alcoólica a quente, com refluxo. Assim, será possível obter a proporção ideal entre NaOH e amostra graxa que potencialize sua função coletora em sistemas de flotação.

O estudo trouxe uma discussão inicial sobre o efeito sinérgico da composição mista e proporção entre saturação/insaturação para os coletores obtidos a partir de amostras graxas amazônicas. Cabe um estudo detalhado sobre a modelagem química da interação e sinergia destas espécies no sistema de flotação e, especialmente, no filme hidrofóbico sobre as partículas minerais.

Finalmente, os coletores alternativos avaliados para o sistema apatita/carbonatos pode ser aplicado em estudos envolvendo outros sistemas passíveis de seletividade, onde o coletor aniônico possa ser empregado.